REPORT DOCUMENTATION PAGE	Form Approved OMB No. 0704-0188

1. AGENCY USE ONLY *(Leave blank)*	2. REPORT DATE	3. REPORT TYPE AND DATES COVERED
	18 Apr 97	

4. TITLE AND SUBTITLE
MODAL FREQUENCY DETECTION IN COMPOSITE BEAMS USING FIBER OPTIC SENSORS

5. FUNDING NUMBERS

6. AUTHOR(S)
GILBERT WARREN SANDERS

7. PERFORMING ORGANIZATION NAME(S) AND ADDRESS(ES)
UNIVERSITY OF MISSOURI-ROLLA

8. PERFORMING ORGANIZATION REPORT NUMBER
97-023

9. SPONSORING/MONITORING AGENCY NAME(S) AND ADDRESS(ES)
DEPARTMENT OF THE AIR FORCE
AFIT/CI
2950 P STREET
WRIGHT-PATTERSON AFB OH 45433-7765

10. SPONSORING/MONITORING AGENCY REPORT NUMBER

11. SUPPLEMENTARY NOTES

12a. DISTRIBUTION AVAILABILITY STATEMENT

DISTRIBUTION STATEMENT A
Approved for public release;
Distribution Unlimited

12b. DISTRIBUTION CODE

13. ABSTRACT *(Maximum 200 words)*

14. SUBJECT TERMS	15. NUMBER OF PAGES
	95
	16. PRICE CODE

17. SECURITY CLASSIFICATION OF REPORT	18. SECURITY CLASSIFICATION OF THIS PAGE	19. SECURITY CLASSIFICATION OF ABSTRACT	20. LIMITATION OF ABSTRACT

Standard Form 298 (Rev. 2-89) (EG)
Prescribed by ANSI Std. 239.18
Designed using Perform Pro, WHS/DIOR, Oct 94

MODAL FREQUENCY DETECTION

IN COMPOSITE BEAMS USING FIBER OPTIC SENSORS

by

GILBERT WARREN SANDERS, 1973-

A THESIS

Presented to the Faculty of the Graduate School of the

UNIVERSITY OF MISSOURI-ROLLA

In Partial Fulfillment of the Requirements for the Degree

MASTERS OF SCIENCE IN ELECTRICAL ENGINEERING

1997

Approved by

Steve E. Watkins, Advisor

Kelvin T. Erickson

K. Chandrashekhara

ABSTRACT

Extrinsic Fabry-Perot interferometric (EFPI) fiber optic sensors were used to determine the first five modal frequencies of laminated glass/epoxy composite beams. EFPI fiber optic sensors and piezoelectric (PZT) ceramic sensor both found identical modal frequencies of the composite beams, however, EFPI fiber optic sensors showed more sensitivity and better signal-to-noise ratios. The analytical classical beam theory and a finite element model validated the EFPI modal frequency measurements. Several 8-ply glass/epoxy composite beams, each 26.04 cm long and 2.33 cm wide were fabricated. Five damaged beams with specified delaminations as well as two different undamaged beams were tested for modal frequencies. Five different delaminations with sizes ranging from 1.27 cm to 6.35 cm long were incorporated in the midplane of the beams. Each modal frequency shifted with a change of delamination size and location. Classical beam theory was used to simulate modal frequency data sets for 1097 different prescribed delamination sizes and locations. These data sets were applied for training and testing a feedforward backpropagation neural network. Finally the neural network was tested against the EFPI fiber optic sensor modal frequency results. The delamination size and location predictions resulted from neural network's simulation had an average error of 5.9% and 4.7% respectively.

ACKNOWLEDGMENT

The author would like to thank my advisor Dr. Steve E. Watkins for his help, suggestions, and direction during my graduate career. Sincere thanks are also extended to my committee members Dr. K. Chandrashekhara and Dr. Kelvin T. Erickson, who have taken the time to review my work. The financial support of Hitachi and the United States Air Force is gratefully acknowledged. Thanks are also given to McDonnell Douglas Corp. for sensors and other research equipment. I would also like to thank Farhad Akhavan, Yuping Jiang, and Sean Bentley for their help in lab and class.

I would like to thank friends: Sully, Jeff, Robin, Jonny, Paul, Joe, Craig, Raj, Mike, Sot, Matt, Darren and Elliot for keeping me on track. Also, thanks to the football teams for allowing me to play and coach.

Finally, special thanks go to my family: mom, dad, Garrett, Natalie, and Ashley for their love and support. Without them, my life would not be as pleasant.

TABLE OF CONTENTS

	Page
ABSTRACT	iii
ACKNOWLEDGMENT	iv
LIST OF ILLUSTRATIONS	vii
LIST OF TABLES	ix
SECTION	
I. INTRODUCTION	1
II. LITERATURE REVIEW	4
A. SMART STRUCTURES AND SENSING	4
B. USE OF FIBER OPTIC SENSORS	5
C. COMPOSITE MATERIAL ANALYSIS	6
D. NEURAL NETWORK APPLICATIONS	7
III. THEORY	8
A. SENSORS AND ACTUATORS	8
1. Fabry-Perot Interferometer	8
2. Extrinsic Fabry-Perot Interferometric Sensors	9
3. Piezoelectric Sensors and Actuators	11
B. COMPOSITE MATERIAL FABRICATION	12
C. COMPOSITE MATERIAL ANALYSIS	14
IV. EXPERIMENTAL PROCEDURES	19
A. FREQUENCY RESPONSE TESTING	19
B. NEURAL NETWORK SETUP	22

V. EXPERIMENTAL RESULTS 25

A. COMPOSITE BEAM MODAL FREQUENCIES 25

B. DELAMINATED COMPOSITE BEAM MODAL FREQUENCIES 29

C. NEURAL NETWORK RESULTS 34

VI. DISCUSSION 43

A. MODAL FREQUENCIES FOR UNDAMAGED COMPOSITE BEAMS 43

B. MODAL FREQUENCIES FOR UNDAMAGED COMPOSITE BEAMS 44

C. NEURAL NETWORK INSIGHT AND IMPROVEMENTS ... 44

VII. CONCLUSIONS 46

APPENDIX

A. MATLAB CODE FOR THE CLASSICAL BEAM THEORY 48

B. MODAL FREQUENCIES GENERATED BY THE CLASSICAL BEAM THEORY 61

C. INPUT AND OUTPUT FOR THE FINITE ELEMENT MODEL 88

BIBLIOGRAPHY 91

VITA 95

LIST OF ILLUSTRATIONS

Page

Figure

1. EFPI fiber optic modal frequency sensor..... 10

2. Orientation of composite lamina..... 13

3. Heating and cooling curve for the glass/epoxy composite plate fabrication..... 14

4. Cantilever composite beam with prescribed delamination location..... 15

5. Experimental setup for determining modal frequencies in a cantilever composite beam..... 20

6. Photograph of the experimental setup..... 21

7. A feed forward, backpropagation neural network with five inputs and two outputs..... 23

8. Frequency response of (a) an EFPI fiber optic sensor and (b) a PZT ceramic sensor mounted on an undamaged glass/epoxy beam. The beam is 2.33 cm wide..... 27

9. Frequency response of (a) an EFPI fiber optic sensor and (b) a PZT ceramic sensor mounted on an undamaged glass/epoxy beam. The beam is 2.54 cm wide..... 28

10. Frequency response of (a) an EFPI fiber optic sensor and (b) a PZT ceramic sensor mounted on glass/epoxy beam containing a 5.08 cm delamination..... 31

11. Frequency response of an EFPI fiber optic sensor mounted on a glass/epoxy beam containing a 1.27 cm delamination..... 32

12. Frequency response of an EFPI fiber optic sensor mounted on a glass/epoxy beam containing a 2.54 cm delamination..... 32

13. Frequency response of an EFPI fiber optic sensor mounted on a glass/epoxy beam containing a 3.81 cm delamination..... 33

14. Frequency response of an EFPI fiber optic sensor mounted on a glass/epoxy beam containing a 6.35 cm delamination..... 33

15. Actual modal frequencies of a glass/epoxy composite beam for five prescribed delamination sizes..... 37

16. Neural network predicted modal frequencies of a glass/epoxy composite beam for five prescribed delamination sizes..... 38

17. Actual modal frequencies of four different 2.54 cm delamination locations in a glass/epoxy composite beam..... 39

18. Neural network predicted modal frequencies of four different 2.54 cm delamination locations in a glass/epoxy composite beam..... 40

19. Actual modal frequencies of four different 6.35 cm delamination locations in a glass/epoxy composite beam..... 41

20. Neural network predicted modal frequencies of four different 6.35 cm delamination locations in a glass/epoxy composite beam..... 42

LIST OF TABLES

Page

Table

I: Experimental modal frequencies of an undamaged beam compared to MATLAB generated frequencies of classical beam theory and frequencies calculated using a finite element model (FEM)..... 26

II: Comparison of modal frequencies of two composite beams having different widths..... 26

III: Experimental modal frequencies of delaminated composite beams..... 29

IV: Comparison of experimental and classical beam theory modal frequencies for different delamination sizes..... 30

V: Experimental delamination size compared to predicted neural network delamination size..... 34

VI: Experimental delamination location compared to predicted neural network delamination location..... 35

I. INTRODUCTION

Fiber reinforced composite materials are being used more frequently in many different engineering fields. The automobile, aerospace, naval, and civil industries all use composite materials in some way. Composite materials are gaining popularity because of high strength, low weight, resistance to corrosion, impact resistance, and high fatigue strength. Other advantages include ease of fabrication, flexibility in design, and variable material properties to meet almost any application [1].

With this increase in structural applications for composite materials comes an increase in safety awareness. Unlike steel or cement, it is difficult to see damage to composite materials with the naked eye. The delamination of laminated composite structures is an important failure mode and consequently has received much attention recently [2]. Delaminations affect the strength and integrity of the composite structure.

Embedded or surface mounted sensors can be used to continuously monitor the composite material. Real time measurements of strain, temperature, or composite material failure can be determined by many different types of sensors: fiber optic, piezoelectric, or LVDT. Long term health monitoring, fatigue deformation, and delamination formation can also be monitored with sensors [3].

Fiber optic sensors hold many advantages over conventional electrical sensors. Fiber optic sensors are light weight, small in size, have high sensitivity, and have a large bandwidth. Fiber optic sensors are all-passive (dielectric) which provides immunity to electromagnetic interference and reduces noise [4]. Also, small size, environmental ruggedness, and high temperature resistance allow fiber optic sensors to be embedded

inside the composite structure. Conventional electrical sensors cannot be imbedded into the composites because high temperatures change their performance permanently [2]. Electrical sensors are also large compared to fiber optic sensors and have soldered electrical connections.

Fiber optic sensors can potentially perform four functions in smart structures applications. First, they can monitor strain, temperature, and pressure during the manufacturing process. Second, they perform a non-destructive evaluation of structural integrity at any point during the manufacturing process. The fiber optic sensors can also be used as a health monitoring system for the composite structure. Finally, they can complement performance monitoring and control systems [3].

Smart structures is a term used to describe a system that uses a sensor or network of sensors, a processor, and actuators to sense the environment, interpret data, make decisions, and respond to the decision. In this study a single fiber optic sensor and a single piezoelectric lead zironate titanate (PZT) actuator are used to perform real time health monitoring of a glass/epoxy composite beam. The sensor chosen for this experiment is an extrinsic Fabry-Perot interferometric (EFPI) fiber optic sensor.

In this research, the first five modal frequencies of several glass/epoxy composite beams with and without various prescribed delaminations are measured with EFPI fiber optic sensors. Classical beam theory, a finite element model, and a piezoelectric (PZT) sensor are all used to validate the accuracy of the modal frequencies measured using the EFPI fiber optic sensors. The classical beam theory is also used to calculate modal frequencies for variations on prescribed delamination size and location. These modal

frequencies are used to train a backpropagation neural network to predict the size and location of the prescribed delaminations.

The next section is a review of the literature that gives background information as well as alternate sources for the theories and applications discussed in this study. The third section is an overview of the theoretical concepts used to measure and compare the experimental results. Then the exact procedures used to complete the experiments are outlined. The fifth section gives the results of the experiments followed by the discussion of these results in the sixth section. The last section is a conclusion of this study.

II. LITERATURE REVIEW

A. SMART STRUCTURES AND SENSING

A "smart" structure is one which incorporates a system that uses a sensor or network of sensors, a processor, and actuators to sense the environment, interpret data, make decisions, and respond to the decisions. The development of a full smart structures system requires the coordination of many different engineering disciplines. The materials, structures, actuators, sensors, signal processing, and systems must all work together to make smart structures a reality.

The level of activity in smart structures research has greatly increased in the last decade [2]. One particular area of interest is applying smart structures to monitor real time damage assessment. An early study involved simple embedded fiber optic grids that located damage by monitoring loss of signal from the optical fibers near the damage location [5]. A similar experiment was conducted on a composite lattice [6]. A simple type of fiber optic sensor involved the strain induced modulation of the coherent interference pattern leaving the fiber. This was the basis for early fiber optic technology [7]. Now more sensitive techniques using optical interference have been developed. These include the Fabry-Perot interferometer, the Mach-Zehner interferometer, and the Michelson interferometer [8]. The suitability of fiber optic sensors in smart structures applications was demonstrated in a study incorporating solid state actuators and neural processing [9].

B. USE OF FIBER OPTIC SENSORS

Fiber optic sensors are ideal for smart structures applications and for use with composite materials. They have low weight, small size, high sensitivity, and a large bandwidth. Fiber optic sensors are all-passive (dielectric) which provides immunity to electromagnetic interference and reduces noise. Also, small size, environmental ruggedness, and high temperature resistance allow fiber optic sensors to be embedded inside the composite structure.

In the area of dynamic testing, the extrinsic Fabry-Perot interferometric (EFPI) fiber optic sensor is the most widely studied. A Fabry-Perot interferometer as a fiber optic sensor was first introduced in 1982 [10]. In a later study intrinsic Fabry-Perot interferometric fiber optic sensors were embedded into composite material and used as ultrasound sensors [11]. Next, EFPI fiber optic sensors were used as strain sensors for composite and metal beams as well as for composite plates [12,13,14,15,16]. Many signal processing techniques and sensor configurations were also discussed in these studies. Fatigue testing was done on a full-scale F-15 aircraft and the EFPI fiber optic sensor was applied to smart structure applications and nondestructive health monitoring [17,18,19]. Modal frequencies and mode shapes were detected using fiber optic sensors in 1994 [20]. In 1995, EFPI fiber optic sensors were used to detect delaminations in composite beams [21]. References 20 and 21 both relate directly to the present study. As an alternative to EFPI fiber optic sensors, fiber Bragg gratings and birefringent integrated fiber optic sensors have been used for vibration sensing of composite structures [22,23].

C. COMPOSITE MATERIAL ANALYSIS

Delamination detection in smart composite structures has received much attention recently because delaminations are an important failure mode for laminated composites. Delaminations affect the strength and integrity of the composite structure and may cause structural failure at a load lower than the design load. The effects of delamination on buckling load, postbuckling deformation, and delamination growth under various geometrical parameters, dynamic and static loading conditions, material properties, and boundary conditions have been studied extensively for the past few years [24,25]. These studies predicted the size and location of delaminations in composite structures. Interlaminar fracture toughness based on static models have been used to predict the size of delamination cracks in composite laminates [26]. The use of dynamic testing to detect and quantify the effects of internal damage on modal parameters has been studied on a limited basis over the past twenty years.

Shifts in natural frequencies have been used to identify damage generated by various mechanical loadings including prescribed delamination [27]. Effects of prescribed delamination position and size on the natural frequencies of the graphite epoxy beam specimens have been investigated analytically and experimentally [28,29]. The analytical approach was based on classical beam theory and imposed the constraint of identical transverse displacements for the upper and lower sublaminates. A finite element model has been utilized to detect and suppress delamination based on such piezoelectric behaviors [30]. Piezoelectric sensors have been used to measure the natural frequencies of composite beams before and after prescribed delaminations and therefore indicate the

presence and size of the delamination [31]. These results were compared to theoretical predictions of an in-house finite element model based on shear deformation theory [32].

Fiber optic sensors have been used to measure acoustic signatures, changes in strain profiles, delamination, and other indications of changes in structural characteristics of fabricated composite structures [6,11,16,21]. Fiber optic sensors have found increasing applications in development of smart composite structures because of their superior advantages including compatibility with their host structures and the ability to be easily multiplexed [9].

D. NEURAL NETWORK APPLICATIONS

Neural networks have been used as effective tools to predict and generalize unknown parameters in physical systems [33]. Recently neural network simulations have been accurate, robust, and fast in response to changes in dynamic characteristics of composite structures. In particular, they have been utilized in such applications as damage assessment and fatigue monitoring of composite structures [34,35]. Neural networks have joined feedback control circuits and programmable logic controllers as processing elements in smart structures. Neural networks are especially suited for applications in which large numbers of sensors and actuators are used. Neural networks have parallel computing architecture that allows multiple inputs and outputs to be processed in nanoseconds. Also, neural networks can learn from experimental data and adapt to changing conditions. This fast processing speed and adaptability provide many possible applications for neural networks in smart structures.

III. THEORY

A. SENSORS AND ACTUATORS

Extrinsic Fabry-Perot interferometric (EFPI) fiber optic sensors are the primary sensors used in this study. EFPI fiber optic sensors are used to experimentally measure the modal frequencies of a cantilever glass/epoxy composite beam. Piezoelectric devices are also used as sensors and actuators. A piezoelectric (PZT) ceramic sensor is used on three different beams to verify the accuracy of the EFPI fiber optic sensors. A PZT ceramic actuator is used on all seven beams. The PZT ceramic actuator is used to vibrate the beam at different frequencies so a frequency response can be measured for the beam.

1. Fabry-Perot Interferometer. The Fabry-Perot interferometer consists of two mirrors of reflectance R_1 and R_2 separated by a distance L. The reflectance of the system is given by the ratio of reflected power P_r to the incident power P_i. Assuming the mirrors are of equal reflectivity ($R_1 = R_2 = R$):

$$\frac{P_r}{P_i} = \frac{2R(1-\cos\phi)}{1+R-2R^2(\cos\phi)} \tag{1}$$

where ϕ is the round trip phase shift of the coherent light inside the cavity [2]. The phase shift is given by:

$$\phi = 4\pi nL/\lambda \tag{2}$$

where L is the cavity length, n is the index of refraction of the cavity, and λ is the free space wavelength of the coherent light source. For this study, the cavity media is air (n = 1.0) and the laser diode wavelength is 1310 nm. The finesse F is a parameter used to describe the sensitivity of the interferometer. Finesse is defined as the ratio of the phase

change between adjacent transmittance peaks to the phase change between half-maximum points on either side of a peak [4]. It can be written as:

$$F = \frac{4R}{(1-R)^2}. \tag{3}$$

Therefore, as R increases, so does F.

2. Extrinsic Fabry-Perot Interferometric Sensors. An EFPI fiber optics sensor is schematically shown in Figure 1(a). The EFPI fiber optic sensor utilizes multiple-beam interference between two polished end faces of a single mode fiber and a multimode fiber. The Fresnel reflection from the glass-air interface at the front of the air gap (reference reflection) and the reflection from the air-glass interface at the far end of the air gap (sensing reflection) interfere in the single mode fiber. The far end of the multimode fiber is shattered so the reflections from the far end do not add to the detector's noise. The phase of the light between the two endfaces in the air gap region is modulated in response to vibration via the strain-optic effect. The active sensing length, or gauge length, is length of the capillary tube that is cemented around the two fibers.

The EFPI fiber optic sensors used in this study had gauge lengths of 8mm and cavity lengths, L, of 100 μm. They also had low finesse, ($R << 1$) so equation (1) can be approximated by:

$$\frac{P_r}{P_i} = 2R(1 - \cos\phi). \tag{4}$$

The sensor detects vibration by changes in ϕ as a function of L (see equation 2). As vibration modulates the axial sensor, strain changes proportionally. This change in reflected power is detected by the fiber optic support system.

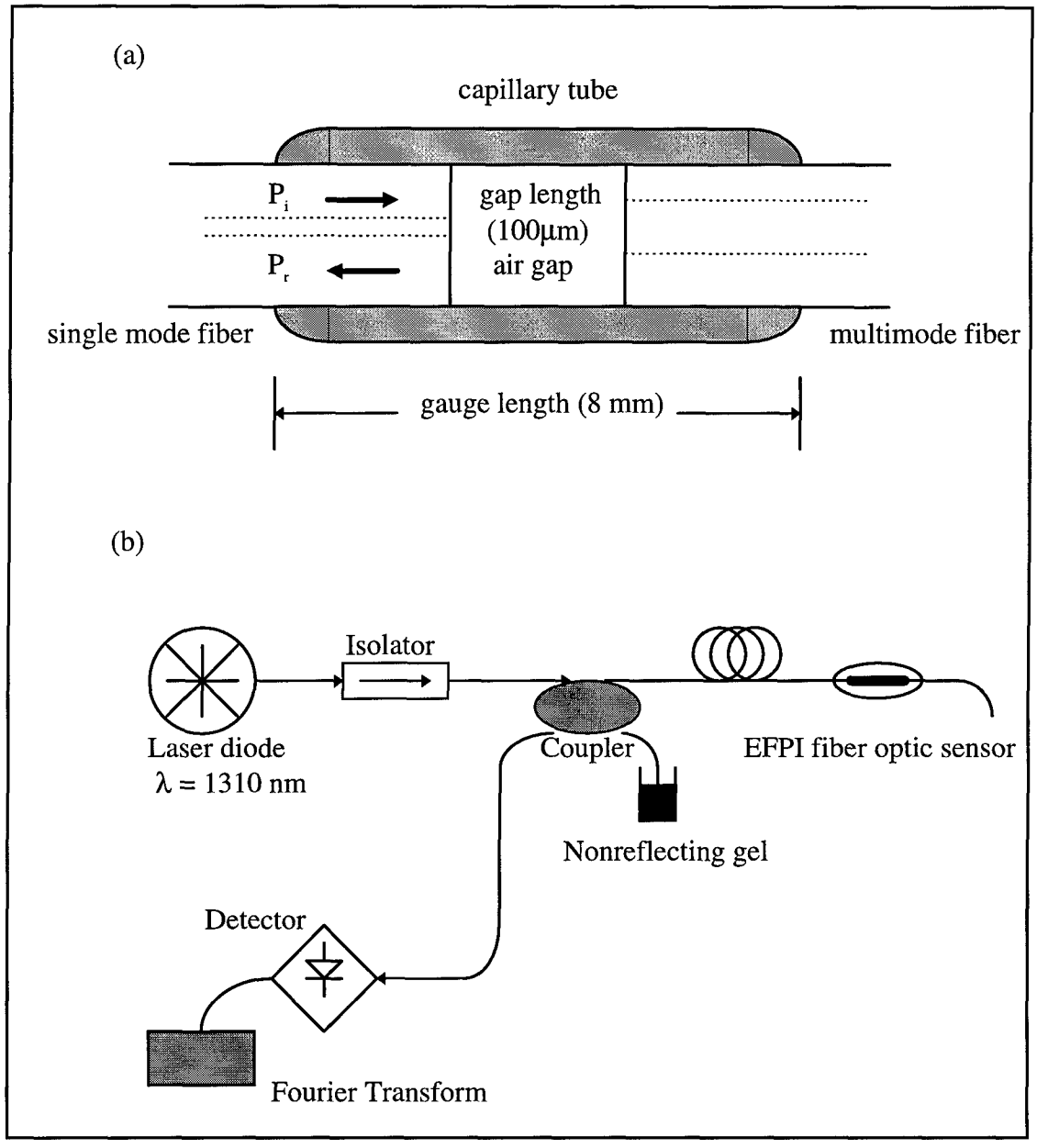

Figure 1. EFPI fiber optic modal frequency sensor. (a) EFPI fiber optic sensor. (b) Fiber optic support system.

The schematic of this source/detector support system for the EFPI fiber optic sensors is displayed in Figure 1(b). A laser source provides the input light beam into the single mode fiber. A coupler branches the reflected interference fringes to a detector.

The reflected optical fringe response of the EFPI fiber optic modal frequency sensor is converted into electrical signals by a fast response detector. The modal frequency content of the electrical signal is obtained by a Fourier transform unit, which is a spectrum analyzer is used in this study.

3. Piezoelectric Ceramic Sensors and Actuators. The piezoelectric effect refers to the conversion of applied mechanical stress in a piezoelectric material into electric field [3]. An applied electric field can also produce mechanical stress in the material. Sensing is based on the first case and actuation on the latter. A material must be anisotropic and electrically poled in order for the piezoelectric effect to occur [3].

The response of a piezoelectric material is determined by:

$$\mathbf{D} = d\mathbf{X} + \varepsilon_r \varepsilon_0 \mathbf{E} \tag{5}$$

and

$$\mathbf{x} = s\mathbf{X} + d\mathbf{E} \tag{6}$$

where **D** is the electric displacement vector, **E** is the electric field vector, ε_r is the relative dielectric constant, ε_0 is the free space dielectric constant, **X** is the stress applied to the material, **x** is the strain, s is the mechanical compliance at a particular value of E, and d is the piezoelectric strain coefficient. **D**, **X**, **x**, and **E** are vectors and d, s, ε_r are tensors. By rearranging equations (5) and (6) and assuming **D** is constant, the strain becomes:

$$\mathbf{x} = \{d - [(s\varepsilon_r\varepsilon_0)/d]\}\mathbf{E}. \tag{7}$$

In this study, identical PZT ceramic patches were used as sensors and actuators. However, a major difference exists between using PZT ceramic material as a sensor and as a actuator. PZT ceramic material converts strain into small electric fields, typically kilovolts/meter, for sensor applications. For actuator applications the electric field must

be very large, approximately 1 megavolt/meter, to produce a mechanical strain (50 GPa to 100 GPa). Typically strain levels that can be applied by PZT ceramic actuators are 0.1%.

B. COMPOSITE MATERIAL FABRICATION

Two 27.94 cm x 27.94 cm glass/epoxy composite plates were fabricated in the Composite Fabrication Laboratory at the University of Missouri-Rolla. The plates were eight layer symmetric laminates $[0/90/0/90]_s$. The lamina orientation can be seen in Figure 2. The material properties of the composite plates are the following: E_{11} = 42.34 GPa, E_{22} = 11.72 GPa, G_{12} = 7.10 GPa, ν_{12} = 0.27, and ρ = 1901.5 kg/m^3, where E_{11} and E_{22} are the principal moduli, G_{22} is the shear modulus, ν_{12} is the Poisson ratio, and ρ is the density. The plates were fabricated using a 75 ton Drake Model #44-806 hydraulic hot press. The fabrication curve used to control the hot press during plate fabrication can be seen in Figure 3. The plain solid line is the manufacturer's recommended fabrication curve. The squares are the actual temperatures measured by the hot press during plate fabrication. A diamond saw was used to cut the first plate into beams 27.94 cm long, 2.54 cm wide, and 0.18 cm thick. Teflon strips, 0.005 cm thick, were inserted in the midplane of the second composite plate before fabrication. The delamination placement can be seen in figure 4. The plate was then cut into ten beams 27.94 cm long, 2.33 cm wide, and 0.15 cm thick. The beams contained 0 cm, 1.27 cm, 2.54 cm, 3.81 cm, 5.08 cm, and 6.35 cm delaminations, respectively, located at the center of the beam.

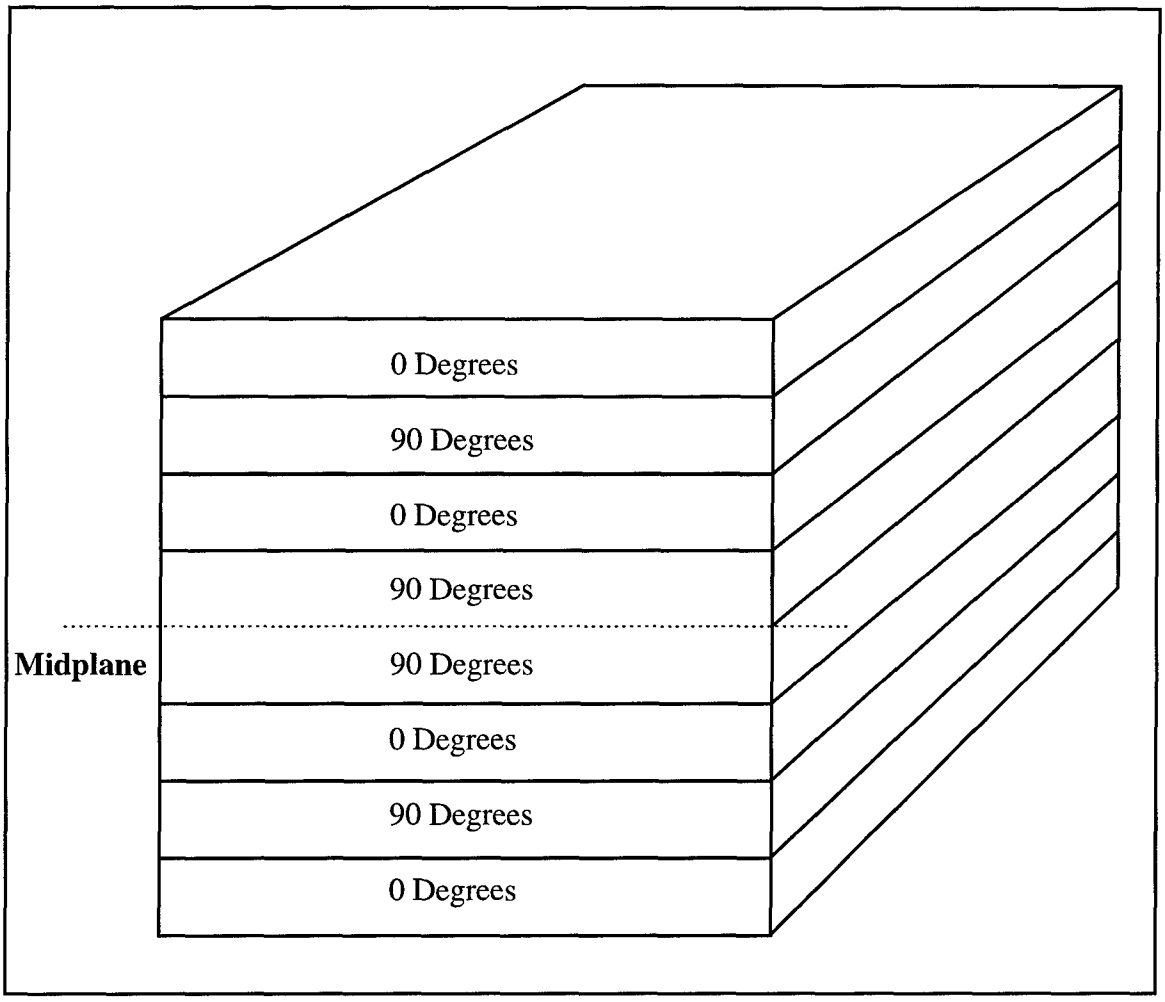

Figure 2. Orientation of composite lamina.

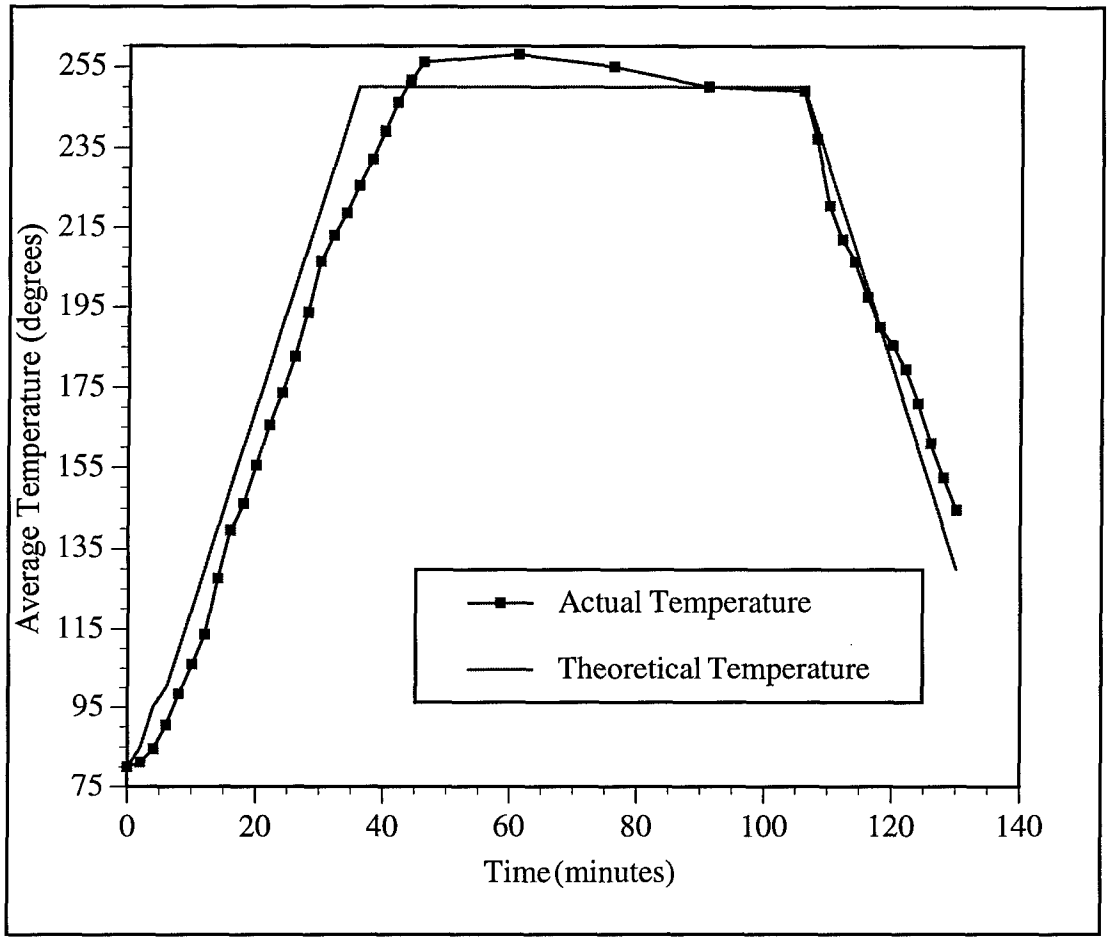

Figure 3. Heating and cooling curve for the glass/epoxy composite plate fabrication.

C. COMPOSITE MATERIAL ANALYSIS

Classical beam theory approximation is a one-dimensional model used to evaluate the effects of delamination position and size on the beam natural frequencies [28]. The formulation is based on a constrained vibration model with the assumption of infinitesimal and identical transverse displacements of the upper and lower sublaminates. The model allows for independent extensional and bending stiffness and does not include bending/extensional coupling stiffness terms. Therefore this model works best for symmetric laminates. Figure 4 represents the delamination model of a beam of unit

width, thickness h, and length L. Delamination is assumed to be uniform across the width of the beam. The delamination has length l_2 and goes from $x = l_1$ to $x = l_1 + l_2$ parallel to the neutral axis and at a distance of h_2 from the upper surface of the beam.

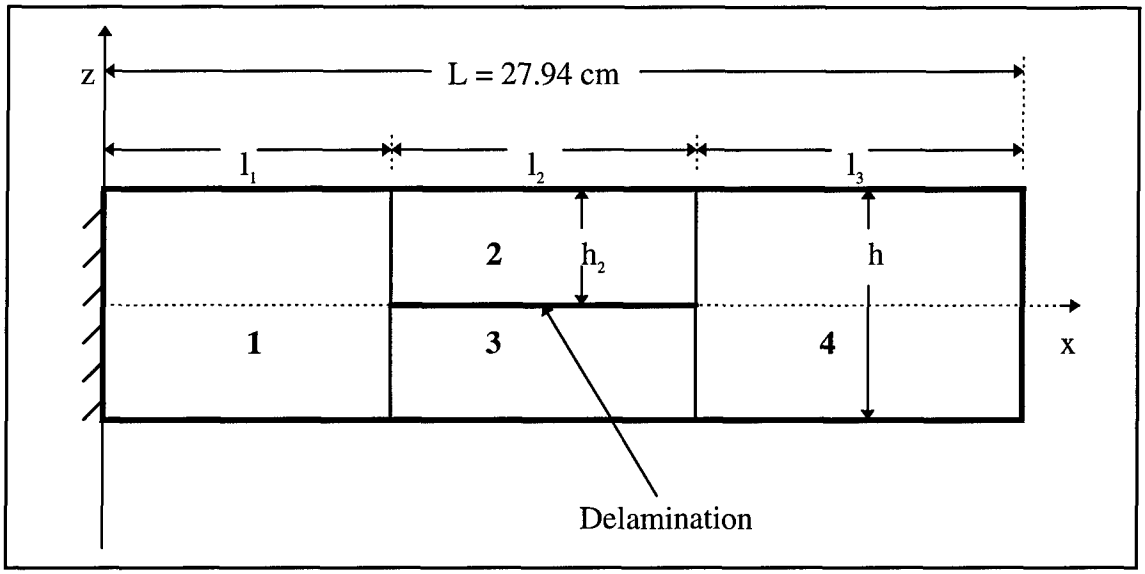

Figure 4. Cantilever composite beam with prescribed delamination location. Segments 1and 4 are the base laminates and segments 2 and 3 are sublaminates above and below the prescribed delamination.

The delaminated beam is divided into four sections (see figure 4) and each segment is characterized by an extensional stiffness A_i, a bending stiffness D_i, and a mass density per unit length m_i. The governing differential equations for each segment are the following:

$$D_i \frac{d^4 w_i}{dx^4} - m_i \omega^2 w_i = 0 \tag{5}$$

and

$$\frac{dP_i}{dx} = A_i \frac{d^2 u_i}{dx^2} = 0 \tag{6}$$

where u_i and w_i are axial and transverse deflections and P_i is the axial force in each segment (note $P_1 = P_4 = 0$). The solution to equations (5) and (6) has the form:

$$w_i = C_{i1}\cosh(kx) + C_{i2}\sinh(kx) + C_{i3}\cos(kx) + C_{i4}\sin(kx) \tag{7}$$

and

$$u_i = B_{i0} + B_{i1}x \tag{8}$$

where k is

$$k^4 = \frac{m_i \omega^2}{D_i} \tag{9}$$

for i = 1,2,3,4. There are 20 unknown constants in Equations (7) and (8). However, the deflections of segments 2 and 3 are forced to vibrate together by setting $C_{21} = C_{31}$, $C_{22} = C_{33}$, $C_{23} = C_{33}$, and $C_{24} = C_{34}$. These constraints are for analysis of midplane delaminations. Therefore only 16 boundary and continuity conditions are needed for the 16 remaining unknowns in Equations (7) and (8). For a cantilever beam, one end of the beam is clamped and the other end is freely vibrating. The 16 geometric boundary, continuity, moment balance, shear force balance, and compatibility for axial midplane displacements conditions are thereby set. These conditions yield 16 homogeneous equations with 16 unknowns. The 16 coupled equations can be seen in Appendix A, program Delam.m. In matrix form the equations are:

$$[Q_{ij}(k)][V_j] = [0] \tag{10}$$

where $Q_{ij}(k)$ are the coefficients of the unknown constants and V_j are the elements of a column vector containing the unknown constants. The expressions for the 256 constants in Equation (10) are given elsewhere [29]. For a non-trivial solution, the determinant of the coefficient matrix $Q_{ij}(k)$ must equal zero. Using MATLAB the expressions are

symbolically derived for the 256 constants as a function of k and other beam parameters. Numerically the determinant of $Q_{ij}(k)$ is calculated for different values of k. If there is a sign change in the determinant of $Q_{ij}(k)$ for two adjacent values of k, then the determinant of $Q_{ij}(k)$ has a root in between these two adjacent values. The root is accurately determined by repeated bisection of the interval between the two adjacent k values (Appendix A, program Final.m). The modal frequencies are then found using equation (9). The bending/extensional coupling is not allowed in this model.

The finite element model discussed in this study was used to determine the theoretical modal frequencies for an undamaged glass/epoxy composite beam. Free vibrations of clamped composite beams based on the classical theory which neglects the effects of transverse shear deformation and rotary inertia have been considered to determine the five modal frequencies of a glass/epoxy beam [36,37]. For a symmetric cantilever composite beam the equation for the modal frequencies is:

$$f_n = \frac{k_n L}{2\pi L^2}\sqrt{\frac{D_{11}}{\rho A}} \tag{11}$$

where L is the length, A is the cross-sectional area, ρ is the mass density, and D_{11} is the flexural stiffness of the laminated composite beam. The mode parameter k_n satisfies the following equation:

$$\cos(k_n L)\cosh(k_n L) + 1 = 0. \tag{12}$$

First-order shear deformation and rotary inertia should be included for more accurate vibration analysis of laminated composite beams [38]. In this study the results from a finite element model based on a higher order shear deformation theory are also used [32]. Results can be seen in Appendix C. The finite element model accounts for the

effects of in-plane inertia and rotary inertia in the formulation of the mass matrix. Also the Poisson effect is incorporated in the formulation of the beam constitutive equation.

Lagrange linear interpolation functions and Hermite cubic interpolation functions are used to interpolate the generalized displacements. The element equation after assembling the elements becomes:

$$([K] - \omega^2[M])\{\Delta\} = 0 \tag{13}$$

where [K] is the element stiffness matrix, [M] is the mass matrix, ω is the angular frequency, and $\{\Delta\}$ is the mode shape. Equation (13) can be solved after imposing the boundary conditions. The natural frequencies of a cantilever composite beam are the object in this study. Therefore the boundary conditions are:

$$u = 0, w = 0, \phi = 0 \tag{14}$$

for the clamped edge. Using the results from a Fortran finite element code, natural frequency solutions are obtained for the free vibration of laminated composite beams.

IV. EXPERIMENTAL PROCEDURES

A. FREQUENCY RESPONSE TESTING

Two 27.94 cm x 27.94 cm glass/epoxy composite plates were fabricated with an eight layer symmetric laminate structure $[0/90/0/90]_{2S}$. The first plate was cut into beams 27.94 cm x 2.54 cm x 0.18 cm which contained no delaminations. Teflon strips, 0.005 cm thick, were inserted in the midplane of the second composite plate. This plate was then cut into ten beams 27.94 cm long, 2.33 cm wide, and 0.15 cm thick. The beams contained 0 cm, 1.27 cm, 2.54 cm, 3.81 cm, 5.08 cm, and 6.35 cm delaminations respectively located at the center of the beam.

Figure 5 shows the experimental setup. A PZT ceramic patch, for use as an actuator, was bonded to the underside of the each beam 3.81 cm from one end. Eccobond 57 C Conductive Epoxy was used to bond the PZT ceramic patch to copper foil. The foil was then attached to the beam using general purpose Super Glue. A second PZT ceramic patch, for use as a sensor, was bonded in the same manner 2.54 cm from the opposite end of two different undamaged beams and the 5.08 cm delaminated beam. An extrinsic Fabry-Perot fiber optic sensor (EFPI) was mounted 2.54 cm from the end of each beam using Super Glue. Each beam was clamped 1.91 cm from the end closest to the actuating PZT ceramic patch. The cantilever beam length was 26.04 cm.

An HP35665A spectrum analyzer was programmed to produce a sine sweep ranging from 1 Hz to 1000 Hz, with an entry step size of 0.1 Hz, a resolution of 801 points per sweep, and a source voltage of 1 V_p. Trial and error were used to determine the settings that produced the best results. The output signal was amplified with a Piezo

Systems, Inc. piezo amplifier, model 60.101. The amplifier was connected to the actuating PZT ceramic patch. The EFPI fiber optic sensor was connected to a fiber optic support system using a butt coupler and index matching gel. The fiber optic support system, model FOSS-1300-2, was manufactured by the F&S Fiber Sensor Technologies. The fiber optic support system contains a laser diode (λ=1300 nm), an optical isolator, a 3 dB fiber coupler, and a high speed photodetector as seen in Figure 1. The fiber optic support system and the PZT ceramic sensor output signals were connected to the inputs of the spectrum analyzer (see Figure 5). The actual experimental setup can be seen in the photograph in Figure 6.

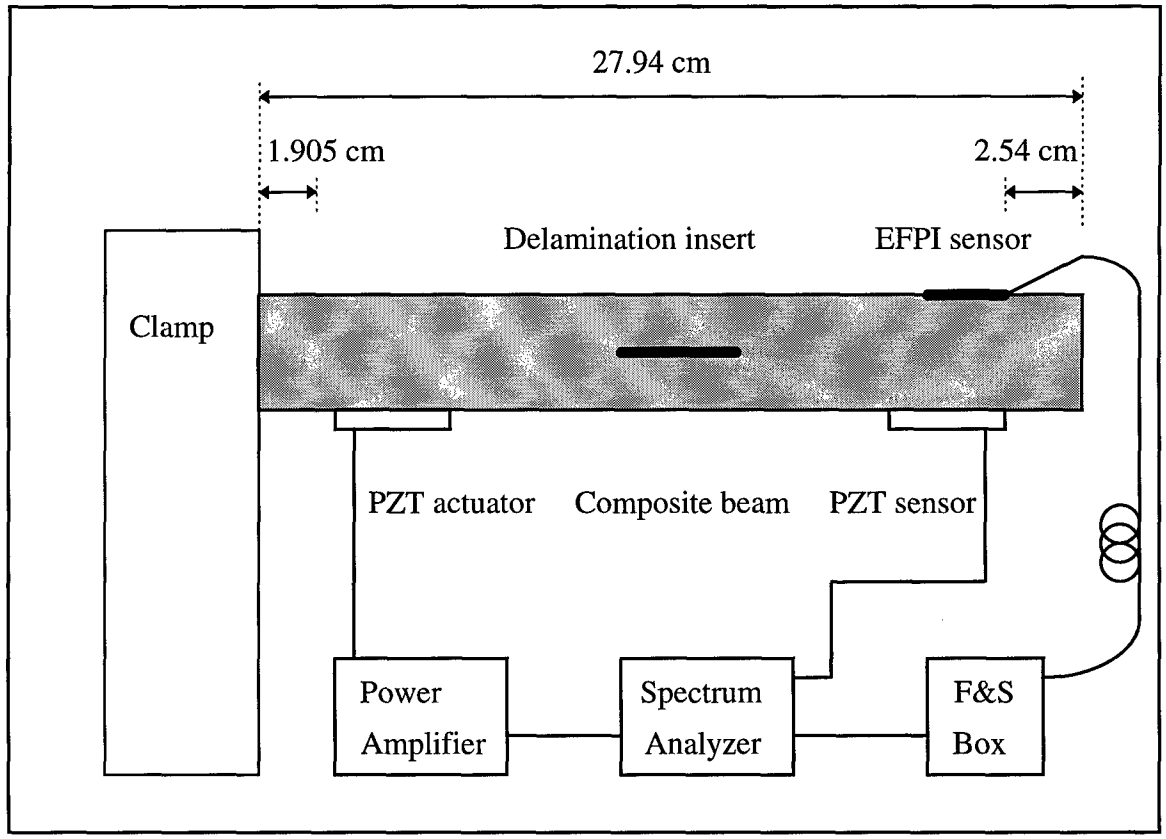

Figure 5. Experimental setup for determining modal frequencies in a cantilever composite beam.

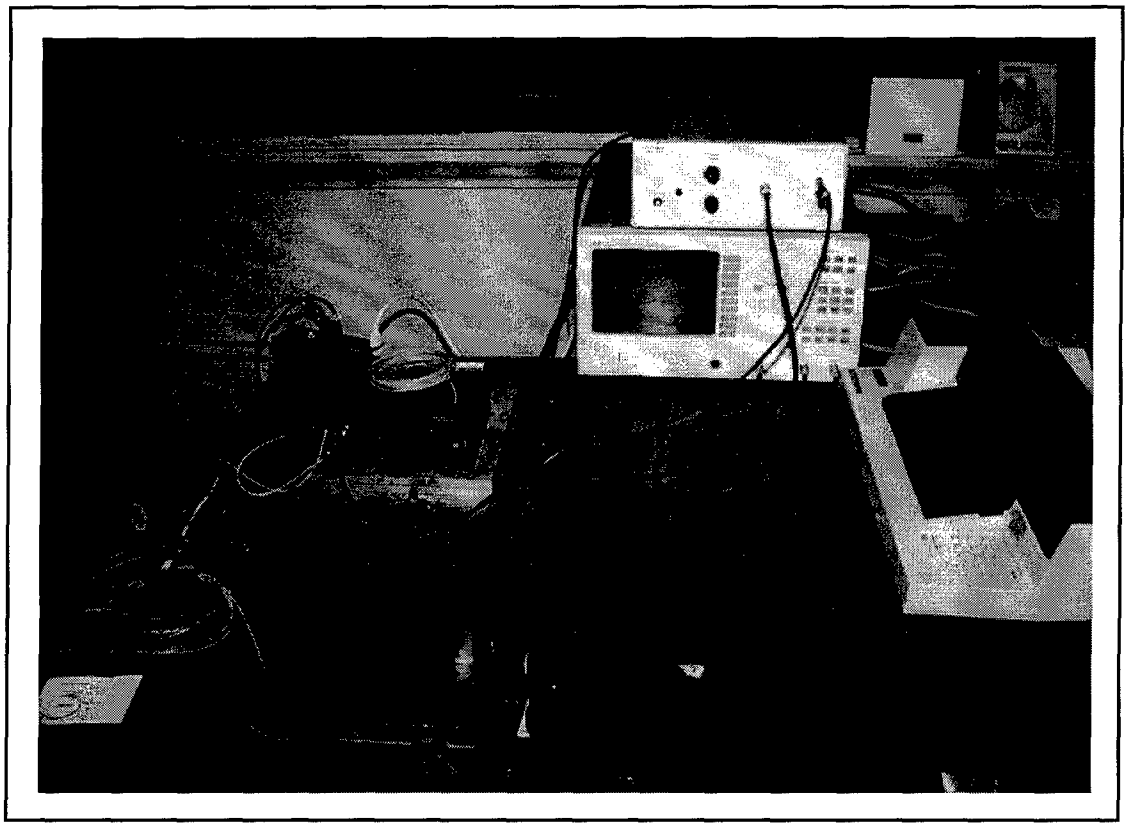

Figure 6. Actual photograph of the experimental setup. The composite beam containing a PZT ceramic actuator and a EFPI fiber optic sensor is at the far left of the picture. Next to the beam is the fiber optic support system (F&S box). The spectrum analyzer is on the table with the piezo amplifier on top of it. The plotter is to the far right.

The sine sweep was initiated using the spectrum analyzer and the amplifier. The output signals from the fiber optic support system and the PZT ceramic patch were collected by the spectrum analyzer in the frequency domain, and the first five modal frequencies were determined and plotted. Both undamaged and delaminated glass/epoxy cantilever beams were tested and the modal frequencies were successfully found. The experimental modal frequencies were verified with calculated modal frequencies obtained from classical beam theory and from the finite element model.

B. NEURAL NETWORK SETUP

A backpropagation neural network with one input layer, three hidden layers, and one output layer was used to predict delamination size and delamination location. There are no established procedures for choosing the optimal number of hidden layers and processing elements per layer. Incorporation of more processing elements enhances the generalization capability of the network for a larger number of training data points. The input layer has five processing units and each corresponds to one of the first five modal frequencies calculated using MATLAB simulations based on classical beam theory. The first hidden layer has four processing elements (neurons), the second hidden layer has five processing elements, and the third hidden layer has four processing elements. The output layer consists of two processing elements. The network predicts delamination size and delamination location. NeuralWorks Professional II software was used to design, train, and test the neural network on a Pentium 133 MHz personal computer. A basic schematic of the neural network is shown in Figure 7.

In this study the hyperbolic tangent function was used as the activation (transfer) function. Training consisted of providing a set of 1066 calculated input modal frequencies and output delamination size and delamination location to the network. Each input set consisted of five modal frequencies for each delamination size. The delamination sizes ranged from zero to 20.22 cm. There were two to ten delamination locations for each delamination size. The number of delamination locations depended on delamination size because delaminations cannot exceed the beam length. The network iteratively adjusted the weights of each of the nodes to obtain the desired outputs. The normalized cumulative delta rule is used to train the network. During the backward

propagation, weights in nodes were adjusted based on the errors using the gradient descent equation [39].

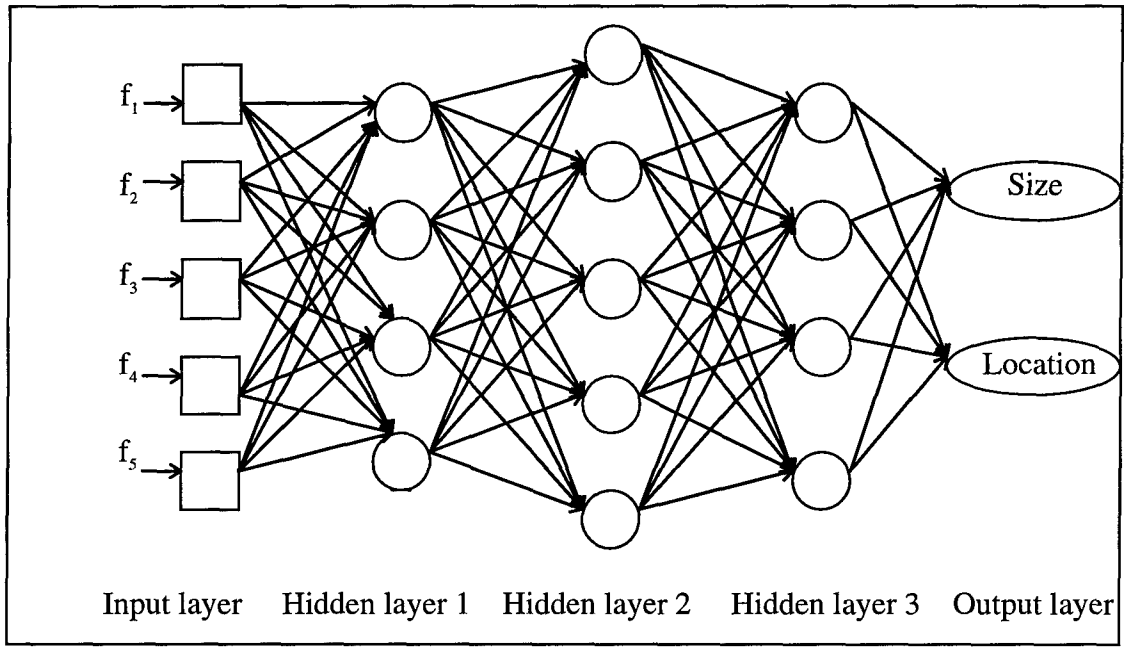

Figure 7. A feed forward, backpropagation neural network with five inputs and two outputs.

To optimize the performance of the network, learning rate and momentum coefficients can be adjusted. Among the neural network parameters, learning rate and momentum coefficients are the critical variables that effect the convergence of the network. The learning rate started at 0.5 and was reduced as iterations increased and the momentum coefficient started at 0.3. The initial learning rate and momentum coefficients were chosen after several trials to find optimum performance.

At the beginning of the training, the network produced outputs which most likely differ from the desired values. The procedure was repeated until the difference between the desired and actual outputs was reduced to a preset convergence limit. The training

was stopped after 160,000 cycles. The root-mean-squared error converged to 0.0005 at approximately 100,000 cycles. After 100,000 cycles, the root-mean-squared error varied from 0.0005 to 0.1. The root-mean-squared error stayed at approximately 0.0005 until single error spikes of 0.1 would appear. The spikes were nonperiodic and did not occur very often. These spikes were assumed to be point errors and were neglected. Therefore, the system converged. The network simulation took about 90 seconds to complete on a Pentium 133 MHz personal computer.

V. EXPERIMENTAL RESULTS

A. COMPSITE BEAM MODAL FREQUENCIES

Figure 8 shows the experimental frequency response of an undamaged composite beam. The response functions were generated using a curve fitting procedure built into the HP35665A spectrum analyzer. Each peak corresponds to a modal frequency of the beam. Figure 8(a) is the response from the EFPI fiber optic sensor while Figure 8(b) is the response of the PZT ceramic sensor.

As described earlier, both classical beam theory and a finite element method were used to calculate modal frequencies of the undamaged test beam. Table I compares the experimental frequencies with those obtained from the classical theory and the finite element model. Experimental modal frequencies are in better agreement with the calculated modal frequencies from the classical beam theory than with those from the finite element model. The calculated difference in modal frequencies between the finite element model and the classical beam theory is also shown in Table I. For high modes there is less difference between the modal frequencies calculated from the finite element model and classical beam theory.

The effect of the beam width on modal frequencies was also observed. Two undelaminated beams, one having a width of 2.54 cm and the other having a width of 2.33 cm, were tested. As stated earlier, Figure 8 is the frequency response of the 2.33 cm wide beam. Figure 9 is the frequency response for the 2.54 cm wide beam. Again, the frequencies are identical for the EFPI fiber optic sensor and the PZT ceramic sensor. The peaks, or modal frequencies, of the two different beams shifted with the change in width.

Table II shows the result of the modal testing. The average difference between the modal frequencies of the two beams is 12.9%. However, the average difference in the finite element code between a 2.54 cm beam and a 2.33 cm beam is 26.2%. Also, the average difference in the modal frequencies of the two beams calculated by the classical beam theory is 20.7%.

Table I: Experimental modal frequencies of an undamaged beam compared to MATLAB generated frequencies of classical beam theory and frequencies calculated using a finite element model (FEM).

Modal Frequencies	Experiment (Hz)	Classical Theory (Hz)	Difference Exp-Theory	Finite Element (Hz)	Difference Exp-FEM	Difference Theory-FEM
1	13.5	16.7	19.2%	15.3	11.7%	8.4%
2	88.4	100.8	12.3%	96.2	8.1%	4.5%
3	250.8	282.1	11.1%	270.8	7.4%	4.0%
4	491.8	552.9	11.0%	534.9	8.1%	3.3%
5	815.2	913.9	10.8%	893.1	8.7%	2.3%

Table II: Comparison of modal frequencies of two composite beams having different widths.

Modal Frequencies	2.54 cm Wide Beam (Hz)	2.33 cm Wide Beam(Hz)	Difference	Difference in FEM	Difference in Theory
1	12.2	13.5	9.6%	26.1%	23.3%
2	75.9	88.4	14.1%	26.2%	20.1%
3	213.3	250.8	14.9%	26.2%	20.1%
4	425.5	491.8	13.5%	26.2%	20.1%
5	714.0	815.2	12.4%	26.2%	20.1%

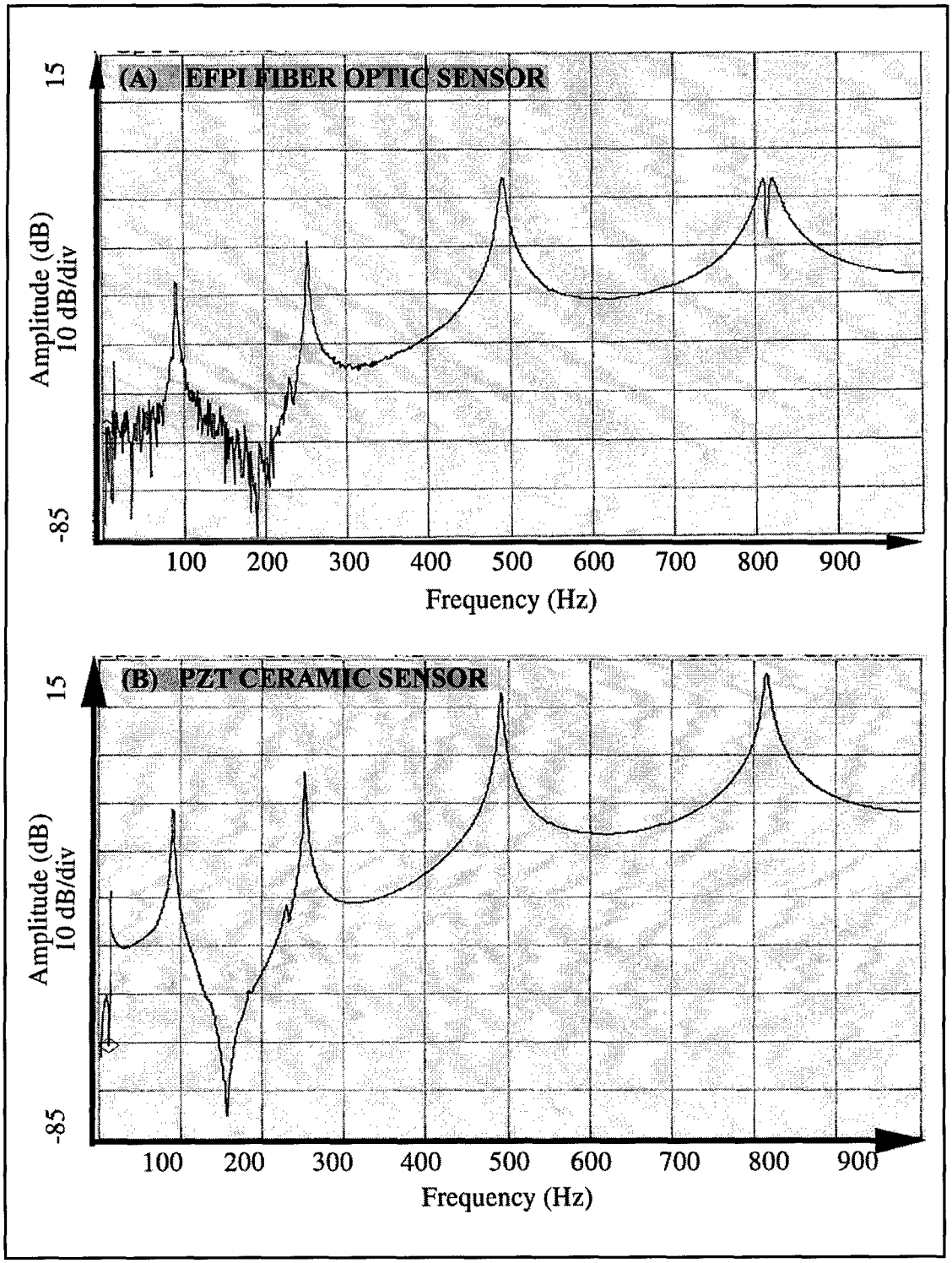

Figure 8. Frequency response of (a) an EFPI fiber optic sensor and (b) a PZT ceramic sensor mounted on an undamaged glass/epoxy beam. The beam is 2.33 cm wide.

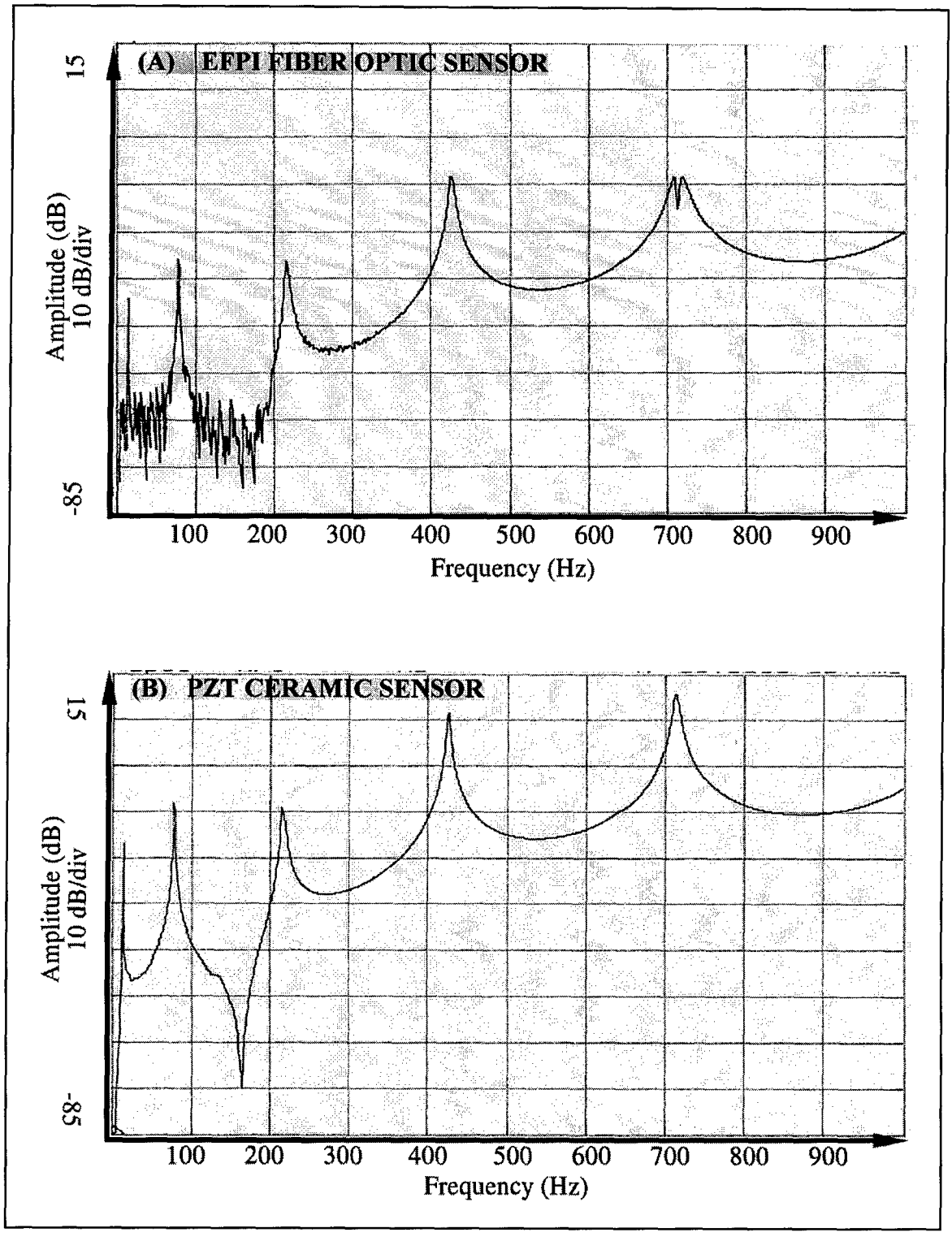

Figure 9. Frequency response of (a) an EFPI fiber optic sensor and (b) a Pzt ceramic sensor mounted on an undamaged glass/epoxy beam. The beam is 2.54 cm wide.

B. DELAMINATED COMPOSITE BEAM MODAL FREQUENCIES

The five delaminated composite beams were tested after the two undamaged beams. Figure 10 shows the frequency response of a EFPI fiber optic sensor and a PZT ceramic sensor mounted on beam containing a 5.08 cm delamination incorporated into the midplane. Again the modal frequencies were identical for both sensors. Figure 11 through Figure 14 show the frequency responses of beams with 1.27 cm, 2.54 cm, 3.81 cm, and 6.35 cm delaminations respectively.

The experimental values for the modal frequencies are found in Table III. Examination of Figure 8 and Figures 10 through 14 reveal the modal frequencies of the delaminated beams are shifted. Table III summaries these shifts in modal frequencies for the 2.33 cm wide undamaged beam and the five different delaminated beams.

Table III: Experimental modal frequencies of delaminated composite beams.

Modal Frequencies	Undamaged (Hz)	1.27 cm Delam (Hz)	2.54 cm Delam (Hz)	3.81 cm Delam (Hz)	5.08 cm Delam (Hz)	6.35 cm Delam (Hz)
1	13.5	17.2	15.9	15.9	13.5	14.7
2	88.4	93.4	95.9	98.4	94.7	94.7
3	250.8	256.9	260.7	254.5	233.4	210.8
4	491.8	502.9	515.5	527.9	519.2	490.5
5	815.2	835.1	818.9	750.3	684.1	621.6

The experimental modal frequencies for each delamination size listed in Table III were compared to the calculated classical beam theory modal frequencies found in Appendix B. Table IV show the results of this comparison. A percent difference was

also calculated. The percent difference ranges from zero to 16.5% with an average difference of 5.6%.

Table IV: Comparison of experimental and classical beam theory modal frequencies for different delamination sizes.

Delamination Size (cm)	Modal Frequencies	Experiment (Hz)	Classical Theory (Hz)	Difference
1.27	1	17.2	15.8	8.9%
	2	93.4	94.4	1.0%
	3	256.9	280.9	8.5%
	4	502.9	524.4	4.1%
	5	835.1	901.7	7.4%
2.54	1	15.9	15.6	2.3%
	2	95.9	90.4	6.1%
	3	260.7	273.1	4.5%
	4	515.5	508.4	1.4%
	5	818.9	828.6	1.2%
3.81	1	15.9	15.3	4.3%
	2	98.4	86.8	13.4%
	3	254.5	254.4	0.0%
	4	527.9	494.4	6.8%
	5	750.3	724.3	3.6%
5.08	1	13.5	15.0	10.2%
	2	94.7	83.8	12.9%
	3	233.4	228.9	1.9%
	4	519.2	486.5	6.7%
	5	684.1	661.1	3.5%
6.35	1	14.7	14.4	2.2%
	2	94.7	81.3	16.5%
	3	210.8	203.1	3.8%
	4	490.5	465.4	5.4%
	5	621.6	638.8	2.7%

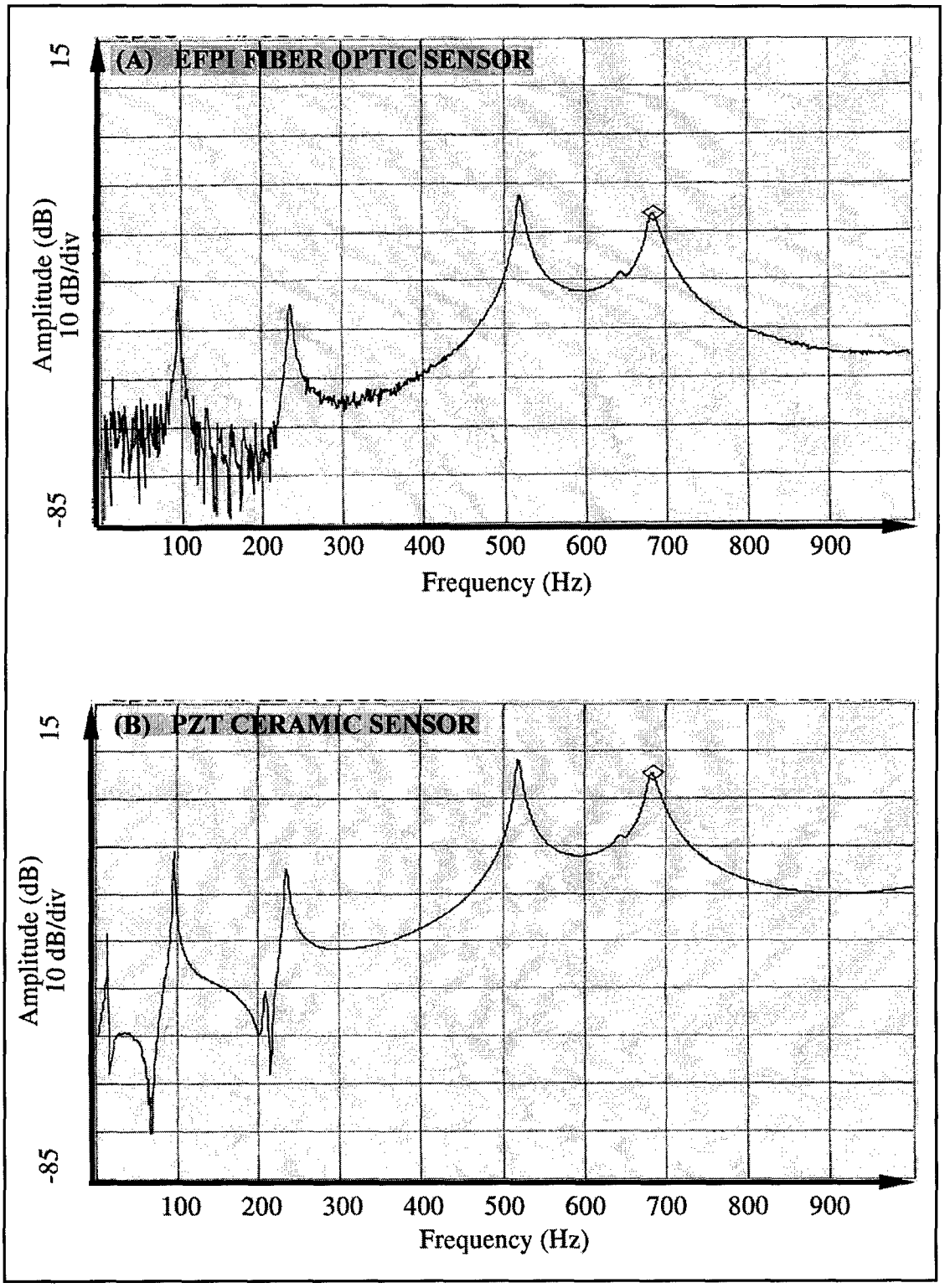

Figure 10. Frequency response of (a) an EFPI fiber optic sensor and (b) a PZT ceramic sensor mounted on glass/epoxy beam containing a 5.08 cm delamination.

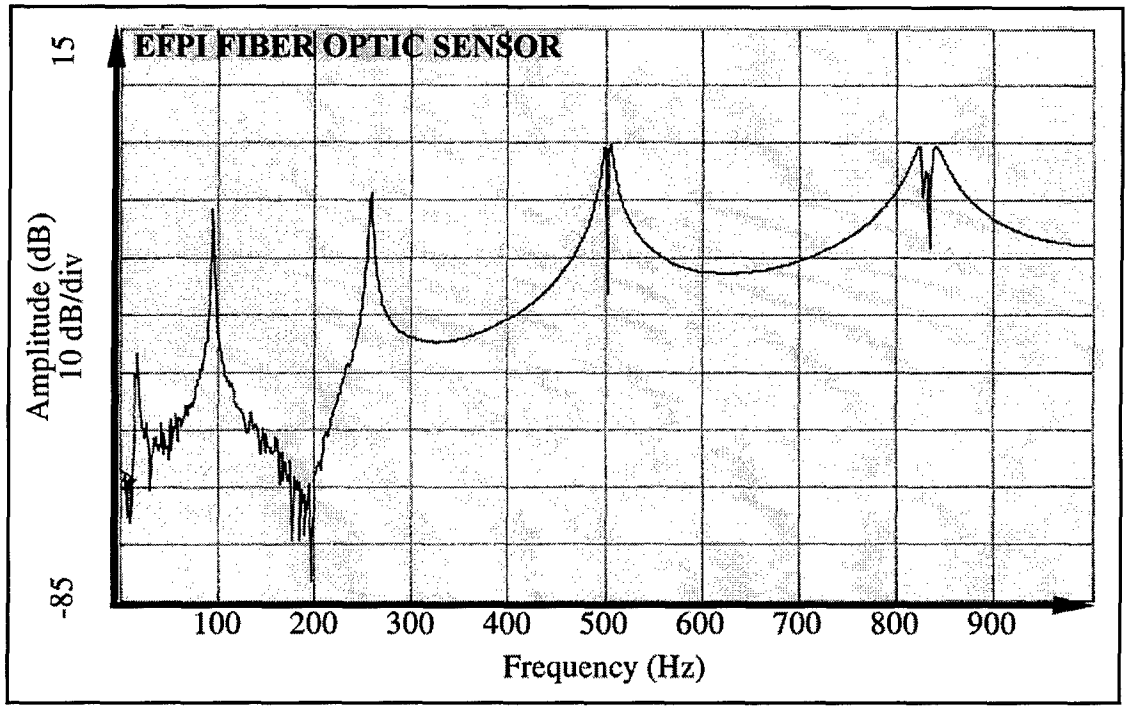

Figure 11. Frequency response of an EFPI fiber optic sensor mounted on a glass/epoxy beam containing a 1.27 cm delamination.

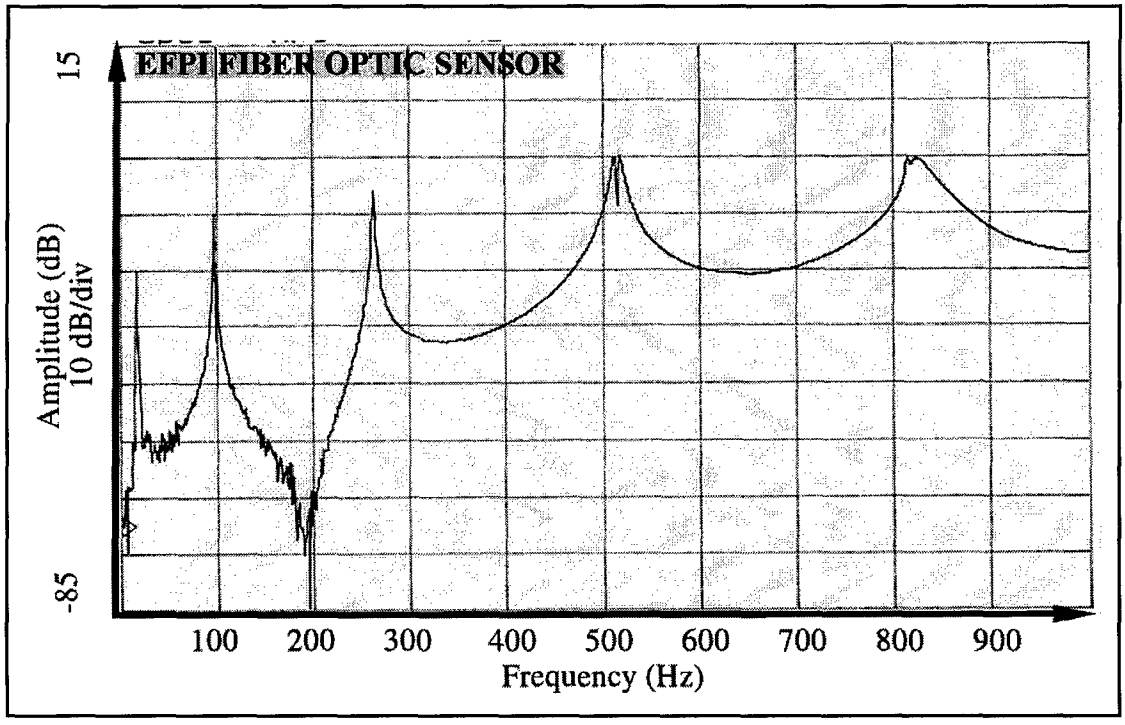

Figure 12. Frequency response of an EFPI fiber optic sensor mounted on a glass/epoxy beam containing a 2.54 cm delamination.

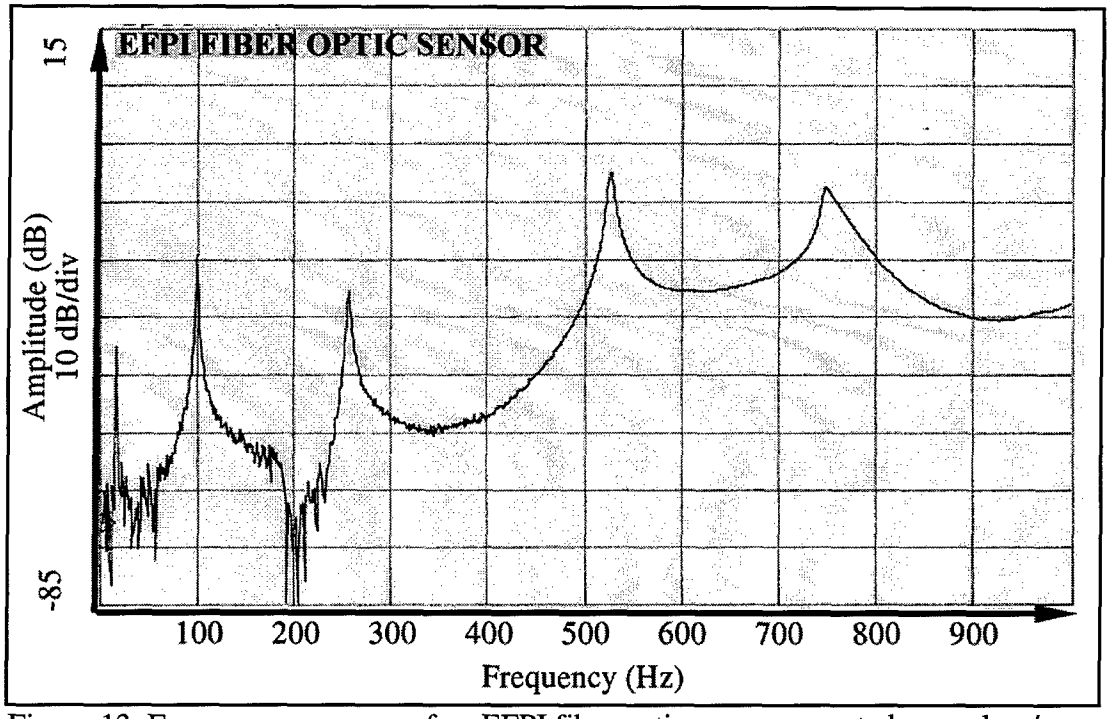

Figure 13. Frequency response of an EFPI fiber optic sensor mounted on a glass/epoxy beam containing a 3.81 cm delamination.

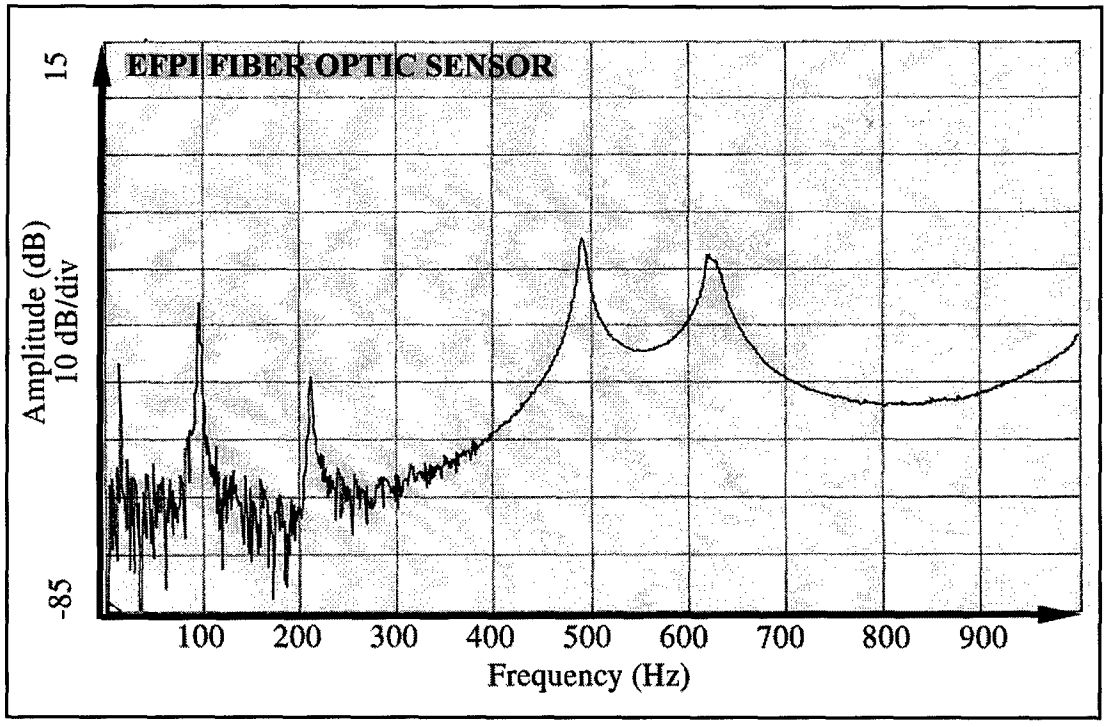

Figure 14. Frequency response of an EFPI fiber optic sensor mounted on a glass/epoxy beam containing a 6.35 cm delamination.

C. NEURAL NETWORK RESULTS

The neural network used in this experiment was discussed in Section IV. Figure 15 shows the variation of the actual modal frequencies used to test the network for the five different delamination sizes: 1.27 cm, 2.54 cm, 3.81 cm, 5.08 cm, and 6.35 cm. Each delamination was incorporated into the midplane in the center of the beam. The modal frequencies are normalized to a maximum of 100%. Figure 16 shows the variation of modal frequencies predicted by the neural network for the five different delamination sizes. Table V confirms that the data in Figure 15 and Figure 16 are in good agreement. Table V compares the experimental delamination sizes to the predicted neural network delamination sizes. The average error of the neural network delamination size predictions was 5.9%. The error values ranged from 0.9% to 10.7%.

Table V: Experimental delamination size compared to predicted neural network delamination size.

Experimental Delamination Size (cm)	Neural Network Prediction (cm)	Percent Error
1.27	1.29	1.2%
2.54	2.81	10.6%
3.81	4.22	10.7%
5.08	5.40	6.3%
6.35	6.41	0.9%

The neural network was also used to predict delamination location. In neural network simulations, four randomly selected delamination locations for each of the five delamination sizes were used tested. The values for the predicted delamination locations

are shown in Table VI. The average error between the actual delamination location and the neural network predicted delamination location was 4.7%. The error values were evenly distributed ranging from zero percent to 13.9%.

Table VI: Experimental delamination location compared to predicted neural network delamination location.

Actual Size (cm)	Actual Location (cm)	Predicted Location (cm)	Percent Error
1.27	3.18	3.20	0.6%
	11.11	10.92	1.7%
	13.02	11.76	9.7%
	17.40	17.65	1.4%
2.54	5.46	6.22	13.9%
	13.02	13.32	2.3%
	15.94	16.55	6.3%
	20.13	19.42	3.5%
3.81	8.19	9.12	11.3%
	13.02	13.74	5.5%
	16.57	17.15	3.5%
	18.67	19.33	3.5%
5.08	8.83	8.83	0.0%
	13.02	13.54	4.1%
	14.85	15.55	4.7%
	15.11	15.07	0.3%
6.35	5.27	5.74	8.9%
	13.02	12.52	3.8%
	17.84	17.88	0.0%
	19.94	19.71	1.2%

Figure 17 shows that the normalized modal frequencies are relatively constant with different delamination locations for a 2.54 cm delamination size. Again, Figure 18 shows that the neural network predicted delamination locations are in good agreement with the actual delamination location for a 2.54 cm delamination size (see figure 17). However, figure 19 shows that the normalized modal frequencies change with different delamination locations for a 6.35 cm delamination. Comparing figure 19 and figure 20 confirms that the neural network predicted delamination locations agree with the actual delamination location for a 6.35 cm delamination size.

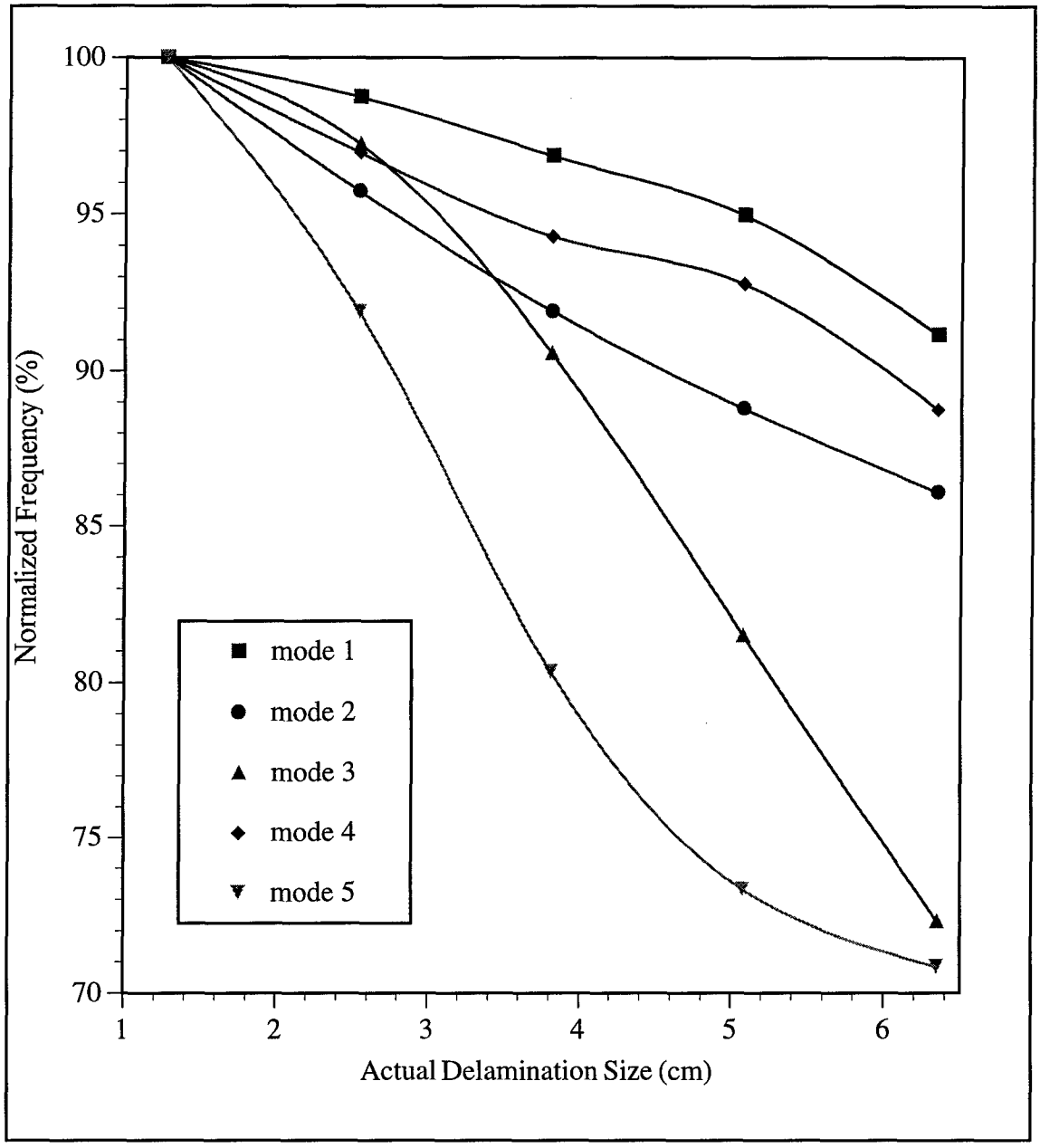

Figure 15. Actual modal frequencies of a glass/epoxy composite beam for five prescribed delamination sizes.

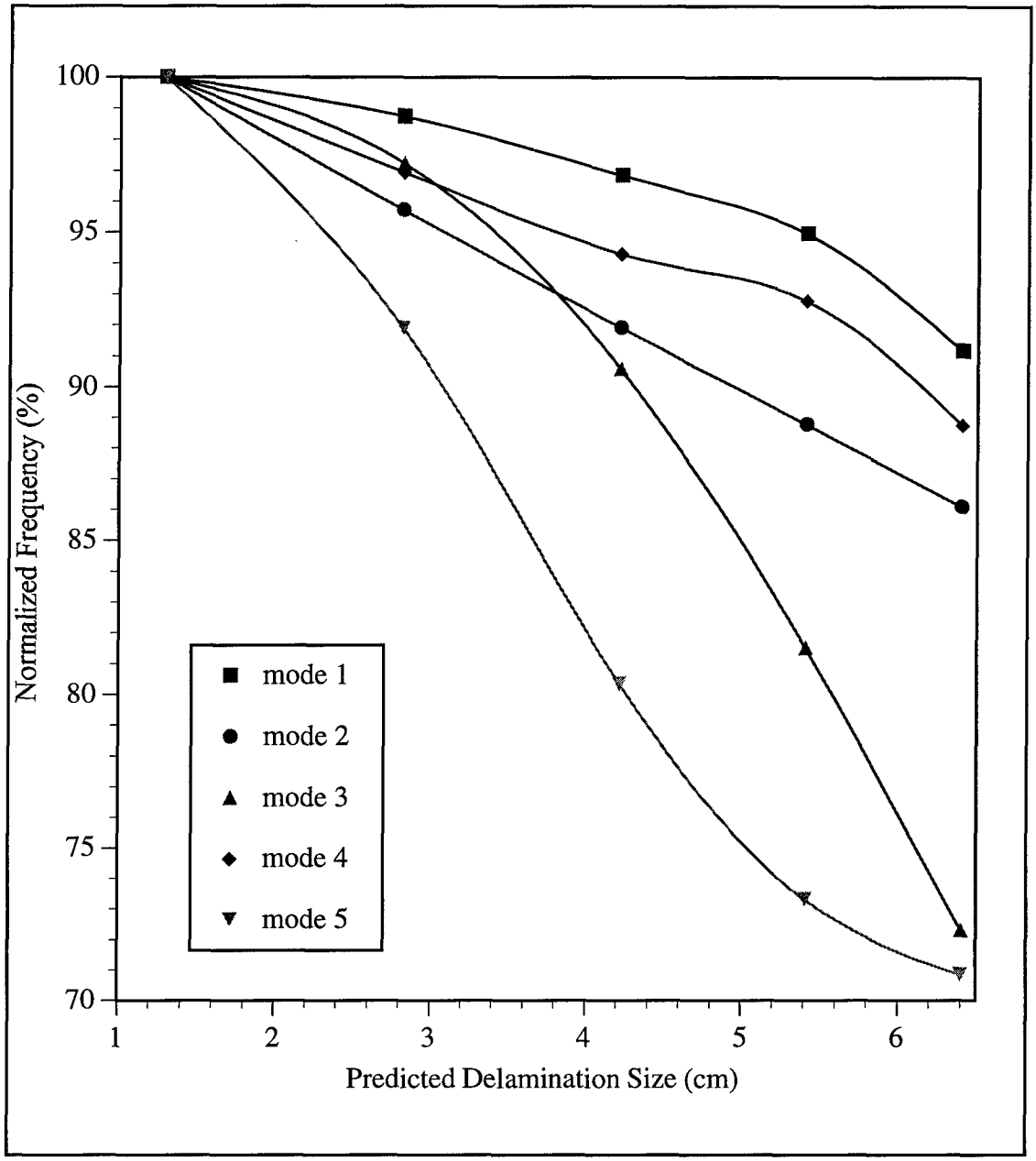

Figure 16. Neural network predicted modal frequencies of a glass/epoxy composite beam for five prescribed delamination sizes.

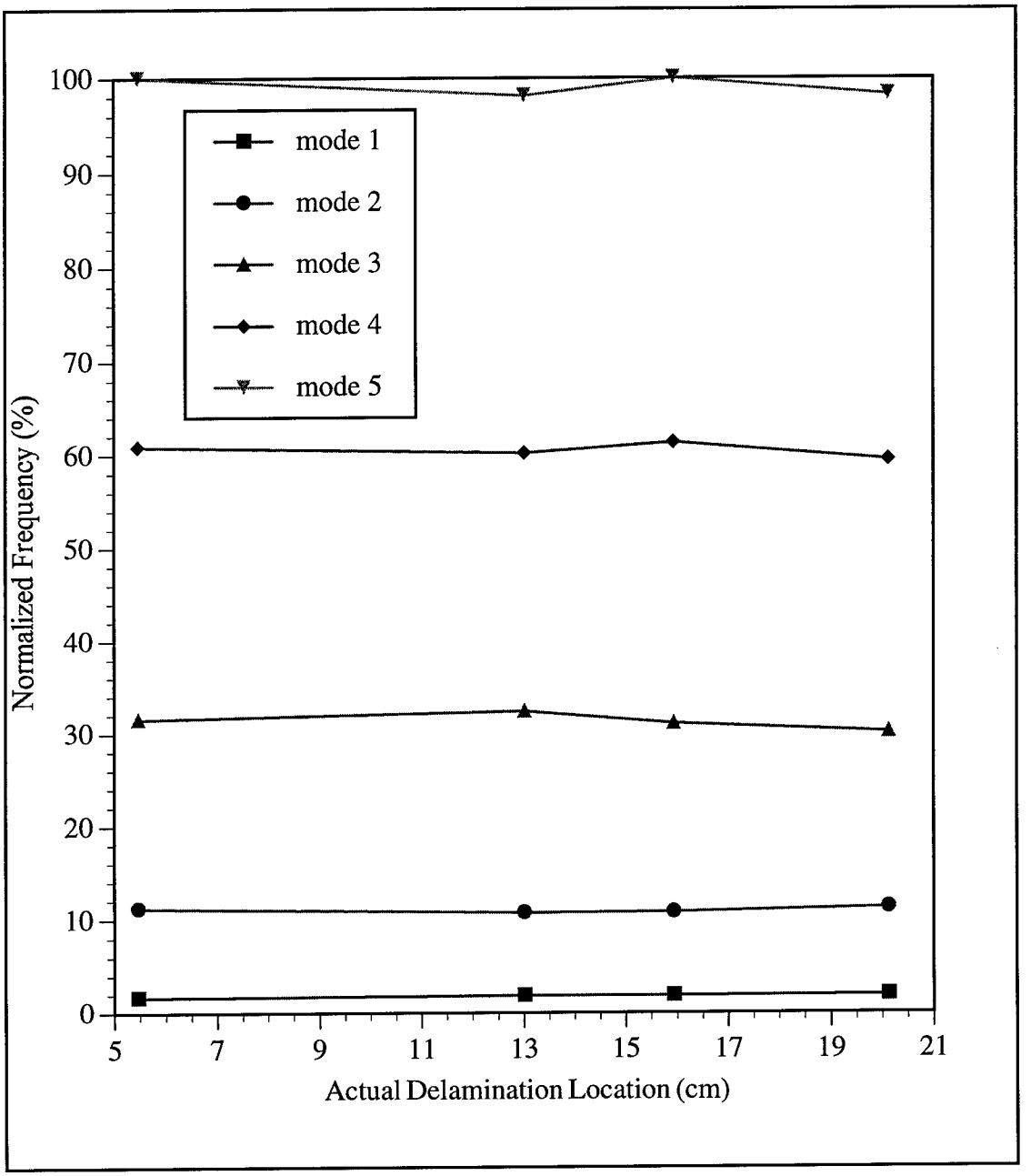

Figure 17. Actual modal frequencies of four different 2.54 cm delamination locations in a glass/epoxy composite beam.

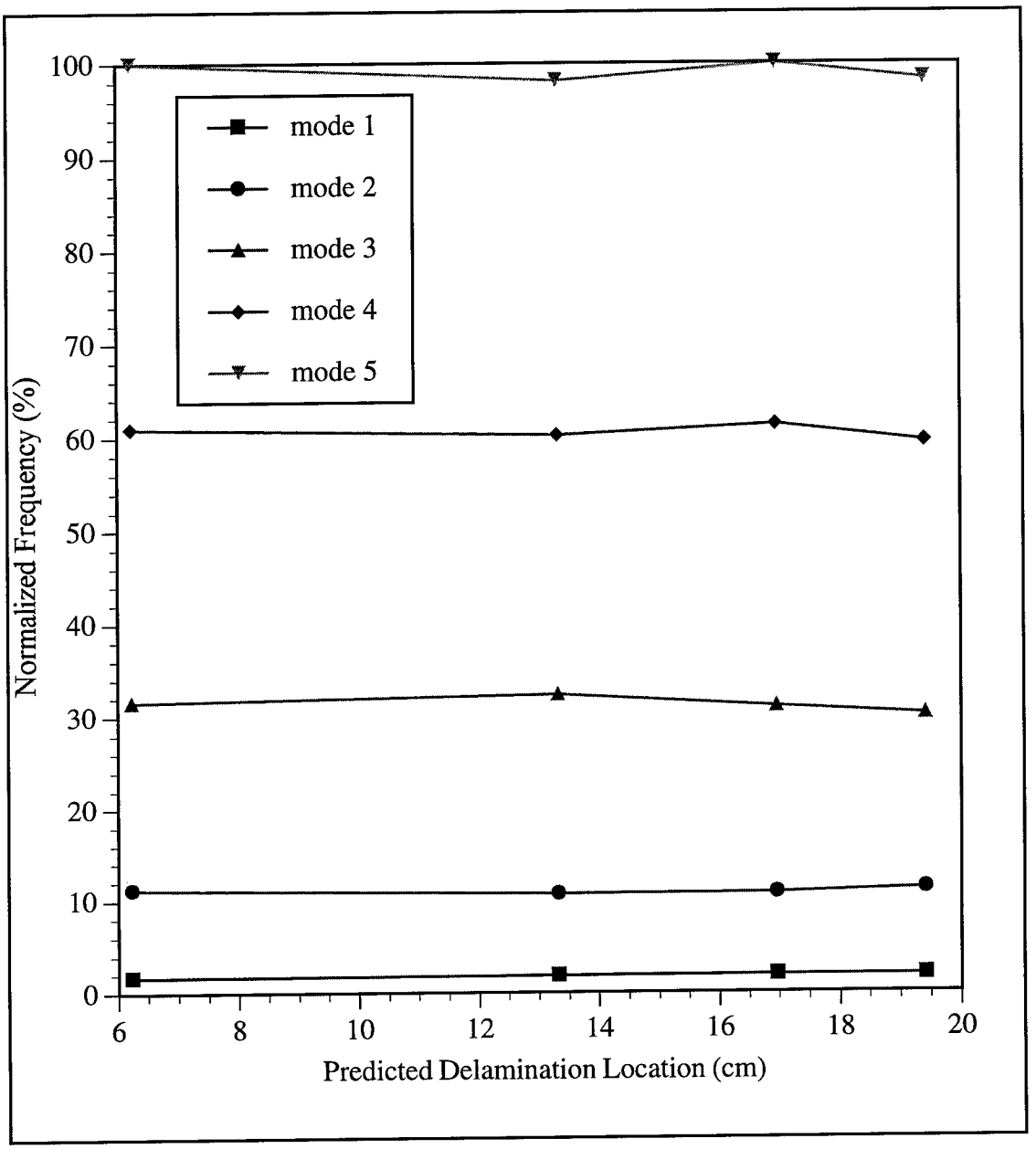

Figure 18. Neural network predicted modal frequencies of four different 2.54 cm delamination locations in a glass/epoxy composite beam.

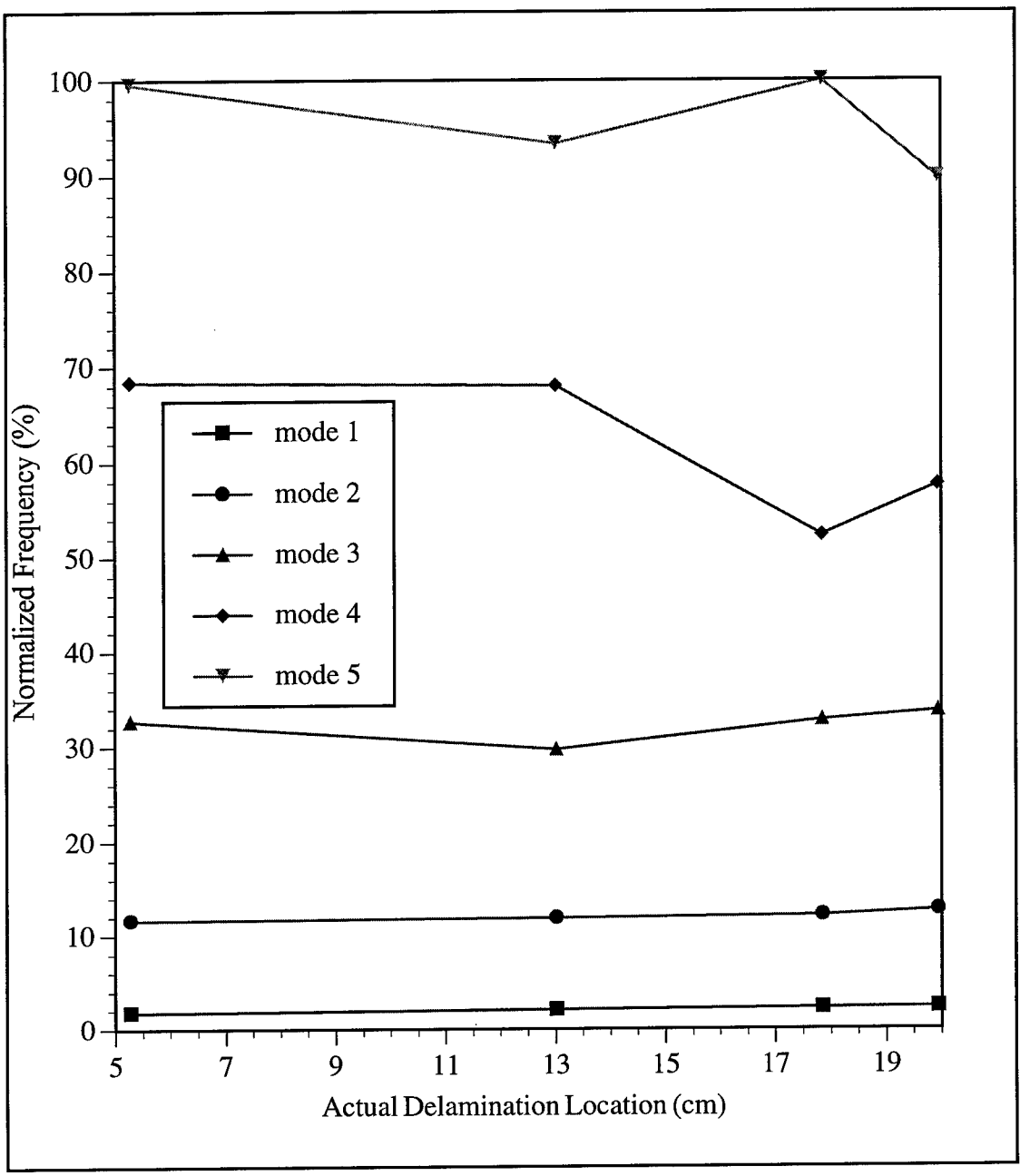

Figure 19. Actual modal frequencies of four different 6.35 cm delamination locations in a glass/epoxy composite beam.

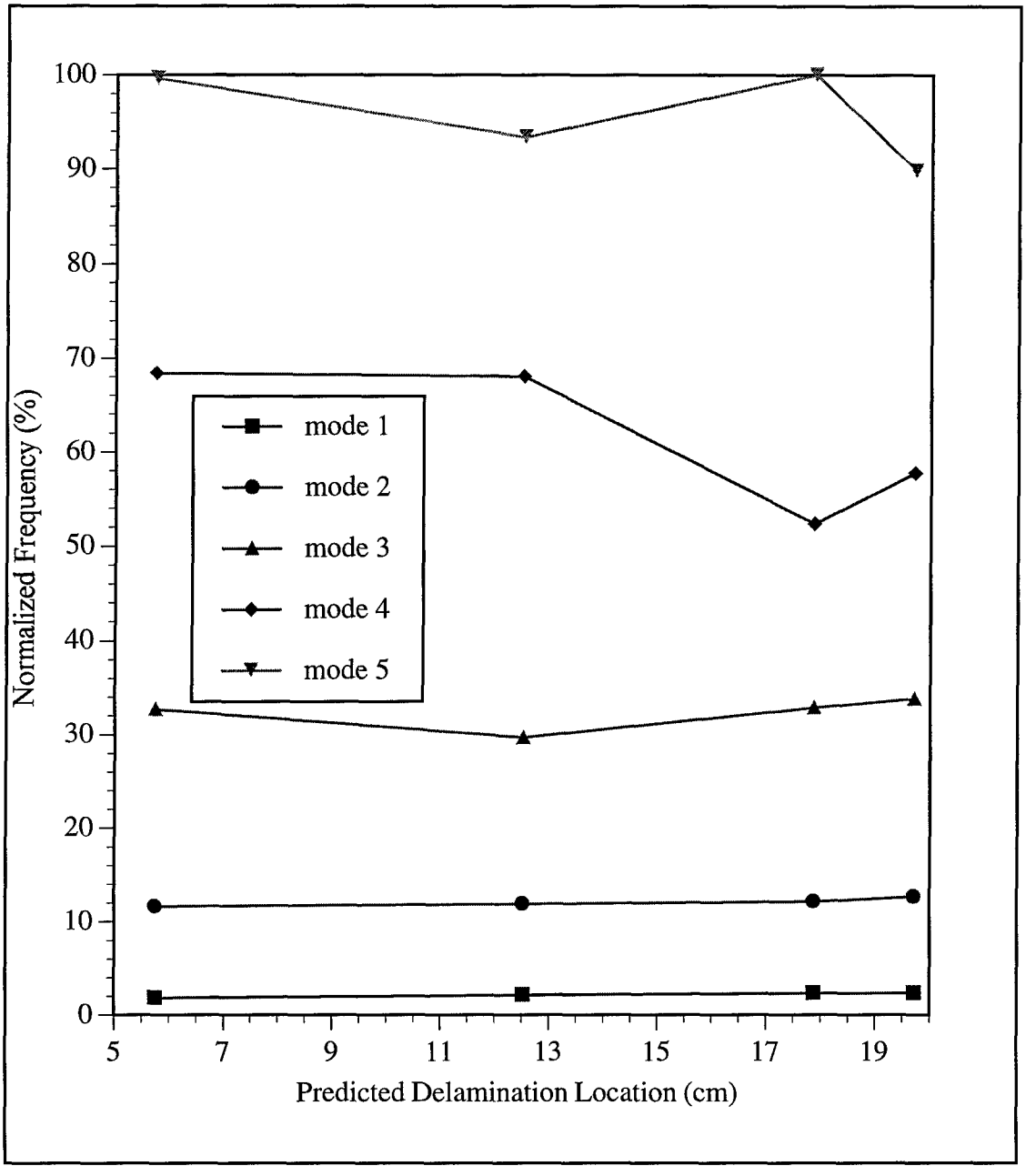

Figure 20. Neural network predicted modal frequencies of four different 6.35 cm delamination locations in a glass/epoxy composite beam.

VI. DISCUSSION

A. MODAL FREQUENCIES FOR UNDAMAGED COMPOSITE BEAMS

The EFPI fiber optic sensor and the PZT ceramic sensor gave identical modal frequencies in each experiment as shown in Figures 8, 9, and 10. The signal-to-noise ratio was higher for the EFPI fiber optic sensor than the PZT ceramic patch, however, as the butt couple changed for each measurement, the signal-to-noise ratio varied for the EFPI fiber optic sensor. The EFPI fiber optic sensor has better sensitivity than a PZT ceramic sensor assuming superior fiber optic splices. There were fine structure differences between the EFPI fiber optic sensors and the PZT ceramic sensors, but the major structures were the same.

The experimental modal frequencies, calculated classical beam theory modal frequencies, and calculated finite element model frequencies are compared in Table I. The largest percentage difference between the modal frequencies is observed in the first mode. The percent difference decreases with the higher order modes. The percent difference between the classical beam theory and the finite element model also follows this trend. In another modal frequency study the opposite was observed [31]. The lower order modes had the least percent difference. The reason for this difference between studies is unknown.

Beam width is the first variable used to experimentally test shifts in modal frequencies predicted by the classical beam theory and the finite element model used in this study. Using Table II, Figure 8, and Figure 9, the 2.54 cm wide beam clearly has lower modal frequencies than the 2.33 cm beam. This shift is expected because a wider beam is stiffer than a narrower beam assuming identical material properties. Both the

classical beam theory and the finite element model predicted that modal frequencies decrease as beam width increases. However, the classical beam theory and the finite element model over-predict the change of modal frequencies due to different beam widths as seen in Table II.

B. MODAL FREQUENCIES FOR DELAMINATED COMPOSITE BEAMS

Table III compares the first five modal frequencies of an undamaged glass/epoxy composite beam to five other beams containing various sized delaminations incorporated in their midplanes. All the beams have identical material properties and dimensions, since variation in material and dimensions can cause significant modal frequency shifts as shown in Table II. These delamination-induced shifts can be seen in Figures 10 through 14. For larger delamination sizes and high modes, the modal frequencies are down shifted to lower frequencies. As delamination size increases, the modal frequencies decrease.

Table IV compares the modal frequencies obtained experimentally for each delamination size to the modal frequencies calculated by the classical beam theory. The average difference is 5.6% with no definite pattern. Therefore, no obvious descripancies are apparent with either the experimental results or the classical beam theory calculations.

C. NEURAL NETWORK INSIGHTS AND IMPROVEMENTS

The normalized predicted neural network delamination size trends shown in Figure 16 are very similar to the actual normalized delamination size trends in Figure 15. The same holds true for the actual delamination locations (cf. Figures 17 and 19)

compared to the predicted neural network delamination locations (cf. Figures 18 and 20). These matching trends, combined with a 5.9% average error for predicted delamination sizes and a 4.7% average error for predicted delamination locations, confirm the ability of the neural network to accurately predict delamination size and location.

Figure 17 shows that the normalized modal frequencies do not change with different delamination locations for a 2.54 cm delamination size. Again, Figure 18 shows that the neural network predicted delamination locations are in good agreement with the actual delamination location for a 2.54 cm delamination size. However, Figure 19 shows that for a 6.35 cm delamination, the modal frequencies vary with different delamination locations. Higher modes show the most variation. Delamination locations farther away from the clamped end of the beam tend to vary more than delaminations close to the clamp. Figure 20 again confirms that the neural network predicted delamination locations are in good agreement with the actual delamination locations. Also, increasing the delamination size, from 2.54 cm to 6.35 cm, results in more variation of normalized frequency as a function of delamination location. By comparing Figures 15 through 20, the neural network delamination size and location predictions follow the actual delamination sizes and locations closely. So, apart from the slight oscillatory behavior, the neural network performed successfully in predicting the prescribed delamination sizes and delamination locations in glass/epoxy composite beams.

VII. CONCLUSIONS

In this study, EFPI fiber optic sensors were used to measure modal frequencies in composite beams. The EFPI fiber optic sensor results were compared to results from PZT ceramic sensors. These experimental results were validated by classical beam theory and a finite element model. A feedforward backpropagating neural network was used to predict the experimental results based on the classical beam theory results.

EFPI fiber optic sensors are superior to the PZT ceramic sensors because of sensitivity, size, ruggedness, ability to be embedded into the composite structure, and immunity to electromagnetic interference. However, the sensitivity is a function of the connection of the EFPI fiber optic sensor to the fiber optic support system. The EFPI fiber optic sensors and PZT ceramic sensors measured identical modal frequencies in glass/epoxy composite beams.

From the change in modal frequencies measured by the EFPI fiber optic sensors delamination of the composite beam can be determined. For smaller delamination sizes the first five modal frequencies increased from the modal frequencies of an undamaged beam. For larger delamination sizes the first two modal frequencies increased while the next three modal frequencies decreased compared to an undamaged beam. Beam dimensions also have an effect on modal frequencies. Modal frequencies shift up as beam width or thickness is increased.

Classical beam theory and a finite element model were used to compare with and validate the experimental modal frequencies. Both of these techniques were used to validate the modal frequencies measured by the EFPI fiber optic sensors and the PZT ceramic sensors for the undamaged beams. The finite element model did not account for

beam delaminations, so only the classical beam theory could be used to compare with the experimental modal frequencies from the damaged beams.

Using modal frequencies calculated by MATLAB simulations based on classical beam theory, a backpropagation neural network was trained to predict delamination size and location in a composite beam. The error of the neural network predicted delamination sizes ranged from 0.9% to 10.7% with an average error of 5.9%. The predicted delamination location error also ranged from zero percent to 13.9% with an average error of 4.7%. The network always overpredicted delamination size and generally overpredicted delamination location. However, the neural network successfully predicted delamination sizes and locations in glass/epoxy composite beams.

The neural network approach is well suited to applications that predict size and location of delaminations in composite lamina. Further work related to this study includes improvements to the accuracy of the predictions and alternatives to the specific neural network and training approaches. Improvement of the neural network performance can be achieved by training the network with more information. In particular, incorporation the modal shapes are possible. The modal shapes can be found experimentally, with the classical beam theory, and with the finite element model. Also improving the modeling of the classical beam theory equations could reduce the error of the calculated modal frequencies. This study was only concerned with delaminations in the midplane of the beam, however, this technique could be expanded to include prescribed delaminations located between other laminate layers. The neural network architecture could also be changed, e.g., number of layers or number of neurons.

APPENDIX A

MATLAB CODE FOR THE CLASSICAL BEAM THEORY

The following appendix contains six MATLAB programs and one text file that implement the classical beam theory discussed in section three of the text. The first program, Delam.m, solves 16 coupled equations. The only input into the program is beam thickness. The equations are solved symbolically so they can be used for any application. The results of Delam.m can be seen in Function.txt. The second program, Property.m, solves for the material properties of the beam. Beam width, thickness, length, number of layers, orientation of layers, and the lamina properties are all input into the program (all parameters are in English units). The material properties (D1, D2, D3, D4, A2, A3, m1, m2, m3, and m4) are saved into a workspace named matrix. Next, Deter.m, is a function that solves for the determinate of the 16x16 matrix created by the 16 coupled equations. Deter.m loads the workspace, matrix, and uses the 16 equations found in Function.txt to solve the determinate. The main program in the appendix is Final.m. This program uses the function Deter.m to solve for five roots, i.e., modal frequencies) of 1000 different delaminations at up to 11 different locations in the beam. The program is set-up so no delamination can start within an inch of the clamp holding the beam or end more than an inch from the free end of the beam. The program takes approximately 24 hours to run on a Pentium 133 MHz processor. A 1097 x 8 matrix is formed and saved into a workspace named final. The matrix contains the first five modal frequencies associated with each delamination, the delamination size, and the beginning and ending location of each delamination. Single.m is a program identical to Final.m, but it allows the user to solve for modal frequencies of a single delamination size. The output is save into a workspace named final2. The last program is Form.m. This program changes the ascii code generated by MATLAB into a text file that can be read by the neural network software.

```
%Delam.m Program
%Modal Frequency Generation for Neural Network

%Generates 16 coupled equations symbolically

%B21=B31;                          %Segments 2 and 3 forced to vibrate together
%B22=B32;
%B23=B33;
%B24=B34;

%Beam dimensions
h=.061;
h2=h/2;
h3=h2;

%Initializing constants
B(1)=0;                            %B11
B(2)=0;                            %B12
B(3)=0;                            %B13
B(4)=0;                            %B14
B(5)=0;                            %B21,B31
B(6)=0;                            %B22,B32
B(7)=0;                            %B23,B33
B(8)=0;                            %B24,B34
B(9)=0;                            %B41
B(10)=0;                           %B42
B(11)=0;                           %B43
B(12)=0;                           %B44
B(13)=0;                           %C20
B(14)=0;                           %C21
B(15)=0;                           %C30
B(16)=0;                           %C31

k1 = sym('((m1*omega^2)/D1)^(1/4)');   %Vibration modes
k2 = sym('((m2*omega^2)/D2)^(1/4)');
k3 = sym('((m3*omega^2)/D3)^(1/4)');
k4 = sym('((m4*omega^2)/D4)^(1/4)');

u2 = sym('B(13)+B(14)*x');             %Axial modes
u3 = sym('B(15)+B(16)*x');

%Initial equation
W = sym('[B(1)*cosh(k1*x)+B(2)*sinh(k1*x)+B(3)*cos(k1*x)+B(4)*sin(k1*x);
B(5)*cosh(k2*x)+B(6)*sinh(k2*x)+B(7)*cos(k2*x)+B(8)*sin(k2*x);
B(5)*cosh(k3*x)+B(6)*sinh(k3*x)+B(7)*cos(k3*x)+B(8)*sin(k3*x);
B(9)*cosh(k4*x)+B(10)*sinh(k4*x)+B(11)*cos(k4*x)+B(12)*sin(k4*x)]');

%16 coupled equations
h1 = sym(W,1,1);                   %Equation 1 @x=0
h2 = diff(h1,'x');                 %Equation 2
w4 = sym(W,4,1);
h3 = diff(w4,'x',2);               %Equation 3 @x=L
h4 = diff(w4,'x',3);               %Equation 4
h5 = symsub(h1,sym(W,2,1));        %Equation 5 @x=x1
dw2 = diff(sym(W,2,1),'x');
h6 = symsub(h2,dw2);               %Equation 6

V1 = symmul('-D1',diff(h1,'x',3)); %Force equations
V2 = symmul('-D2',diff(sym(W,2,1),'x',3));
V3 = symmul('-D3',diff(sym(W,3,1),'x',3));
V4 = symmul('-D4',diff(w4,'x',3));

h7 = symsub(V1,symadd(V2,V3));     %Equation 7
```

```
M1 = symmul('D1',diff(h1,'x',2));                    %Moment Equations
M2 = symmul('D2',diff(sym(W,2,1),'x',2));
M3 = symmul('D3',diff(sym(W,3,1),'x',2));
M4 = symmul('D4',diff(w4,'x',2));

P2 = symmul('A2',diff(u2,'x'));                %Axial Force Equations
P3 = symmul('A3',diff(u3,'x'));

h8a = symsub(M1,symadd(M2,M3));
h8 = symsub(h8a,symsub(symmul('(h/2-h3/2)',P3),symmul('(h/2-h2/2)',P2)));
                                                          %Equation 8
h9 = symadd(u2,symmul('(h/2-h2/2)',h2));
                                                  %Equation 9
h10 = symsub(u3,symmul('(h/2-h3/2)',h2));
                                                          %Equation 10
h11 = symadd(P2,P3);                                 %Equation 11

h12 = symsub(sym(W,2,1),w4);                 %Equation 12  @x=x2
h13 = symsub(dw2,diff(w4,'x'));              %Equation 13
h14 = symsub(V4,symadd(V2,V3));                      %Equation 14
h15a = symsub(M4,symadd(M2,M3));
h15 = symsub(h15a,symsub(symmul('(h/2-h3/2)',P3),symmul('(h/2-h2/2)',P2)));
                                                  %Equation 15
h16 = symsub(u2,symsub(u3,symmul('(h/2)',diff(w4,'x'))));
                                                          %Equation 16
```

%----------

Function.txt

Text file that shows the 16 coupled, symbolic equations generated by Delam.m

Equation 1

```
h1 = B(1)*cosh(k1*x)+B(2)*sinh(k1*x)+B(3)*cos(k1*x)+B(4)*sin(k1*x)
```

Equation 2

```
h2 = B(1)*sinh(k1*x)*k1+B(2)*cosh(k1*x)*k1-B(3)*sin(k1*x)*k1+B(4)*cos(k1*x)*k1
```

Equation 3

```
h3 = B(9)*cosh(k4*x)*k4^2+B(10)*sinh(k4*x)*k4^2-B(11)*cos(k4*x)*k4^2-
     B(12)*sin(k4*x)*k4^2
```

Equation 4

```
h4 = B(9)*sinh(k4*x)*k4^3+B(10)*cosh(k4*x)*k4^3+B(11)*sin(k4*x)*k4^3-
     B(12)*cos(k4*x)*k4^3
```

Equation 5

```
h5 = B(1)*cosh(k1*x)+B(2)*sinh(k1*x)+B(3)*cos(k1*x)+B(4)*sin(k1*x)-
     B(5)*cosh(k2*x)-B(6)*sinh(k2*x)-B(7)*cos(k2*x)-B(8)*sin(k2*x)
```

Equation 6

```
h6 = B(1)*sinh(k1*x)*k1+B(2)*cosh(k1*x)*k1-B(3)*sin(k1*x)*k1+B(4)*cos(k1*x)*k1-
     B(5)*sinh(k2*x)*k2-B(6)*cosh(k2*x)*k2+B(7)*sin(k2*x)*k2-B(8)*cos(k2*x)*k2
```

Equation 7

```
h7 = -D1*(B(1)*sinh(k1*x)*k1^3+B(2)*cosh(k1*x)*k1^3+B(3)*sin(k1*x)*k1^3-
     B(4)*cos(k1*x)*k1^3)+D2*(B(5)*sinh(k2*x)*k2^3+B(6)*cosh(k2*x)*k2^3
     +B(7)*sin(k2*x)*k2^3-B(8)*cos(k2*x)*k2^3)+D3*(B(5)*sinh(k3*x)*k3^3
     +B(6)*cosh(k3*x)*k3^3+B(7)*sin(k3*x)*k3^3-B(8)*cos(k3*x)*k3^3)
```

Equation 8

```
h8 = D1*(B(1)*cosh(k1*x)*k1^2+B(2)*sinh(k1*x)*k1^2-B(3)*cos(k1*x)*k1^2-
```

```
B(4)*sin(k1*x)*k1^2)-D2*(B(5)*cosh(k2*x)*k2^2+B(6)*sinh(k2*x)*k2^2-
B(7)*cos(k2*x)*k2^2-B(8)*sin(k2*x)*k2^2)-D3*(B(5)*cosh(k3*x)*k3^2
+B(6)*sinh(k3*x)*k3^2-B(7)*cos(k3*x)*k3^2-B(8)*sin(k3*x)*k3^2)-(1/2*h-
1/2*h3)*A3*B(16)+(1/2*h-1/2*h2)*A2*B(14)

Equation 9
h9 = B(13)+B(14)*x+(1/2*h-1/2*h2)*(B(1)*sinh(k1*x)*k1+B(2)*cosh(k1*x)*k1-
     B(3)*sin(k1*x)*k1+B(4)*cos(k1*x)*k1)

Equation 10
h10 = B(15)+B(16)*x-(1/2*h-1/2*h3)*(B(1)*sinh(k1*x)*k1+B(2)*cosh(k1*x)*k1-
      B(3)*sin(k1*x)*k1+B(4)*cos(k1*x)*k1)

Equation 11
h11 = A2*B(14)+A3*B(16)

Equation 12
h12 = B(5)*cosh(k2*x)+B(6)*sinh(k2*x)+B(7)*cos(k2*x)+B(8)*sin(k2*x)-
      B(9)*cosh(k4*x)-B(10)*sinh(k4*x)-B(11)*cos(k4*x)-B(12)*sin(k4*x)

Equation 13
h13 = B(5)*sinh(k2*x)*k2+B(6)*cosh(k2*x)*k2-B(7)*sin(k2*x)*k2
      +B(8)*cos(k2*x)*k2-B(9)*sinh(k4*x)*k4-B(10)*cosh(k4*x)*k4
      +B(11)*sin(k4*x)*k4-B(12)*cos(k4*x)*k4

Equation 14
h14 = -D4*(B(9)*sinh(k4*x)*k4^3+B(10)*cosh(k4*x)*k4^3+B(11)*sin(k4*x)*k4^3-
      B(12)*cos(k4*x)*k4^3)+D2*(B(5)*sinh(k2*x)*k2^3+B(6)*cosh(k2*x)*k2^3
      +B(7)*sin(k2*x)*k2^3-B(8)*cos(k2*x)*k2^3)+D3*(B(5)*sinh(k3*x)*k3^3
      +B(6)*cosh(k3*x)*k3^3+B(7)*sin(k3*x)*k3^3-B(8)*cos(k3*x)*k3^3)

Equation 15
h15 = D4*(B(9)*cosh(k4*x)*k4^2+B(10)*sinh(k4*x)*k4^2-B(11)*cos(k4*x)*k4^2-
      B(12)*sin(k4*x)*k4^2)-D2*(B(5)*cosh(k2*x)*k2^2+B(6)*sinh(k2*x)*k2^2-
      B(7)*cos(k2*x)*k2^2-B(8)*sin(k2*x)*k2^2)-D3*(B(5)*cosh(k3*x)*k3^2
      +B(6)*sinh(k3*x)*k3^2-B(7)*cos(k3*x)*k3^2-B(8)*sin(k3*x)*k3^2)-(1/2*h-
      1/2*h3)*A3*B(16)+(1/2*h-1/2*h2)*A2*B(14)

Equation 16
h16 = B(13)+B(14)*x-B(15)-B(16)*x+1/2*h*(B(9)*sinh(k4*x)*k4
      +B(10)*cosh(k4*x)*k4-B(11)*sin(k4*x)*k4+B(12)*cos(k4*x)*k4)
```

```
%-----------------------------------------------------------------------------------------------------------------------
%Property.m Program
%Modal Frequency Generation for Neural Network

%Program to solve for the material properties of the beam

%Inputs
b = .917;                %width
h = .061;                %thickness
L = 10.25;               %length
n = 8;                           %number of layers

E11 = 6.14E6;                    % Lamina properties
E22 = 1.7E6;
G12 = 1.03E6;
v12 = .27;
r = .18E-3;

h2 = h/2;
```

```
h3 = h2;
k = h/n;
kk=h/(2*n);

v21 = (E22*v12)/E11;            %Constant equations
Q11 = E11/(1-(v12*v21));
Q12 = (v12*E22)/(1-(v12*v21));
Q22 = E22/(1-(v12*v21));
Q66 = G12;

theta(1) = 0;                                   %Layer orientation
theta(2) = pi/2;
theta(3) = 0;
theta(4) = pi/2;
theta(5) = pi/2;
theta(6) = 0;
theta(7) = pi/2;
theta(8) = 0;

%Loop to solve Q for the different layer orientations
for n = 1:8
Q(n) = Q11*(cos(theta(n)))^4+Q22*(sin(theta(n)))^4 +2*(Q12+2*Q66)*(sin(theta(n)))^2*(cos(theta(n)))^2;
end;

%Solving for the D's
D=0;
for j = 1:8
C = Q(j)*((((h/2)+(1-j)*k)^3)-((h/2)-j*k)^3);
D = C+D;
end;

D1 = (1/3)*D;
D4 = D1;

D=0;
for j = 1:4
C = Q(j)*((((h/4)+(1-j)*kk)^3)-((h/4)-j*kk)^3);
D = C+D;
end;

D2 = (1/3)*D;
D3 = D2;

%Solving for the A's
A = 0;
for j = 1:4;
C = Q(j)*(((h/4)+(1-j)*kk)-((h/4)-j*kk));
A = A+C;
end;

A2 = 1*A;
A3 = A2;

%Solving for the m's
m1 = r*b*h;
m4=m1;
m2 = r*b*h/2;
m3=m2;

save matrix D1 D2 D3 D4 A2 A3 m1 m2 m3 m4 L h h2 h3
```

```
%-----------------------------------------------------------------------------------------------------------------
%Deter.m Program
%Modal Frequency Generation for Neural Network

%Function to determine the numeric value of the determinant of a 16x16 symbolic matrix

function [d] = deter(y)

load matrix
load cor

j=1:16;
B=0*j;

t=tm;                                          %Change of variables
tt=ttm;

omega = 2*pi*y;
k1 = ((m1*omega^2)/D1)^(1/4); %Vibration Modes
k2 = ((m2*omega^2)/D2)^(1/4);
k3 = ((m3*omega^2)/D3)^(1/4);
k4 = ((m4*omega^2)/D4)^(1/4);

a(1,1)=1;                                      %Initializes matrix values
a(1,3)=1;
a(2,2)=1;
a(2,4)=1;
a(11,14)=A2;
a(11,16)=A3;

x=L;
for I=9:12                                     %Starts loop for x=L
        B(i)=1;
        a(3,i) = B(9)*cosh(k4*x)*k4^2+B(10)*sinh(k4*x)*k4^2-B(11)*cos(k4*x)*k4^2-B(12)*sin(k4*x)*k4^2;
        a(4,i) = B(9)*sinh(k4*x)*k4^3+B(10)*cosh(k4*x)*k4^3+B(11)*sin(k4*x)*k4^3-B(12)*cos(k4*x)*k4^3;
        B(i)=0;
end;

x=tt;
for I=9:16                                     %Starts loop for x equal to end of delamination
        B(i)=1;
        a(16,i) = B(13)+B(14)*x-B(15)-B(16)*x+(1/2*h)*(B(9)*sinh(k4*x)*k4+B(10)*cosh(k4*x)*k4-
B(11)*sin(k4*x)*k4+B(12)*cos(k4*x)*k4);
        B(i)=0;
end;

x=t;
for I=1:8                                      %Starts loop for x equal to front of delamination
        B(i)=1;
        a(5,i) = B(1)*cosh(k1*x)+B(2)*sinh(k1*x)+B(3)*cos(k1*x)+B(4)*sin(k1*x)-B(5)*cosh(k2*x)-B(6)*sinh(k2*x)-
B(7)*cos(k2*x)-B(8)*sin(k2*x);
        a(6,i) = B(1)*sinh(k1*x)*k1+B(2)*cosh(k1*x)*k1-B(3)*sin(k1*x)*k1+B(4)*cos(k1*x)*k1-B(5)*sinh(k2*x)*k2-
B(6)*cosh(k2*x)*k2+B(7)*sin(k2*x)*k2-B(8)*cos(k2*x)*k2;
        a(7,i) = -D1*(B(1)*sinh(k1*x)*k1^3+B(2)*cosh(k1*x)*k1^3+B(3)*sin(k1*x)*k1^3-
B(4)*cos(k1*x)*k1^3)+D2*(B(5)*sinh(k2*x)*k2^3+B(6)*cosh(k2*x)*k2^3+B(7)*sin(k2*x)*k2^3-
B(8)*cos(k2*x)*k2^3)+D3*(B(5)*sinh(k3*x)*k3^3+B(6)*cosh(k3*x)*k3^3+B(7)*sin(k3*x)*k3^3-B(8)*cos(k3*x)*k3^3);
        B(i)=0;
end;

for i=1:16
B(i)=1;
x=t;
a(8,i) = D1*(B(1)*cosh(k1*x)*k1^2+B(2)*sinh(k1*x)*k1^2-B(3)*cos(k1*x)*k1^2-B(4)*sin(k1*x)*k1^2)-
D2*(B(5)*cosh(k2*x)*k2^2+B(6)*sinh(k2*x)*k2^2-B(7)*cos(k2*x)*k2^2-B(8)*sin(k2*x)*k2^2)-
```

```
D3*(B(5)*cosh(k3*x)*k3^2+B(6)*sinh(k3*x)*k3^2-B(7)*cos(k3*x)*k3^2-B(8)*sin(k3*x)*k3^2)-(1/2*h-
1/2*h3)*A3*B(16)+(1/2*h-1/2*h2)*A2*B(14);
a(9,i) = B(13)+B(14)*x+(1/2*h-1/2*h2)*(B(1)*sinh(k1*x)*k1+B(2)*cosh(k1*x)*k1-B(3)*sin(k1*x)*k1+B(4)*cos(k1*x)*k1);
a(10,i) = B(15)+B(16)*x-(1/2*h-1/2*h3)*(B(1)*sinh(k1*x)*k1+B(2)*cosh(k1*x)*k1-B(3)*sin(k1*x)*k1+B(4)*cos(k1*x)*k1);
x=tt;
a(15,i) = D4*(B(9)*cosh(k4*x)*k4^2+B(10)*sinh(k4*x)*k4^2-B(11)*cos(k4*x)*k4^2-B(12)*sin(k4*x)*k4^2)-
D2*(B(5)*cosh(k2*x)*k2^2+B(6)*sinh(k2*x)*k2^2-B(7)*cos(k2*x)*k2^2-B(8)*sin(k2*x)*k2^2)-
D3*(B(5)*cosh(k3*x)*k3^2+B(6)*sinh(k3*x)*k3^2-B(7)*cos(k3*x)*k3^2-B(8)*sin(k3*x)*k3^2)-(1/2*h-
1/2*h3)*A3*B(16)+(1/2*h-1/2*h2)*A2*B(14);
B(i)=0;
end;

x=tt;
for i=5:12
B(i)=1;
a(12,i) = B(5)*cosh(k2*x)+B(6)*sinh(k2*x)+B(7)*cos(k2*x)+B(8)*sin(k2*x)-B(9)*cosh(k4*x)-B(10)*sinh(k4*x)-
B(11)*cos(k4*x)-B(12)*sin(k4*x);
a(13,i) = B(5)*sinh(k2*x)*k2+B(6)*cosh(k2*x)*k2-B(7)*sin(k2*x)*k2+B(8)*cos(k2*x)*k2-B(9)*sinh(k4*x)*k4-
B(10)*cosh(k4*x)*k4+B(11)*sin(k4*x)*k4-B(12)*cos(k4*x)*k4;
a(14,i) = -D4*(B(9)*sinh(k4*x)*k4^3+B(10)*cosh(k4*x)*k4^3+B(11)*sin(k4*x)*k4^3-
B(12)*cos(k4*x)*k4^3)+D2*(B(5)*sinh(k2*x)*k2^3+B(6)*cosh(k2*x)*k2^3+B(7)*sin(k2*x)*k2^3-
B(8)*cos(k2*x)*k2^3)+D3*(B(5)*sinh(k3*x)*k3^3+B(6)*cosh(k3*x)*k3^3+B(7)*sin(k3*x)*k3^3-B(8)*cos(k3*x)*k3^3);
B(i)=0;
end;

d =det(a);



%-----------------------------------------------------------------------------------------------------------------------
%Final.m Program
%Modal Frequency Generation for Neural Network

%Finds the first five modal frequencies for different delamination sizes and locations in a composite beam
freq = [0,0,0,0,0,0,0,0,0,0,0,0,0,0,0,0,0,0,0,0,0,0,0];        % watch out for the size of these
                                                               matrices
uuuu= [0,0,0,0,0,0,0,0,0,0,0,0,0,0,0,0,0,0,0,0,0,0,0,0,0,0,0];
uuu= [0,0,0,0,0,0,0,0,0,0,0,0,0,0,0,0,0,0,0,0,0,0,0,0,0,0,0];
uu = [0,0,0,0,0,0,0,0,0,0,0,0,0,0,0,0,0,0,0,0,0,0,0,0,0,0,0];
u = [0,0,0,0,0,0,0,0,0,0,0,0,0,0,0,0,0,0,0,0,0,0,0,0,0,0,0];

range = 1000;          % the frequencies are between 0 and range
nmax1 = 20;            % number of initial intervals
nmax2 = 10;            % range/(nmax1*nmax2*nmax3*nmax4) is the accuracy on the frequency
nmax3 = 10;            % make sure you put round numbers otherwise you get "truncated errors"
                 from maple
nmax4 = 10;
p = nmax1/range;
nroots = 5;            % number of roots to find
% ------------------------
%Loop to calculate 1000 different delaminations and locations
Z=11;
C=0;
q=0;
L=10.25;
x(2)=1;                                    %Delamination locations
x(3)=8.25/(Z-1);
x(4)=2*(8.25/(Z-1));
x(5)=3*(8.25/(Z-1));
x(6)=4*(8.25/(Z-1));
x(7)=5*(8.25/(Z-1));
x(8)=6*(8.25/(Z-1));
x(9)=7*(8.25/(Z-1));
```

```
x(10)=8*(8.25/(Z-1));
x(11)=9*(8.25/(Z-1));

for g=1:200                                    %Changes delamination size by 0.04"
t = 5.145-(.02*g);
tt = 5.10501+(.02*g);
delam=tt-t;                                    %Delamination size
x(1)=t;
if q<Z
        C=C+1;
end;

for q=1:Z;                                     %Changes delamination location
tm=x(q);
ttm=delam+x(q);
save cor tm ttm
if ttm < 9.25                                  %If delamination extends out of beam

%-------------------------
%Prgram to find n (numeric) roots of the determinant of 16x16 matrix (symbolic)
i=1;
m=1;
u(1) = deter(0.001);
for j=1:nmax1
        u(j+1) = deter(j/p);
end;
while m < nmax1+1
        index=0;
        if u(m)*u(m+1) < 0
                uu(1) = u(m);
                uu(nmax2) = u(m+1);
                k=1;
                while k< nmax2
                        y = (m-1+k/nmax2)/p;
                                if k < nmax2-1
                                        uu(k+1)=deter(y);
                                end;
                                if uu(k)*uu(k+1) < 0
                                        uuu(1)=uu(k);
                                        uuu(nmax3)=uu(k+1);
                                        l=1;
                                        while l < nmax3
                                                yy = (m-1+(k-1+
                                                    (l/nmax3))/nmax2)/p;
                                                        if l < nmax3-1
                                                                uuu(l+1)=deter(yy);
                                                        end;

                                                if uuu(l)*uuu(l+1) < 0
                                                        uuuu(1) = uuu(l);
                                                        uuuu(nmax4) = uuu(l+1);
                                                        ll=1;
                                                        while ll < nmax4
                                                                yyy = (m-1+(k-1+
                                                  ((l1)+ll/nmax4)/
                                                 nmax3)/nmax2)/p;

                                                                        if ll < nmax4-1
                                                                      uuuu(ll+1) =
                                                    deter(yyy);
                                                                                end;
                                                        if uuuu(ll)*uuuu(ll+1) < 0;
                                                                freq(i) = (2*yyy
                                                 -1/(nmax2*nmax3
```

```
                                                    *nmax4*p))/2;
                                                                i=i+1;
                                                                index=1;
                                                                break;
                                                        end;
                                                    ll = ll+1;
                                                    end;
                                                end;
                                            if index == 1
                                            break;
                                            end;
                                            l=l+1;
                                            end;
                                    end;
                                if index == 1
                                break;
                                end;
                                k=k+1;
                        end;
                if i == nroots+1
                        break;
                end;
                end;
m=m+1;
end;
%-------------------------

MF(C,1)=freq(1);        %Loads values into matrix MF
MF(C,2)=freq(2);
MF(C,3)=freq(3);
MF(C,4)=freq(4);
MF(C,5)=freq(5);
MF(C,6)=delam;
MF(C,7)=tm;
MF(C,8)=ttm;
C=C+1;
end;                            %Ends if loop
end;                            %Ends location loop
end;                            %Ends size loop
S = size(MF);
save final MF S                 %Saves workspace into final


%-----------------------------------------------------------------------------------------------------------------------
Single.m Program
%Modal Frequency Generation for Neural Network

%Does the same operation as final.m, however allows for the determination of modal frequencies for single delamination size

freq = [0,0,0,0,0,0,0,0,0,0,0,0,0,0,0,0,0,0,0,0,0,0,0];     % watch out for the size of these
                                                            matrices
uuuu= [0,0,0,0,0,0,0,0,0,0,0,0,0,0,0,0,0,0,0,0,0,0,0];
uuu= [0,0,0,0,0,0,0,0,0,0,0,0,0,0,0,0,0,0,0,0,0,0,0];
uu = [0,0,0,0,0,0,0,0,0,0,0,0,0,0,0,0,0,0,0,0,0,0,0];
u = [0,0,0,0,0,0,0,0,0,0,0,0,0,0,0,0,0,0,0,0,0,0,0];
range = 1000;       % the frequencies are between 0 and range
nmax1 = 20;         % number of initial intervals
nmax2 = 10;         % range/(nmax1*nmax2*nmax3*nmax4) is the accuracy on the frequency
nmax3 = 10;         % make sure you put round numbers otherwise you get "truncated errors" from maple
nmax4 = 10;
p = nmax1/range;
nroots = 5;         % number of roots to find
% -------------------------
```

```
%Loop to calculate 1000 different delaminations and locations
Z=11;
C=1;
q=0;
L=10.25;
x(2)=1;                         %Delamination locations
x(3)=8.25/(Z-1);
x(4)=2*(8.25/(Z-1));
x(5)=3*(8.25/(Z-1));
x(6)=4*(8.25/(Z-1));
x(7)=5*(8.25/(Z-1));
x(8)=6*(8.25/(Z-1));
x(9)=7*(8.25/(Z-1));
x(10)=8*(8.25/(Z-1));
x(11)=9*(8.25/(Z-1));

%Enter delamination size below
t = 5.125-(0.5/2);              %Changes delamination size by 0.1"
tt = 5.125+(0.5/2);
delam=tt-t;                             %Delamination size
x(1)=t;


for q=1:Z;                      %Changes delamination location

%if q<Z
        %C=C+1;
%end;

tm=x(q);
ttm=delam+x(q);
save cor tm ttm
if ttm > 9.25
C=C+1;
end;

if ttm < 9.25                           %If delamination extends out of beam

%--------------------------
%prgram to find n (numeric) roots of the determinant of 16x16 matrix (symbolic)

i=1;
m=1;
u(1) = deter(0.001);
for j=1:nmax1
        u(j+1) = deter(j/p);
end;
while m < nmax1+1
        index=0;
        if u(m)*u(m+1) < 0
                uu(1) = u(m);
                uu(nmax2) = u(m+1);
                k=1;
                while k< nmax2
                        y = (m-1+k/nmax2)/p;
                                if k < nmax2-1
                                        uu(k+1)=deter(y);
                                end;
                                if uu(k)*uu(k+1) < 0
                                        uuu(1)=uu(k);
                                        uuu(nmax3)=uu(k+1);
                                        l=1;
                                        while l < nmax3
                                                yy = (m-1+(k-1+
```

```
                                                    (l/nmax3))/nmax2)/p;
                                                                        if l < nmax3-1
                                                                                uuu(l+1)=deter(yy);
                                                                        end;

                                                                    if uuu(l)*uuu(l+1) < 0

                                                                        uuuu(1) = uuu(l);
                                                                        uuuu(nmax4) = uuu(l+1);
                                                                        ll=1;
                                                                        while ll < nmax4
                                                                                yyy = (m-1+(k-1+
                                                                ((l-1)+ll/nmax4)/
                                                               nmax3)/nmax2)/p;

                                                                                        if ll<nmax4-1
                                                                                        uuuu(ll+1) =
                                                                    deter(yyy);
                                                                                        end;
                                                                        if uuuu(ll)*uuuu(ll+1) < 0;
                                                                                freq(i) = (2*yyy
                                                                -1/(nmax2*nmax3
                                                                 *nmax4*p))/2;
                                                                                i=i+1;
                                                                                index=1;
                                                                                break;
                                                                        end;
                                                                    ll = ll+1;
                                                                    end;
                                                            end;
                                                        if index == 1
                                                                break;
                                                        end;
                                                        l=l+1;
                                                        end;
                                                end;
                                            if index == 1
                                                    break;
                                            end;
                                            k=k+1;
                                    end;
                            if i == nroots+1
                                    break;
                            end;
                            end;
m=m+1;
end;
%-------------------------

MF(C,1)=freq(1);            %loads values into matrix MF
MF(C,2)=freq(2);
MF(C,3)=freq(3);
MF(C,4)=freq(4);
MF(C,5)=freq(5);
MF(C,6)=delam;
MF(C,7)=tm;
MF(C,8)=ttm;
C=C+1;
end;                                %ends if loop
end;                                %ends location loop
%end;                               %ends size loop
S = size(MF);
save final MF S             %saves workspace into final
```

```
%-------------------------------------------------------------------------------------------------------------
%Form.m Program
%Modal Frequency Generation for Neural Network

%Changes ascii code to text file so the five modal frequencies, delamination size, and delamination location can be used to train the
neural network (from average.mat)

fod = fopen('E:\FARHAD\GIL\IMPORTAN\outtest2.txt','w+');
load average
outcount = fprintf(fod,'%6.3f   %6.3f   %6.3f   %6.3f   %6.3f   %6.3f   %6.3f\n',MN')
fclose(fod);
```

APPENDIX B

MODAL FREQUENCIES GENERATED BY THE CLASSICAL BEAM THEORY

The following appendix contains the data generated using the MATLAB codes implementing the classical beam theory. The first five columns are the first five modal frequency for a glass-epoxy composite beam. The units on modal frequencies are hertz (Hz). The sixth column is the delamination size. The delamination size is measured in inches (the rest of the thesis uses MKS units). The final column is the delamination location, also measured in inches. The location is described at the center of the delamination. It was found by averaging the beginning and ending of each delamination location.

DATA GENETERATED USING CLASSICAL BEAM THEORY

Mode 1	Mode 2	Mode 3	Mode 4	Mode 5	Size	Location
16.075	100.775	282.125	552.875	913.925	0.000	5.125
16.075	100.775	282.125	552.875	913.925	0.000	1.000
16.075	100.775	282.125	552.875	913.925	0.000	0.825
16.075	100.775	282.125	552.875	913.925	0.000	1.650
16.075	100.775	282.125	552.875	913.925	0.000	2.475
16.075	100.775	282.125	552.875	913.925	0.000	3.300
16.075	100.775	282.125	552.875	913.925	0.000	4.125
16.075	100.775	282.125	552.875	913.925	0.000	4.950
16.075	100.775	282.125	552.875	913.925	0.000	5.775
16.075	100.775	282.125	552.875	744.025	0.000	6.600
16.075	100.775	282.125	650.075	755.075	0.000	7.425
16.075	100.225	282.125	550.075	913.925	0.040	5.105
15.925	100.425	281.925	552.825	913.125	0.040	1.000
15.925	100.375	281.775	552.775	913.825	0.040	0.825
15.925	100.725	282.025	551.375	909.425	0.040	1.650
16.025	100.725	281.225	550.625	913.025	0.040	2.475
16.025	100.625	280.925	552.525	912.175	0.040	3.300
16.025	100.375	281.525	552.175	909.425	0.040	4.125
16.075	100.275	282.125	550.175	913.675	0.040	4.950
16.075	100.225	281.725	551.325	911.025	0.040	5.775
16.075	100.375	280.825	552.825	910.425	0.040	6.600
16.075	100.525	280.525	550.925	915.025	0.040	7.425
16.025	94.425	282.125	544.425	913.875	0.080	5.085
15.825	100.225	281.875	552.775	912.175	0.080	1.000
15.825	100.075	281.425	552.725	913.575	0.080	0.825
15.875	100.675	281.875	544.425	906.225	0.080	1.650
15.925	100.725	280.325	544.425	912.325	0.080	2.475
15.925	100.425	279.425	552.275	910.225	0.080	3.300
16.025	100.025	280.925	551.325	905.525	0.080	4.125
16.025	94.425	282.125	544.425	913.575	0.080	4.950
16.075	94.425	281.325	544.425	908.025	0.080	5.775
16.075	94.425	279.425	552.825	907.175	0.080	6.600
16.075	100.325	278.925	544.425	910.225	0.080	7.425
16.025	94.425	282.125	544.425	913.725	0.120	5.065
15.725	100.025	281.775	552.675	910.925	0.120	1.000
15.725	94.425	281.225	552.675	913.125	0.120	0.825
15.775	100.625	281.725	544.425	902.575	0.120	1.650
15.875	100.725	279.375	544.425	911.775	0.120	2.475
15.925	100.275	278.675	552.075	908.075	0.120	3.300
15.925	94.425	280.525	550.425	901.825	0.120	4.125
16.025	94.425	282.075	544.425	913.425	0.120	4.950
16.025	94.425	280.875	544.425	904.425	0.120	5.775
16.075	94.425	278.225	552.725	904.325	0.120	6.600
16.075	100.125	277.425	544.425	914.075	0.120	7.425
16.025	94.425	282.075	542.375	913.525	0.160	5.045
15.625	94.425	281.675	552.425	909.375	0.160	1.000
15.575	94.425	281.025	552.575	912.375	0.160	0.825
15.725	100.575	281.525	544.425	894.425	0.160	1.650
15.825	100.675	278.425	544.425	911.275	0.160	2.475
15.875	100.075	277.575	551.925	905.625	0.160	3.300
15.925	94.425	280.075	544.425	894.425	0.160	4.125
15.925	94.425	282.075	542.425	913.225	0.160	4.950
16.025	94.425	280.375	544.425	901.775	0.160	5.775
16.075	94.425	276.925	552.575	901.675	0.160	6.600
16.075	94.425	275.925	544.425	912.625	0.160	7.425
15.925	94.425	282.025	540.025	913.125	0.200	5.025
15.525	94.425	281.625	552.125	907.575	0.200	1.000
15.425	94.425	280.825	552.375	911.375	0.200	0.825
15.625	100.575	281.275	544.425	894.425	0.200	1.650
15.725	100.625	277.425	543.175	910.825	0.200	2.475
15.825	94.425	276.575	551.725	903.025	0.200	3.300

Mode 1	Mode 2	Mode 3	Mode 4	Mode 5	Size	Location
15.925	94.425	279.425	544.425	894.425	0.200	4.125
15.925	94.425	282.025	540.075	912.925	0.200	4.950
16.025	94.425	279.425	544.425	894.425	0.200	5.775
16.075	94.425	275.675	552.325	894.425	0.200	6.600
16.075	94.425	274.425	543.025	910.575	0.200	7.425
15.925	94.425	281.925	537.725	912.525	0.240	5.005
15.425	94.425	281.525	551.675	905.425	0.240	1.000
15.375	94.425	280.675	552.075	910.025	0.240	0.825
15.525	100.525	280.925	542.925	892.875	0.240	1.650
15.675	100.625	276.525	541.675	910.275	0.240	2.475
15.775	94.425	275.625	551.525	900.225	0.240	3.300
15.875	94.425	279.275	544.425	892.425	0.240	4.125
15.925	94.425	281.925	537.775	912.425	0.240	4.950
16.025	94.425	279.275	544.425	894.425	0.240	5.775
16.025	94.425	274.375	551.925	894.425	0.240	6.600
16.075	94.425	273.175	540.925	908.125	0.240	7.425
15.925	94.425	281.925	535.525	911.775	0.280	4.985
15.325	94.425	281.425	551.025	903.075	0.280	1.000
15.275	94.425	280.425	551.675	908.325	0.280	0.825
15.425	100.425	280.625	541.125	890.125	0.280	1.650
15.625	100.575	275.575	540.275	909.425	0.280	2.475
15.725	94.425	274.425	551.325	894.425	0.280	3.300
15.875	94.425	278.925	544.425	889.425	0.280	4.125
15.925	94.425	281.925	535.525	911.675	0.280	4.950
16.025	94.425	278.675	544.425	891.925	0.280	5.775
16.025	94.425	273.125	551.525	894.425	0.280	6.600
16.075	94.425	271.875	538.875	911.075	0.280	7.425
15.925	94.425	281.825	533.375	910.675	0.320	4.965
15.225	94.425	281.275	550.275	900.425	0.320	1.000
15.175	94.425	280.325	551.125	906.225	0.320	0.825
15.375	100.425	280.225	539.275	887.525	0.320	1.650
15.575	100.525	274.425	539.025	908.925	0.320	2.475
15.725	94.425	273.825	551.025	894.025	0.320	3.300
15.825	94.425	278.625	544.275	887.425	0.320	4.125
15.925	94.425	281.825	533.375	910.675	0.320	4.950
15.925	94.425	278.025	543.925	888.625	0.320	5.775
16.025	94.425	271.875	550.925	893.525	0.320	6.600
16.075	94.425	270.575	536.775	907.325	0.320	7.425
15.925	94.425	281.675	531.375	909.325	0.360	4.945
15.125	94.425	281.125	544.425	894.425	0.360	1.000
15.075	94.425	280.125	550.375	903.775	0.360	0.825
15.275	100.425	279.425	537.425	885.225	0.360	1.650
15.425	100.425	273.625	537.825	907.875	0.360	2.475
15.675	94.425	272.925	550.625	890.725	0.360	3.300
15.825	94.425	278.325	542.725	885.375	0.360	4.125
15.925	94.425	281.675	531.375	909.325	0.360	4.950
15.925	94.425	277.325	543.225	885.325	0.360	5.775
16.025	94.425	270.625	550.175	891.775	0.360	6.600
16.075	94.425	269.325	534.425	906.525	0.360	7.425
15.875	94.425	281.525	529.425	907.625	0.400	4.925
15.025	94.425	280.925	544.425	894.425	0.400	1.000
14.425	94.425	279.425	544.425	900.925	0.400	0.825
15.225	100.425	279.275	535.575	883.075	0.400	1.650
15.425	100.375	272.675	536.775	906.575	0.400	2.475
15.625	94.425	272.225	550.125	887.325	0.400	3.300
15.775	94.425	278.075	541.025	883.375	0.400	4.125
15.875	94.425	281.425	529.425	907.625	0.400	4.950
15.925	94.425	276.625	542.525	882.075	0.400	5.775
16.025	94.425	269.425	544.425	890.175	0.400	6.600
16.075	94.425	268.125	532.525	902.025	0.400	7.425
15.875	94.425	281.325	527.525	905.575	0.440	4.905
14.425	94.425	280.675	544.425	891.275	0.440	1.000
14.425	94.425	279.425	544.425	894.425	0.440	0.825

Mode 1	Mode 2	Mode 3	Mode 4	Mode 5	Size	Location
15.175	100.375	278.725	533.725	881.125	0.440	1.650
15.375	100.275	271.725	535.775	904.425	0.440	2.475
15.575	94.425	271.425	544.425	883.875	0.440	3.300
15.775	94.425	277.775	539.275	881.525	0.440	4.125
15.875	94.425	281.275	527.625	905.425	0.440	4.950
15.925	94.425	275.825	541.775	878.875	0.440	5.775
16.025	94.425	268.175	544.425	888.425	0.440	6.600
16.075	94.425	266.925	530.375	900.125	0.440	7.425
15.875	94.425	281.075	525.725	903.125	0.480	4.885
14.425	94.425	280.325	544.425	887.925	0.480	1.000
14.425	94.425	279.325	544.425	894.275	0.480	0.825
15.075	100.325	278.125	531.925	879.375	0.480	1.650
15.325	100.175	270.775	534.425	902.875	0.480	2.475
15.525	94.425	270.775	544.425	880.425	0.480	3.300
15.725	94.425	277.525	537.425	879.425	0.480	4.125
15.875	94.425	281.025	525.875	902.875	0.480	4.950
15.925	94.425	275.025	540.925	875.825	0.480	5.775
16.025	94.425	266.925	544.425	886.725	0.480	6.600
16.075	94.425	265.775	528.225	891.425	0.480	7.425
15.825	94.425	280.825	524.025	900.225	0.520	4.865
14.425	94.425	279.425	543.675	884.425	0.520	1.000
14.425	94.425	278.925	544.425	890.575	0.520	0.825
15.025	100.275	277.425	530.175	877.675	0.520	1.650
15.275	100.075	269.425	533.925	900.325	0.520	2.475
15.525	94.425	270.125	544.425	876.925	0.520	3.300
15.725	94.425	277.225	535.525	877.925	0.520	4.125
15.825	94.425	280.675	524.225	894.425	0.520	4.950
15.925	94.425	274.175	540.175	872.825	0.520	5.775
16.025	94.425	265.775	544.425	884.425	0.520	6.600
16.075	94.425	264.425	526.125	894.125	0.520	7.425
15.825	94.375	280.425	522.375	894.425	0.560	4.845
14.425	94.425	279.425	541.775	881.275	0.560	1.000
14.425	94.425	278.575	543.725	886.675	0.560	0.825
14.425	100.225	276.775	528.425	876.125	0.560	1.650
15.225	94.425	268.925	533.025	894.425	0.560	2.475
15.425	94.425	269.425	544.425	873.575	0.560	3.300
15.675	94.425	276.925	533.575	876.125	0.560	4.125
15.825	94.275	280.275	522.725	894.425	0.560	4.950
15.925	94.425	273.325	539.275	869.425	0.560	5.775
16.025	94.425	264.425	543.925	882.775	0.560	6.600
16.075	94.425	263.625	523.925	885.675	0.560	7.425
15.775	93.925	280.125	520.775	893.075	0.600	4.825
14.425	94.425	279.025	539.425	878.025	0.600	1.000
14.425	94.425	278.075	541.725	882.675	0.600	0.825
14.425	100.175	276.025	526.875	874.425	0.600	1.650
15.175	94.425	268.075	532.175	893.725	0.600	2.475
15.425	94.425	268.875	544.425	870.275	0.600	3.300
15.675	94.425	276.675	531.525	874.175	0.600	4.125
15.825	93.875	279.425	521.275	892.275	0.600	4.950
15.925	94.175	272.425	538.275	867.225	0.600	5.775
16.025	94.425	263.425	542.125	880.525	0.600	6.600
16.075	94.425	262.625	521.875	885.525	0.600	7.425
15.775	93.575	279.425	519.275	888.775	0.640	4.805
14.425	94.425	278.425	537.625	874.425	0.640	1.000
14.425	94.425	277.575	539.425	878.675	0.640	0.825
14.425	100.075	275.225	525.325	872.925	0.640	1.650
15.125	94.425	267.175	531.275	889.425	0.640	2.475
15.425	94.425	268.325	543.875	867.075	0.640	3.300
15.625	94.425	276.375	529.425	872.075	0.640	4.125
15.825	93.425	279.325	519.425	887.825	0.640	4.950
15.925	93.825	271.425	537.125	864.425	0.640	5.775
16.025	94.425	262.325	540.175	877.825	0.640	6.600
16.075	94.425	261.625	519.425	876.925	0.640	7.425

Mode 1	Mode 2	Mode 3	Mode 4	Mode 5	Size	Location
15.775	93.175	279.175	517.825	883.925	0.680	4.785
14.425	94.425	277.825	535.325	871.925	0.680	1.000
14.375	94.425	276.925	537.175	874.425	0.680	0.825
14.425	94.425	274.375	523.825	871.325	0.680	1.650
15.075	94.425	266.375	530.325	884.425	0.680	2.475
15.375	94.425	267.775	542.075	864.025	0.680	3.300
15.625	94.375	276.025	527.375	869.425	0.680	4.125
15.775	93.075	278.775	518.625	882.875	0.680	4.950
15.925	93.425	270.525	535.825	862.225	0.680	5.775
16.025	94.425	261.225	537.925	874.425	0.680	6.600
16.075	94.425	260.675	517.725	875.525	0.680	7.425
15.725	92.825	278.675	516.425	878.625	0.720	4.765
14.425	94.425	277.075	532.925	869.125	0.720	1.000
14.325	94.425	276.225	534.425	870.825	0.720	0.825
14.425	94.425	273.425	522.425	869.425	0.720	1.650
15.025	94.425	265.525	529.375	879.425	0.720	2.475
15.325	94.425	267.275	540.125	861.175	0.720	3.300
15.575	93.925	275.625	525.275	867.075	0.720	4.125
15.775	92.675	278.125	517.375	877.525	0.720	4.950
15.925	93.125	269.425	534.325	859.425	0.720	5.775
16.025	94.425	260.125	535.675	871.175	0.720	6.600
16.075	94.425	259.425	515.675	864.425	0.720	7.425
15.725	92.425	278.075	515.125	872.825	0.760	4.745
14.325	94.425	276.275	530.425	866.575	0.760	1.000
14.225	94.425	275.425	531.925	867.125	0.760	0.825
14.425	94.425	272.525	521.125	867.525	0.760	1.650
14.425	94.425	264.425	528.275	873.775	0.760	2.475
15.325	94.425	266.775	537.875	858.525	0.760	3.300
15.575	93.625	275.225	523.175	864.075	0.760	4.125
15.775	92.275	277.425	516.225	871.725	0.760	4.950
15.925	92.825	268.425	532.675	857.875	0.760	5.775
15.925	94.425	259.025	533.175	867.225	0.760	6.600
16.025	94.425	258.875	513.625	865.525	0.760	7.425
15.725	92.075	277.425	513.875	866.425	0.800	4.725
14.275	94.425	275.375	527.925	864.225	0.800	1.000
14.175	94.425	274.425	529.175	863.625	0.800	0.825
14.425	94.425	271.575	519.425	865.225	0.800	1.650
14.425	94.425	263.925	527.075	867.425	0.800	2.475
15.275	94.425	266.275	535.425	856.025	0.800	3.300
15.525	93.275	274.425	521.075	860.575	0.800	4.125
15.775	91.925	276.625	515.125	865.625	0.800	4.950
15.925	92.425	267.425	530.775	855.925	0.800	5.775
15.925	94.425	257.925	530.425	862.775	0.800	6.600
16.025	94.425	258.025	511.675	855.575	0.800	7.425
15.675	91.725	276.675	512.675	859.425	0.840	4.705
14.175	94.425	274.425	525.425	862.175	0.840	1.000
14.125	94.425	273.675	526.275	860.375	0.840	0.825
14.425	94.425	270.575	518.775	862.575	0.840	1.650
14.425	94.425	263.225	525.775	860.775	0.840	2.475
15.225	94.425	265.825	532.725	853.775	0.840	3.300
15.525	92.875	274.275	518.925	856.575	0.840	4.125
15.725	91.525	275.775	514.025	859.225	0.840	4.950
15.875	92.175	266.375	528.675	854.225	0.840	5.775
15.925	94.425	256.925	527.625	857.625	0.840	6.600
16.025	94.425	257.175	509.425	850.025	0.840	7.425
15.675	91.375	275.875	511.525	852.425	0.880	4.685
14.125	94.425	273.375	522.875	860.325	0.880	1.000
14.025	94.425	272.625	523.325	857.425	0.880	0.825
14.425	94.425	269.425	517.725	859.425	0.880	1.650
14.425	94.425	262.525	524.275	853.775	0.880	2.475
15.225	94.425	265.325	529.425	851.725	0.880	3.300
15.525	92.525	273.725	516.925	852.075	0.880	4.125
15.725	91.175	274.425	512.925	852.575	0.880	4.950

Mode 1	Mode 2	Mode 3	Mode 4	Mode 5	Size	Location
15.875	91.875	265.275	526.325	852.625	0.880	5.775
15.925	94.225	255.925	524.425	852.075	0.880	6.600
16.025	94.425	256.375	507.775	840.425	0.880	7.425
15.625	91.075	275.025	510.425	844.425	0.920	4.665
14.075	94.425	272.225	520.425	858.725	0.920	1.000
13.925	94.425	271.525	520.375	854.425	0.920	0.825
14.425	94.425	268.575	516.775	855.825	0.920	1.650
14.425	94.425	261.875	522.625	844.425	0.920	2.475
15.175	94.425	264.425	526.675	844.425	0.920	3.300
15.425	92.175	273.075	514.425	844.425	0.920	4.125
15.725	90.825	273.875	511.875	844.425	0.920	4.950
15.875	91.575	264.175	523.675	851.125	0.920	5.775
15.925	94.025	254.425	521.425	844.425	0.920	6.600
16.025	94.425	255.575	505.925	835.925	0.920	7.425
15.625	90.725	274.125	509.375	836.925	0.960	4.645
14.025	94.425	271.025	517.925	857.275	0.960	1.000
13.925	94.425	270.325	517.425	852.425	0.960	0.825
14.375	94.425	267.525	515.825	851.625	0.960	1.650
14.425	94.425	261.225	520.725	839.175	0.960	2.475
15.175	94.425	264.425	523.325	844.425	0.960	3.300
15.425	91.775	272.425	513.025	841.275	0.960	4.125
15.725	90.425	272.775	510.825	838.825	0.960	4.950
15.875	91.275	263.075	520.825	844.425	0.960	5.775
15.925	93.775	253.925	518.175	839.425	0.960	6.600
16.025	94.425	254.425	504.075	830.775	0.960	7.425
15.625	90.375	273.125	508.375	828.625	1.000	4.625
13.925	94.425	269.425	515.625	856.075	1.000	1.000
13.825	94.425	269.025	514.425	850.425	1.000	0.825
14.325	94.425	266.425	514.425	844.425	1.000	1.650
14.425	94.425	260.575	518.625	831.825	1.000	2.475
15.125	94.425	263.925	519.425	844.425	1.000	3.300
15.425	91.425	271.625	511.125	835.025	1.000	4.125
15.675	90.125	271.625	509.425	831.875	1.000	4.950
15.875	90.925	261.925	517.675	844.425	1.000	5.775
15.925	93.575	253.025	514.425	832.425	1.000	6.600
16.025	94.425	254.125	502.275	830.025	1.000	7.425
15.575	90.075	272.025	507.375	820.175	1.040	4.605
13.875	94.425	268.425	513.375	855.025	1.040	1.000
13.775	94.425	267.675	511.675	844.425	1.040	0.825
14.275	94.425	265.375	514.175	841.125	1.040	1.650
14.425	94.425	259.425	516.275	824.425	1.040	2.475
15.075	94.125	263.425	516.175	844.425	1.040	3.300
15.425	91.075	270.825	509.325	828.225	1.040	4.125
15.675	89.425	270.425	508.525	824.425	1.040	4.950
15.875	90.675	260.775	514.275	844.425	1.040	5.775
15.925	93.375	252.125	511.175	825.175	1.040	6.600
16.025	94.425	253.375	500.525	820.025	1.040	7.425
15.575	89.425	270.875	506.425	811.425	1.080	4.585
13.825	94.425	267.025	511.175	854.075	1.080	1.000
13.725	94.425	266.275	508.925	844.425	1.080	0.825
14.225	94.425	264.325	513.425	834.425	1.080	1.650
14.425	94.425	259.425	513.675	817.425	1.080	2.475
15.075	93.775	262.925	512.375	844.175	1.080	3.300
15.425	90.725	269.425	507.625	820.925	1.080	4.125
15.675	89.425	269.175	507.225	818.125	1.080	4.950
15.875	90.425	259.425	510.675	844.425	1.080	5.775
15.925	93.175	251.225	507.525	817.525	1.080	6.600
16.025	94.425	252.675	494.425	810.025	1.080	7.425
15.525	89.425	269.425	505.525	802.725	1.120	4.565
13.775	94.425	265.625	509.175	853.175	1.120	1.000
13.675	94.425	264.425	506.325	844.425	1.120	0.825
14.175	94.425	263.275	512.675	827.825	1.120	1.650
14.425	94.425	258.875	510.775	810.625	1.120	2.475

Mode 1	Mode 2	Mode 3	Mode 4	Mode 5	Size	Location
15.025	93.425	262.425	508.425	843.025	1.120	3.300
15.375	90.375	268.925	506.025	813.175	1.120	4.125
15.675	89.175	267.825	505.875	811.425	1.120	4.950
15.875	90.175	258.425	506.775	844.425	1.120	5.775
15.925	93.025	250.375	503.725	809.425	1.120	6.600
16.025	94.425	252.025	494.425	800.025	1.120	7.425
15.525	89.125	268.375	504.425	793.875	1.160	4.545
13.725	94.425	264.125	507.275	852.325	1.160	1.000
13.625	94.425	263.275	503.825	844.425	1.160	0.825
14.125	94.425	262.275	511.925	820.175	1.160	1.650
14.425	94.425	258.375	507.625	804.175	1.160	2.475
15.025	93.075	261.875	504.425	841.875	1.160	3.300
15.375	90.025	267.825	504.425	805.075	1.160	4.125
15.625	88.825	266.425	504.425	805.075	1.160	4.950
15.825	89.425	257.275	502.675	843.075	1.160	5.775
15.925	92.825	244.425	494.425	801.625	1.160	6.600
16.025	94.425	251.325	494.425	792.625	1.160	7.425
15.425	88.825	267.025	503.825	785.075	1.200	4.525
13.675	94.425	262.625	505.525	851.425	1.200	1.000
13.575	94.425	261.675	501.425	844.075	1.200	0.825
14.075	94.425	261.225	511.175	811.875	1.200	1.650
14.425	94.425	257.875	504.175	794.425	1.200	2.475
14.425	92.725	261.325	500.425	840.725	1.200	3.300
15.325	89.425	266.675	503.075	794.425	1.200	4.125
15.625	88.525	264.425	502.825	794.425	1.200	4.950
15.825	89.425	256.075	494.425	841.425	1.200	5.775
15.925	92.625	244.425	494.425	793.425	1.200	6.600
16.025	94.425	250.675	494.175	784.275	1.200	7.425
15.425	88.525	265.625	503.025	776.325	1.240	4.505
13.625	94.425	261.075	503.925	850.425	1.240	1.000
13.525	94.425	260.075	494.425	843.325	1.240	0.825
14.025	94.425	260.225	510.375	803.175	1.240	1.650
14.425	94.425	257.425	500.425	792.575	1.240	2.475
14.425	92.375	260.675	494.425	839.425	1.240	3.300
15.325	89.325	265.425	501.725	788.075	1.240	4.125
15.625	88.225	263.425	501.075	793.275	1.240	4.950
15.825	89.375	254.425	493.925	839.425	1.240	5.775
15.925	92.425	244.425	491.875	785.275	1.240	6.600
16.025	94.425	250.025	492.725	777.275	1.240	7.425
15.425	88.275	264.125	502.225	767.725	1.280	4.485
13.575	94.425	259.425	502.425	844.425	1.280	1.000
13.425	94.425	258.425	494.425	842.675	1.280	0.825
13.925	94.425	259.225	509.425	794.025	1.280	1.650
14.425	94.425	256.925	494.425	787.525	1.280	2.475
14.425	92.025	260.025	492.425	838.125	1.280	3.300
15.325	89.025	264.075	500.525	779.375	1.280	4.125
15.625	87.925	261.875	494.425	787.925	1.280	4.950
15.825	89.125	253.675	489.275	837.575	1.280	5.775
15.925	92.275	244.425	487.825	777.075	1.280	6.600
16.025	94.425	244.425	491.325	769.425	1.280	7.425
15.425	87.925	262.525	501.425	759.275	1.320	4.465
13.525	94.425	257.925	501.175	844.425	1.320	1.000
13.375	94.175	256.725	494.425	842.075	1.320	0.825
13.925	94.425	258.275	508.625	784.425	1.320	1.650
14.425	94.425	256.575	492.325	782.925	1.320	2.475
14.425	91.675	259.275	488.425	836.525	1.320	3.300
15.275	88.675	262.675	494.425	770.625	1.320	4.125
15.625	87.625	260.275	494.425	783.025	1.320	4.950
15.825	88.925	252.525	484.425	835.225	1.320	5.775
15.925	92.075	244.425	483.675	768.875	1.320	6.600
16.025	94.425	244.425	490.025	765.025	1.320	7.425
15.425	87.675	260.925	500.625	751.025	1.360	4.445
13.425	94.425	256.425	494.425	844.425	1.360	1.000

Mode 1	Mode 2	Mode 3	Mode 4	Mode 5	Size	Location
13.325	93.825	255.075	493.725	841.425	1.360	0.825
13.875	94.425	257.375	507.625	775.225	1.360	1.650
14.425	94.425	256.125	487.925	778.925	1.360	2.475
14.425	91.325	258.425	484.425	834.425	1.360	3.300
15.275	88.375	261.175	494.425	761.875	1.360	4.125
15.575	87.375	258.575	494.425	778.625	1.360	4.950
15.825	88.675	251.325	479.425	832.575	1.360	5.775
15.925	91.925	244.425	479.425	760.875	1.360	6.600
16.025	94.425	244.425	488.775	756.525	1.360	7.425
15.375	87.425	259.225	494.425	743.025	1.400	4.425
13.425	94.425	254.425	494.425	844.375	1.400	1.000
13.275	93.525	253.375	492.225	840.725	1.400	0.825
13.875	94.425	256.425	506.425	765.775	1.400	1.650
14.375	94.425	255.725	483.325	775.425	1.400	2.475
14.425	90.925	257.675	480.675	832.525	1.400	3.300
15.275	88.025	259.425	494.425	753.225	1.400	4.125
15.575	87.075	256.875	492.325	774.425	1.400	4.950
15.825	88.425	250.125	474.425	829.425	1.400	5.775
15.925	91.725	244.425	475.375	752.925	1.400	6.600
16.025	94.425	244.425	487.575	750.525	1.400	7.425
15.375	87.175	257.425	494.425	735.275	1.440	4.405
13.375	94.075	253.275	494.425	841.875	1.440	1.000
13.225	93.175	251.675	490.875	839.425	1.440	0.825
13.825	94.425	255.625	505.175	756.525	1.440	1.650
14.375	94.125	255.325	478.575	772.425	1.440	2.475
14.425	90.625	256.775	476.925	829.425	1.440	3.300
15.225	87.725	257.875	494.425	744.425	1.440	4.125
15.575	86.825	255.125	489.425	771.275	1.440	4.950
15.825	88.225	244.425	469.425	826.375	1.440	5.775
15.925	91.525	244.275	471.225	744.425	1.440	6.600
16.025	94.425	244.425	486.425	741.925	1.440	7.425
15.325	86.875	255.675	494.425	727.875	1.480	4.385
13.325	93.725	251.775	494.425	838.825	1.480	1.000
13.175	92.825	250.025	489.425	838.775	1.480	0.825
13.775	94.425	254.425	503.725	744.425	1.480	1.650
14.325	93.725	254.425	473.725	769.425	1.480	2.475
14.425	90.275	255.775	473.325	826.925	1.480	3.300
15.225	87.425	256.175	494.425	736.425	1.480	4.125
15.575	86.525	253.375	486.875	768.325	1.480	4.950
15.775	87.925	244.425	464.425	822.775	1.480	5.775
15.925	91.375	243.625	467.125	737.625	1.480	6.600
16.025	94.425	244.425	485.425	735.825	1.480	7.425
15.325	86.625	253.825	494.425	720.775	1.520	4.365
13.275	93.325	250.275	494.425	835.175	1.520	1.000
13.175	92.425	244.425	488.675	837.375	1.520	0.825
13.725	94.425	253.925	502.075	738.825	1.520	1.650
14.275	93.325	254.425	468.775	767.875	1.520	2.475
14.425	89.425	254.425	469.425	823.575	1.520	3.300
15.225	87.125	254.325	494.425	728.425	1.520	4.125
15.575	86.275	251.575	483.875	765.825	1.520	4.950
15.775	87.775	244.425	459.325	818.875	1.520	5.775
15.925	91.175	242.925	463.025	730.225	1.520	6.600
16.025	94.425	244.425	484.425	729.225	1.520	7.425
15.325	86.375	251.925	494.425	713.925	1.560	4.345
13.225	92.925	244.425	494.425	830.825	1.560	1.000
13.125	92.075	244.425	487.775	835.625	1.560	0.825
13.725	94.425	253.225	500.175	730.575	1.560	1.650
14.275	92.925	254.175	463.775	766.225	1.560	2.475
14.425	89.425	253.625	466.625	819.425	1.560	3.300
15.225	86.825	252.425	494.425	720.725	1.560	4.125
15.525	86.025	244.425	480.725	763.825	1.560	4.950
15.775	87.575	244.425	454.225	814.425	1.560	5.775
15.925	91.025	242.375	458.925	723.075	1.560	6.600

Mode 1	Mode 2	Mode 3	Mode 4	Mode 5	Size	Location
16.025	94.425	244.425	483.425	723.075	1.560	7.425
15.275	86.125	244.425	494.425	707.525	1.600	4.325
13.175	92.525	244.425	494.425	825.725	1.600	1.000
13.075	91.675	244.425	487.025	833.425	1.600	0.825
13.675	93.925	252.525	494.425	722.875	1.600	1.650
14.225	92.425	253.775	458.775	764.425	1.600	2.475
14.425	89.175	252.425	463.575	815.275	1.600	3.300
15.175	86.525	250.525	493.925	713.275	1.600	4.125
15.525	85.775	244.425	477.425	762.175	1.600	4.950
15.775	87.375	244.375	444.425	810.325	1.600	5.775
15.925	90.825	241.775	454.425	716.175	1.600	6.600
16.025	94.425	244.175	482.575	717.775	1.600	7.425
15.275	85.875	244.425	494.425	701.425	1.640	4.305
13.125	92.075	244.425	494.425	819.425	1.640	1.000
13.025	91.275	243.575	486.375	830.675	1.640	0.825
13.625	93.525	251.875	494.425	715.675	1.640	1.650
14.225	92.075	253.375	453.825	763.875	1.640	2.475
14.425	88.825	251.125	460.675	810.425	1.640	3.300
15.175	86.225	244.425	493.425	706.225	1.640	4.125
15.525	85.525	244.425	474.025	760.925	1.640	4.950
15.775	87.175	243.225	444.025	805.675	1.640	5.775
15.925	90.675	241.175	451.025	709.425	1.640	6.600
16.025	94.425	243.425	481.725	713.525	1.640	7.425
15.225	85.625	244.425	494.425	694.425	1.680	4.285
13.125	91.625	244.425	494.425	813.425	1.680	1.000
12.925	90.825	242.075	485.825	827.325	1.680	0.825
13.575	93.075	251.225	493.125	709.075	1.680	1.650
14.175	91.675	252.925	444.425	763.125	1.680	2.475
14.425	88.425	244.425	457.925	805.225	1.680	3.300
15.175	85.925	244.425	492.875	694.425	1.680	4.125
15.525	85.275	244.125	470.525	759.425	1.680	4.950
15.775	86.925	242.125	438.925	800.825	1.680	5.775
15.925	90.425	240.625	444.425	702.925	1.680	6.600
16.025	94.425	242.775	480.875	709.025	1.680	7.425
15.225	85.375	243.875	493.575	690.175	1.720	4.265
13.075	91.175	243.375	494.325	806.275	1.720	1.000
12.925	90.375	240.575	485.375	823.275	1.720	0.825
13.575	92.625	250.675	490.225	703.075	1.720	1.650
14.125	91.225	252.425	444.025	762.575	1.720	2.475
14.425	88.125	244.425	455.425	794.425	1.720	3.300
15.125	85.625	244.375	492.325	693.225	1.720	4.125
15.525	85.075	242.275	466.875	759.275	1.720	4.950
15.775	86.725	241.025	433.925	794.425	1.720	5.775
15.925	90.325	240.125	443.425	694.425	1.720	6.600
16.025	94.425	242.075	480.075	704.425	1.720	7.425
15.175	85.175	241.825	492.725	685.075	1.760	4.245
13.025	90.725	242.125	493.925	794.425	1.760	1.000
12.875	89.425	239.175	485.025	818.575	1.760	0.825
13.525	92.125	250.125	487.075	694.425	1.760	1.650
14.125	90.775	251.925	439.275	762.225	1.760	2.475
14.425	87.775	244.425	453.175	793.675	1.760	3.300
15.125	85.375	242.225	491.775	687.325	1.760	4.125
15.425	84.425	240.375	463.175	758.825	1.760	4.950
15.775	86.575	239.425	429.075	790.625	1.760	5.775
15.925	90.125	239.425	439.425	690.725	1.760	6.600
16.025	94.425	241.375	479.325	700.375	1.760	7.425
15.175	84.425	239.425	491.775	680.325	1.800	4.225
12.925	90.225	240.925	493.675	790.325	1.800	1.000
12.875	89.425	237.825	484.425	813.125	1.800	0.825
13.425	91.625	244.425	483.675	692.925	1.800	1.650
14.075	90.375	251.425	434.425	761.925	1.800	2.475
14.425	87.425	244.425	451.075	787.425	1.800	3.300
15.125	85.075	240.075	491.125	681.875	1.800	4.125

Mode 1	Mode 2	Mode 3	Mode 4	Mode 5	Size	Location
15.425	84.425	238.425	459.425	758.425	1.800	4.950
15.775	86.375	238.925	424.275	785.325	1.800	5.775
15.925	89.425	239.075	436.275	684.425	1.800	6.600
16.025	94.375	240.625	478.575	694.425	1.800	7.425
15.125	84.425	237.575	490.825	675.875	1.840	4.205
12.925	89.425	239.425	493.325	781.775	1.840	1.000
12.825	88.925	236.525	484.425	806.925	1.840	0.825
13.425	91.125	244.425	480.025	688.825	1.840	1.650
14.075	89.425	250.925	430.225	761.675	1.840	2.475
14.425	87.075	243.625	444.425	780.925	1.840	3.300
15.075	84.425	237.875	490.425	676.825	1.840	4.125
15.425	84.375	236.575	455.625	758.125	1.840	4.950
15.725	86.175	237.875	419.425	779.425	1.840	5.775
15.925	89.425	238.575	432.875	679.375	1.840	6.600
15.125	84.425	235.425	489.425	671.725	1.880	4.185
12.925	89.175	238.725	492.925	772.925	1.880	1.000
12.775	88.425	235.325	484.175	800.125	1.880	0.825
13.425	90.625	244.425	476.125	685.225	1.880	1.650
14.025	89.425	250.325	425.925	761.375	1.880	2.475
14.425	86.775	241.925	444.425	774.275	1.880	3.300
15.075	84.425	235.675	489.425	672.225	1.880	4.125
15.425	84.175	234.425	451.825	757.825	1.880	4.950
15.725	85.925	236.875	414.425	774.375	1.880	5.775
15.925	89.425	238.075	429.425	674.025	1.880	6.600
15.075	84.225	233.275	488.775	667.875	1.920	4.165
12.875	88.675	237.725	492.425	763.925	1.920	1.000
12.725	87.925	234.125	483.925	792.675	1.920	0.825
13.375	90.075	244.425	472.075	682.225	1.920	1.650
14.025	89.025	244.425	421.775	761.025	1.920	2.475
14.425	86.425	240.175	444.425	767.425	1.920	3.300
15.075	84.325	233.425	488.725	668.075	1.920	4.125
15.425	83.925	232.825	444.425	757.425	1.920	4.950
15.725	85.775	235.925	410.375	768.775	1.920	5.775
15.925	89.425	237.625	426.425	668.825	1.920	6.600
15.075	84.025	231.125	487.675	664.325	1.960	4.145
12.825	88.125	236.775	491.925	754.425	1.960	1.000
12.675	87.375	233.025	483.675	784.425	1.960	0.825
13.375	89.425	244.425	467.825	679.425	1.960	1.650
13.925	88.575	244.425	417.825	760.525	1.960	2.475
14.425	86.075	238.325	444.425	760.575	1.960	3.300
15.075	84.025	231.225	487.725	664.325	1.960	4.125
15.425	83.775	230.925	444.125	756.825	1.960	4.950
15.725	85.575	234.425	405.925	763.125	1.960	5.775
15.925	89.225	237.175	423.525	663.875	1.960	6.600
15.025	83.825	228.925	486.525	661.075	2.000	4.125
12.775	87.575	235.925	491.275	744.425	2.000	1.000
12.675	86.825	231.925	483.375	776.425	2.000	0.825
13.325	89.025	244.425	463.425	677.625	2.000	1.650
13.925	88.125	244.425	414.125	759.425	2.000	2.475
14.425	85.725	236.425	443.675	753.625	2.000	3.300
15.025	83.825	228.925	486.525	661.075	2.000	4.125
15.425	83.575	229.125	440.275	756.025	2.000	4.950
15.725	85.425	234.025	401.625	757.375	2.000	5.775
15.925	89.025	236.675	420.675	659.125	2.000	6.600
15.025	83.575	226.825	485.275	658.025	2.040	4.105
12.775	87.025	235.075	490.425	737.425	2.040	1.000
12.625	86.275	231.025	482.925	767.875	2.040	0.825
13.275	88.425	244.425	458.925	675.925	2.040	1.650
13.925	87.675	244.425	410.575	758.825	2.040	2.475
14.425	85.425	234.425	442.725	744.425	2.040	3.300
15.025	83.575	226.725	485.175	658.175	2.040	4.125
15.425	83.375	227.275	436.425	754.425	2.040	4.950
15.725	85.225	233.075	394.425	751.625	2.040	5.775

Mode 1	Mode 2	Mode 3	Mode 4	Mode 5	Size	Location
15.925	88.825	236.225	418.025	654.425	2.040	6.600
14.425	83.375	224.425	484.025	655.275	2.080	4.085
12.725	86.425	234.325	489.425	728.925	2.080	1.000
12.575	85.725	230.075	482.575	759.125	2.080	0.825
13.275	87.925	244.425	454.375	674.425	2.080	1.650
13.925	87.225	244.425	407.275	757.525	2.080	2.475
14.425	85.075	232.525	441.925	739.425	2.080	3.300
15.025	83.325	224.425	483.675	655.775	2.080	4.125
15.425	83.175	225.425	432.675	753.425	2.080	4.950
15.725	85.025	232.225	393.375	744.425	2.080	5.775
15.925	88.675	235.775	415.425	650.125	2.080	6.600
14.425	83.175	222.525	482.625	652.775	2.120	4.065
12.675	85.875	233.625	488.425	720.875	2.120	1.000
12.525	85.125	229.225	482.025	750.375	2.120	0.825
13.225	87.375	244.425	444.425	673.725	2.120	1.650
13.875	86.775	244.425	404.225	755.875	2.120	2.475
14.425	84.425	230.525	441.275	732.775	2.120	3.300
14.425	83.075	222.275	482.025	653.725	2.120	4.125
15.425	82.925	223.725	428.925	751.525	2.120	4.950
15.725	84.425	231.375	389.425	739.425	2.120	5.775
15.875	88.425	235.325	413.125	644.425	2.120	6.600
14.425	82.925	220.375	481.175	650.525	2.160	4.045
12.675	85.325	232.925	487.075	713.225	2.160	1.000
12.525	84.425	228.425	481.375	741.675	2.160	0.825
13.175	86.825	244.425	444.425	673.025	2.160	1.650
13.875	86.375	244.425	401.325	753.725	2.160	2.475
14.425	84.425	228.425	440.775	725.925	2.160	3.300
14.425	82.875	220.075	480.175	652.025	2.160	4.125
15.375	82.775	221.925	425.225	744.425	2.160	4.950
15.675	84.425	230.525	385.575	734.075	2.160	5.775
15.875	88.275	234.425	410.925	641.875	2.160	6.600
14.425	82.775	218.275	479.425	644.425	2.200	4.025
12.625	84.425	232.325	485.525	705.925	2.200	1.000
12.425	83.925	227.725	480.575	733.125	2.200	0.825
13.175	86.275	244.425	440.425	672.575	2.200	1.650
13.825	85.925	243.625	394.425	751.175	2.200	2.475
14.425	84.125	226.375	440.325	719.225	2.200	3.300
14.425	82.625	217.875	478.125	650.725	2.200	4.125
15.375	82.625	220.225	421.525	744.425	2.200	4.950
15.675	84.425	229.425	381.875	728.175	2.200	5.775
15.875	88.075	234.425	408.925	638.025	2.200	6.600
14.425	82.575	216.175	478.075	644.425	2.240	4.005
12.575	84.125	231.825	483.725	694.425	2.240	1.000
12.425	83.375	227.025	479.425	724.425	2.240	0.825
13.125	85.725	244.425	435.775	672.275	2.240	1.650
13.825	85.425	242.425	394.425	744.425	2.240	2.475
14.425	83.825	224.325	440.025	712.575	2.240	3.300
14.425	82.425	215.675	475.925	644.425	2.240	4.125
15.375	82.425	218.525	417.925	743.075	2.240	4.950
15.675	84.275	228.925	378.275	722.275	2.240	5.775
15.875	87.875	233.925	407.025	634.325	2.240	6.600
14.425	82.375	214.075	476.375	644.425	2.280	3.985
12.575	83.525	231.325	481.675	693.025	2.280	1.000
12.425	82.825	226.425	478.425	716.925	2.280	0.825
13.125	85.175	244.425	431.225	672.125	2.280	1.650
13.775	85.025	241.275	394.075	744.425	2.280	2.475
14.425	83.525	222.225	439.425	706.125	2.280	3.300
14.425	82.225	213.525	473.525	644.425	2.280	4.125
15.375	82.225	216.875	414.375	739.325	2.280	4.950
15.675	84.075	228.225	374.425	716.375	2.280	5.775
15.875	87.675	233.525	405.325	630.775	2.280	6.600
14.425	82.175	212.025	474.425	643.425	2.320	3.965
12.525	82.925	230.875	479.375	687.375	2.320	1.000

Mode 1	Mode 2	Mode 3	Mode 4	Mode 5	Size	Location
12.375	82.225	225.875	477.075	709.375	2.320	0.825
13.075	84.425	244.425	426.675	672.025	2.320	1.650
13.775	84.425	240.025	392.075	740.425	2.320	2.475
14.375	83.225	220.075	439.425	694.425	2.320	3.300
14.425	81.925	211.375	470.925	644.425	2.320	4.125
15.375	82.075	215.275	410.825	735.125	2.320	4.950
15.675	83.875	227.525	371.425	710.425	2.320	5.775
15.875	87.425	233.025	403.775	627.425	2.320	6.600
14.425	81.925	209.425	472.675	642.175	2.360	3.945
12.425	82.325	230.425	476.775	682.225	2.360	1.000
12.325	81.625	225.325	475.425	702.325	2.360	0.825
13.075	84.075	244.425	422.225	672.025	2.360	1.650
13.725	84.175	238.675	390.275	735.925	2.360	2.475
14.375	82.925	217.925	439.375	693.725	2.360	3.300
14.425	81.775	209.275	468.275	644.425	2.360	4.125
15.325	81.875	213.675	407.375	730.425	2.360	4.950
15.675	83.725	226.875	368.225	704.425	2.360	5.775
15.875	87.225	232.575	402.375	624.275	2.360	6.600
14.425	81.775	207.925	470.725	641.025	2.400	3.925
12.425	81.725	230.075	473.875	677.675	2.400	1.000
12.325	80.925	224.425	473.575	694.425	2.400	0.825
13.025	83.525	244.425	417.875	671.925	2.400	1.650
13.725	83.725	237.275	388.725	730.925	2.400	2.475
14.325	82.625	215.875	439.225	687.825	2.400	3.300
14.425	81.575	207.225	465.425	644.425	2.400	4.125
15.325	81.725	212.125	403.925	725.425	2.400	4.950
15.675	83.525	226.225	365.125	694.425	2.400	5.775
15.875	87.025	232.075	401.125	621.225	2.400	6.600
14.425	81.575	206.025	468.625	640.025	2.440	3.905
12.425	81.125	229.425	470.775	673.675	2.440	1.000
12.275	80.375	224.425	471.425	689.425	2.440	0.825
12.925	82.925	244.425	413.675	671.875	2.440	1.650
13.675	83.325	235.825	387.325	725.525	2.440	2.475
14.325	82.325	213.775	439.025	682.175	2.440	3.300
14.425	81.375	205.175	462.425	644.425	2.440	4.125
15.325	81.525	210.575	400.675	720.075	2.440	4.950
15.675	83.325	225.625	362.175	692.775	2.440	5.775
15.875	86.825	231.575	394.425	618.425	2.440	6.600
14.425	81.375	204.075	466.425	639.125	2.480	3.885
12.425	80.525	229.425	467.425	670.225	2.480	1.000
12.225	79.425	224.125	469.125	684.075	2.480	0.825
12.925	82.425	244.425	409.425	671.675	2.480	1.650
13.675	82.875	234.325	386.075	719.425	2.480	2.475
14.325	82.075	211.625	438.875	676.775	2.480	3.300
14.425	81.225	203.175	459.425	644.425	2.480	4.125
15.325	81.375	209.125	394.425	714.375	2.480	4.950
15.625	83.125	225.075	359.275	686.925	2.480	5.775
15.875	86.575	231.075	394.425	615.725	2.480	6.600
14.425	81.175	202.125	464.225	638.425	2.520	3.865
12.375	79.425	229.275	463.825	667.225	2.520	1.000
12.225	79.175	223.775	466.425	679.075	2.520	0.825
12.925	81.875	244.425	405.575	671.325	2.520	1.650
13.625	82.425	232.725	385.075	713.675	2.520	2.475
14.275	81.775	209.425	438.625	671.625	2.520	3.300
14.425	81.025	201.175	456.225	644.425	2.520	4.125
15.325	81.225	207.675	394.175	708.425	2.520	4.950
15.625	82.925	224.425	356.575	681.175	2.520	5.775
15.875	86.375	230.525	394.425	613.225	2.520	6.600
14.425	81.025	200.225	461.875	637.775	2.560	3.845
12.325	79.325	229.025	460.025	664.425	2.560	1.000
12.175	78.575	223.425	463.625	674.425	2.560	0.825
12.925	81.325	244.325	401.725	670.825	2.560	1.650
13.625	82.075	231.125	384.175	707.375	2.560	2.475

Mode 1	Mode 2	Mode 3	Mode 4	Mode 5	Size	Location
14.275	81.525	207.425	438.275	666.775	2.560	3.300
14.425	80.825	194.425	452.925	644.425	2.560	4.125
15.275	81.025	206.275	391.025	702.275	2.560	4.950
15.625	82.725	223.925	353.925	675.425	2.560	5.775
15.875	86.125	229.425	394.425	610.925	2.560	6.600
14.425	80.825	194.425	459.375	637.275	2.600	3.825
12.325	78.725	228.875	456.075	662.675	2.600	1.000
12.175	77.925	223.225	460.425	670.775	2.600	0.825
12.875	80.775	243.925	394.425	670.125	2.600	1.650
13.575	81.625	229.425	383.425	700.875	2.600	2.475
14.275	81.275	205.425	437.875	662.275	2.600	3.300
14.425	80.675	194.425	444.425	644.425	2.600	4.125
15.275	80.875	204.425	387.925	694.425	2.600	4.950
15.625	82.525	223.425	351.425	669.425	2.600	5.775
15.875	85.925	229.425	394.425	608.825	2.600	6.600
14.425	80.625	194.425	456.825	636.875	2.640	3.805
12.275	78.125	228.675	451.925	661.025	2.640	1.000
12.125	77.375	223.025	457.125	667.375	2.640	0.825
12.875	80.225	243.625	394.425	669.175	2.640	1.650
13.575	81.225	227.775	382.825	694.275	2.640	2.475
14.225	80.925	203.375	437.325	658.025	2.640	3.300
14.425	80.425	194.425	444.425	644.425	2.640	4.125
15.275	80.725	203.625	384.425	689.425	2.640	4.950
15.625	82.325	223.025	344.425	664.125	2.640	5.775
15.875	85.675	228.825	394.425	606.825	2.640	6.600
14.425	80.425	194.425	454.225	636.525	2.680	3.785
12.275	77.575	228.525	444.425	659.425	2.680	1.000
12.075	76.775	222.825	453.575	664.425	2.680	0.825
12.825	79.425	243.275	391.125	667.925	2.680	1.650
13.525	80.825	226.025	382.375	687.575	2.680	2.475
14.225	80.725	201.375	436.675	654.175	2.680	3.300
14.425	80.325	193.675	442.725	644.425	2.680	4.125
15.275	80.525	202.375	381.925	682.925	2.680	4.950
15.625	82.125	222.575	344.425	658.625	2.680	5.775
14.425	80.275	193.025	451.425	636.275	2.720	3.765
12.225	76.925	228.425	443.375	658.775	2.720	1.000
12.075	76.175	222.675	444.425	662.075	2.720	0.825
12.825	79.175	242.825	387.925	666.425	2.720	1.650
13.525	80.425	224.275	381.925	680.875	2.720	2.475
14.175	80.425	194.425	435.875	650.625	2.720	3.300
14.425	80.125	191.925	439.225	644.425	2.720	4.125
15.275	80.375	201.175	379.025	676.425	2.720	4.950
15.625	81.925	222.175	344.425	653.225	2.720	5.775
14.425	80.075	191.275	444.425	636.075	2.760	3.745
12.175	76.375	228.325	439.025	658.075	2.760	1.000
12.025	75.575	222.525	444.425	660.075	2.760	0.825
12.775	78.625	242.325	384.425	664.425	2.760	1.650
13.525	80.075	222.425	381.725	674.175	2.760	2.475
14.175	80.225	194.425	434.425	644.425	2.760	3.300
14.425	79.425	190.175	435.625	644.425	2.760	4.125
15.225	80.225	200.025	376.125	669.425	2.760	4.950
15.625	81.725	221.825	342.425	644.425	2.760	5.775
14.425	79.425	189.425	444.425	635.925	2.800	3.725
12.175	75.825	228.225	434.425	657.575	2.800	1.000
12.025	75.025	222.425	441.875	658.425	2.800	0.825
12.775	78.125	241.775	382.025	662.425	2.800	1.650
13.425	79.425	220.675	381.525	667.575	2.800	2.475
14.175	80.025	194.425	433.725	644.425	2.800	3.300
14.425	79.425	188.425	432.075	644.275	2.800	4.125
15.225	80.025	194.425	373.375	663.175	2.800	4.950
15.575	81.425	221.425	340.525	642.675	2.800	5.775
14.425	79.425	187.925	442.775	635.875	2.840	3.705
12.125	75.225	228.125	430.225	657.275	2.840	1.000

Mode 1	Mode 2	Mode 3	Mode 4	Mode 5	Size	Location
11.925	74.425	222.325	437.725	657.225	2.840	0.825
12.725	77.625	241.175	379.375	659.425	2.840	1.650
13.425	79.275	218.825	381.375	661.075	2.840	2.475
14.125	79.425	193.525	432.425	642.175	2.840	3.300
14.425	79.425	186.825	428.425	642.925	2.840	4.125
15.225	79.425	194.425	370.625	656.575	2.840	4.950
15.575	81.275	221.075	338.725	637.625	2.840	5.775
14.425	79.425	186.325	439.425	635.775	2.880	3.685
12.125	74.425	228.025	425.825	657.125	2.880	1.000
11.925	73.875	222.225	433.525	656.275	2.880	0.825
12.725	77.125	240.525	376.875	657.125	2.880	1.650
13.425	78.925	217.025	381.275	654.425	2.880	2.475
14.125	79.425	191.675	430.875	640.025	2.880	3.300
14.425	79.425	185.225	424.425	641.325	2.880	4.125
15.225	79.425	194.425	367.925	650.075	2.880	4.950
15.575	81.075	220.775	336.925	632.725	2.880	5.775
14.375	79.375	184.425	436.625	635.775	2.920	3.665
12.075	74.125	227.875	421.425	657.025	2.920	1.000
11.925	73.275	222.125	429.275	655.575	2.920	0.825
12.675	76.625	239.425	374.425	654.025	2.920	1.650
13.425	78.575	215.175	381.225	644.425	2.920	2.475
14.125	79.325	189.425	429.175	638.275	2.920	3.300
14.425	79.375	183.675	421.175	639.425	2.920	4.125
15.225	79.425	194.425	365.325	643.625	2.920	4.950
15.575	80.825	220.425	335.375	627.925	2.920	5.775
14.375	79.175	183.225	433.425	635.775	2.960	3.645
12.075	73.575	227.775	417.175	657.025	2.960	1.000
11.875	72.725	222.025	425.025	655.125	2.960	0.825
12.675	76.125	238.925	372.425	650.625	2.960	1.650
13.375	78.225	213.325	381.175	642.625	2.960	2.475
14.075	79.075	187.925	427.275	636.775	2.960	3.300
14.425	79.225	182.175	417.575	637.325	2.960	4.125
15.175	79.375	194.425	362.725	637.225	2.960	4.950
15.575	80.625	220.175	333.825	623.325	2.960	5.775
14.325	79.025	181.725	430.225	635.775	3.000	3.625
12.025	73.025	227.675	412.925	657.025	3.000	1.000
11.875	72.175	221.925	420.775	654.425	3.000	0.825
12.625	75.625	238.125	370.525	644.425	3.000	1.650
13.375	77.875	211.425	381.125	636.875	3.000	2.475
14.075	78.875	186.225	425.175	635.575	3.000	3.300
14.425	79.075	180.675	413.925	634.425	3.000	4.125
15.175	79.225	193.925	360.225	630.925	3.000	4.950
15.575	80.375	219.425	332.425	618.875	3.000	5.775
14.275	78.825	180.225	426.925	635.775	3.040	3.605
12.025	72.425	227.525	408.825	656.925	3.040	1.000
11.825	71.625	221.875	416.525	654.425	3.040	0.825
12.625	75.175	237.175	368.775	643.075	3.040	1.650
13.375	77.525	209.425	381.075	631.375	3.040	2.475
14.025	78.675	184.425	422.925	634.425	3.040	3.300
14.425	78.925	179.225	410.325	632.425	3.040	4.125
15.175	79.025	193.075	357.775	624.425	3.040	4.950
15.575	80.175	219.425	331.125	614.425	3.040	5.775
14.275	78.675	178.775	423.675	635.725	3.080	3.585
11.925	71.925	227.375	404.425	656.875	3.080	1.000
11.825	71.075	221.775	412.325	654.425	3.080	0.825
12.575	74.425	236.125	367.175	638.925	3.080	1.650
13.325	77.175	207.775	381.025	626.175	3.080	2.475
14.025	78.425	182.725	420.425	634.025	3.080	3.300
14.425	78.775	177.825	406.725	629.425	3.080	4.125
15.175	78.875	192.275	355.425	618.775	3.080	4.950
15.525	79.425	219.325	329.425	610.525	3.080	5.775
14.225	78.425	177.375	420.325	635.725	3.120	3.565
11.925	71.425	227.175	400.925	656.675	3.120	1.000

Mode 1	Mode 2	Mode 3	Mode 4	Mode 5	Size	Location
11.775	70.525	221.675	408.225	654.425	3.120	0.825
12.575	74.225	235.025	365.725	634.425	3.120	1.650
13.325	76.825	205.925	380.875	621.225	3.120	2.475
14.025	78.275	181.025	417.875	633.575	3.120	3.300
14.425	78.625	176.425	403.125	626.725	3.120	4.125
15.125	78.725	191.525	353.075	612.875	3.120	4.950
15.525	79.425	219.025	328.825	606.625	3.120	5.775
14.175	78.325	176.025	416.925	635.625	3.160	3.545
11.925	70.875	226.925	394.425	656.275	3.160	1.000
11.775	70.025	221.525	404.175	654.425	3.160	0.825
12.525	73.775	233.875	364.425	630.275	3.160	1.650
13.275	76.525	204.075	380.725	616.575	3.160	2.475
13.925	78.075	179.375	415.125	633.275	3.160	3.300
14.425	78.425	175.175	394.425	623.625	3.160	4.125
15.125	78.525	190.775	350.825	607.125	3.160	4.950
15.525	79.425	218.775	327.775	602.925	3.160	5.775
14.175	78.125	174.425	413.525	635.525	3.200	3.525
11.925	70.375	226.675	393.575	655.775	3.200	1.000
11.725	69.425	221.375	400.275	654.425	3.200	0.825
12.525	73.325	232.675	363.375	625.775	3.200	1.650
13.275	76.175	202.275	380.425	612.275	3.200	2.475
13.925	77.875	177.775	412.275	633.125	3.200	3.300
14.425	78.375	173.925	394.425	620.375	3.200	4.125
15.125	78.375	190.125	344.425	601.525	3.200	4.950
15.525	79.275	218.525	326.875	594.425	3.200	5.775
14.125	77.925	173.375	410.075	635.375	3.240	3.505
11.875	69.425	226.375	390.075	655.025	3.240	1.000
11.725	68.925	221.225	394.425	654.425	3.240	0.825
12.425	72.875	231.375	362.425	621.225	3.240	1.650
13.225	75.875	200.425	380.125	608.275	3.240	2.475
13.925	77.725	176.175	409.275	633.075	3.240	3.300
14.425	78.225	172.675	392.575	617.075	3.240	4.125
15.125	78.175	189.425	344.425	594.425	3.240	4.950
15.525	79.025	218.225	326.075	594.425	3.240	5.775
14.075	77.775	172.125	406.625	635.125	3.280	3.485
11.875	69.375	226.025	386.775	654.075	3.280	1.000
11.675	68.425	220.925	392.725	654.175	3.280	0.825
12.425	72.425	230.025	361.625	616.625	3.280	1.650
13.225	75.575	194.425	379.425	604.425	3.280	2.475
13.925	77.525	174.425	406.175	633.025	3.280	3.300
14.425	78.075	171.525	389.125	613.625	3.280	4.125
15.125	77.925	188.875	344.325	590.775	3.280	4.950
15.525	78.775	217.925	325.325	593.125	3.280	5.775
14.075	77.575	170.875	403.175	634.425	3.320	3.465
11.825	68.925	225.625	383.625	652.825	3.320	1.000
11.675	67.925	220.775	389.175	653.825	3.320	0.825
12.425	72.025	228.575	360.925	611.925	3.320	1.650
13.225	75.275	194.425	379.175	601.225	3.320	2.475
13.925	77.375	173.125	403.025	633.025	3.320	3.300
14.425	77.925	170.375	385.675	610.125	3.320	4.125
15.075	77.825	188.325	342.325	585.675	3.320	4.950
15.525	78.525	217.675	324.425	590.325	3.320	5.775
14.025	77.425	169.425	394.425	634.425	3.360	3.445
11.825	68.425	225.175	380.675	651.325	3.360	1.000
11.625	67.525	220.425	385.775	653.225	3.360	0.825
12.425	71.625	227.125	360.375	607.425	3.360	1.650
13.175	74.425	194.425	378.525	594.425	3.360	2.475
13.875	77.175	171.625	394.425	633.025	3.360	3.300
14.425	77.825	169.275	382.275	606.575	3.360	4.125
15.075	77.625	187.825	340.325	580.675	3.360	4.950
15.425	78.325	217.375	324.125	587.725	3.360	5.775
13.925	77.225	168.525	394.425	634.025	3.400	3.425
11.775	67.925	224.425	377.875	644.425	3.400	1.000

Mode 1	Mode 2	Mode 3	Mode 4	Mode 5	Size	Location
11.625	67.025	220.125	382.425	652.425	3.400	0.825
12.375	71.225	225.625	359.425	602.825	3.400	1.650
13.175	74.425	193.425	377.775	594.425	3.400	2.475
13.875	77.025	170.175	394.425	632.925	3.400	3.300
14.425	77.725	168.225	378.925	603.025	3.400	4.125
15.075	77.425	187.325	338.425	575.875	3.400	4.950
15.425	78.075	217.025	323.625	585.325	3.400	5.775
13.925	77.075	167.375	392.875	633.425	3.440	3.405
11.775	67.425	224.125	375.225	644.425	3.440	1.000
11.575	66.575	219.425	379.375	651.425	3.440	0.825
12.375	70.825	224.025	359.425	594.425	3.440	1.650
13.125	74.425	191.725	376.875	593.175	3.440	2.475
13.875	76.875	168.775	393.075	632.675	3.440	3.300
14.425	77.575	167.225	375.675	594.425	3.440	4.125
15.075	77.275	186.875	336.575	571.275	3.440	4.950
15.425	77.825	216.725	323.225	583.175	3.440	5.775
13.925	76.875	166.275	389.425	632.825	3.480	3.385
11.725	67.025	223.425	372.775	644.425	3.480	1.000
11.575	66.075	219.325	376.425	650.175	3.480	0.825
12.325	70.425	222.425	359.325	593.925	3.480	1.650
13.125	74.175	190.025	375.825	591.125	3.480	2.475
13.825	76.725	167.375	389.425	632.325	3.480	3.300
14.425	77.425	166.225	372.425	594.425	3.480	4.125
15.025	77.075	186.425	334.425	566.825	3.480	4.950
13.875	76.725	165.175	386.025	632.075	3.520	3.365
11.725	66.625	222.775	370.525	642.575	3.520	1.000
11.525	65.625	218.875	373.675	644.425	3.520	0.825
12.325	70.025	220.775	359.125	589.425	3.520	1.650
13.075	73.875	188.375	374.425	589.375	3.520	2.475
13.825	76.575	166.025	386.275	631.825	3.520	3.300
14.425	77.325	165.275	369.225	592.125	3.520	4.125
15.025	76.875	186.075	333.075	562.525	3.520	4.950
13.825	76.525	164.125	382.625	631.225	3.560	3.345
11.675	66.175	222.025	368.425	639.425	3.560	1.000
11.525	65.175	218.325	371.075	644.425	3.560	0.825
12.275	69.425	219.125	358.925	585.425	3.560	1.650
13.075	73.625	186.725	373.425	587.875	3.560	2.475
13.825	76.425	164.425	382.825	631.125	3.560	3.300
14.425	77.175	164.375	366.125	588.525	3.560	4.125
15.025	76.675	185.725	331.425	558.425	3.560	4.950
13.825	76.325	163.125	379.275	630.175	3.600	3.325
11.675	65.725	221.225	366.425	636.575	3.600	1.000
11.425	64.425	217.725	368.625	644.425	3.600	0.825
12.275	69.275	217.425	358.925	581.425	3.600	1.650
13.075	73.375	185.125	371.925	586.675	3.600	2.475
13.775	76.275	163.425	379.425	630.225	3.600	3.300
14.425	77.075	163.525	363.025	584.425	3.600	4.125
15.025	76.425	185.425	329.425	554.425	3.600	4.950
13.775	76.175	162.125	375.925	629.075	3.640	3.305
11.625	65.325	220.325	364.425	633.225	3.640	1.000
11.425	64.325	217.075	366.375	642.225	3.640	0.825
12.225	68.925	215.675	358.875	577.525	3.640	1.650
13.025	73.125	183.525	370.425	585.725	3.640	2.475
13.775	76.125	162.225	375.925	629.075	3.640	3.300
14.425	76.925	162.725	360.025	581.325	3.640	4.125
14.425	76.275	185.125	328.325	550.725	3.640	4.950
13.725	75.925	161.175	372.675	627.775	3.680	3.285
11.625	64.425	219.325	363.175	629.425	3.680	1.000
11.425	63.925	216.325	364.275	639.425	3.680	0.825
12.225	68.575	213.925	358.875	573.825	3.680	1.650
13.025	72.925	181.925	368.775	585.025	3.680	2.475
13.725	76.025	160.925	372.575	627.725	3.680	3.300
14.425	76.775	161.925	357.075	577.825	3.680	4.125

Mode 1	Mode 2	Mode 3	Mode 4	Mode 5	Size	Location
14.425	76.075	184.425	326.875	544.425	3.680	4.950
13.675	75.775	160.225	369.375	626.375	3.720	3.265
11.575	64.425	218.325	361.775	625.925	3.720	1.000
11.425	63.425	215.575	362.375	636.525	3.720	0.825
12.225	68.225	212.175	358.875	570.275	3.720	1.650
12.925	72.675	180.375	367.025	584.425	3.720	2.475
13.725	75.875	159.425	369.175	626.075	3.720	3.300
14.425	76.675	161.175	354.175	574.275	3.720	4.125
14.425	75.875	184.425	325.525	543.725	3.720	4.950
13.675	75.625	159.325	366.175	624.425	3.760	3.245
11.575	64.125	217.225	360.525	622.125	3.760	1.000
11.375	63.075	214.425	360.625	633.275	3.760	0.825
12.175	67.925	210.425	358.825	566.925	3.760	1.650
12.925	72.425	178.875	365.125	584.125	3.760	2.475
13.725	75.775	158.675	365.775	624.275	3.760	3.300
14.375	76.525	160.425	351.325	570.825	3.760	4.125
14.425	75.675	184.425	324.225	540.425	3.760	4.950
13.625	75.425	158.425	362.925	623.075	3.800	3.225
11.525	63.725	216.075	359.425	618.125	3.800	1.000
11.375	62.725	213.775	359.025	629.425	3.800	0.825
12.175	67.575	208.675	358.825	563.725	3.800	1.650
12.925	72.225	177.375	363.175	583.925	3.800	2.475
13.675	75.625	157.525	362.425	622.175	3.800	3.300
14.375	76.375	159.425	344.425	567.425	3.800	4.125
14.425	75.425	184.225	322.925	537.425	3.800	4.950
13.575	75.225	157.625	359.425	621.225	3.840	3.205
11.525	63.375	214.425	358.425	614.075	3.840	1.000
11.325	62.325	212.825	357.625	626.175	3.840	0.825
12.125	67.275	206.875	358.775	560.775	3.840	1.650
12.925	72.025	175.875	361.125	583.775	3.840	2.475
13.675	75.525	156.425	359.125	619.425	3.840	3.300
14.375	76.275	159.175	344.425	564.025	3.840	4.125
14.425	75.275	184.025	321.825	534.425	3.840	4.950
13.575	75.025	156.775	356.725	619.225	3.880	3.185
11.425	62.925	213.625	357.625	609.425	3.880	1.000
11.325	61.925	211.775	356.325	622.275	3.880	0.825
12.125	66.925	205.075	358.725	558.025	3.880	1.650
12.875	71.825	174.425	358.925	583.725	3.880	2.475
13.675	75.425	155.375	355.875	617.425	3.880	3.300
14.325	76.125	158.575	343.275	560.725	3.880	4.125
14.425	75.025	183.875	320.725	531.825	3.880	4.950
13.525	74.425	155.925	353.675	617.075	3.920	3.165
11.425	62.625	212.275	356.925	605.725	3.920	1.000
11.275	61.575	210.675	355.225	618.275	3.920	0.825
12.075	66.675	203.325	358.575	555.425	3.920	1.650
12.875	71.625	173.025	356.775	583.675	3.920	2.475
13.625	75.275	154.375	352.675	614.425	3.920	3.300
14.325	75.925	157.925	340.725	557.425	3.920	4.125
14.425	74.425	183.675	319.425	529.275	3.920	4.950
13.425	74.425	155.225	350.675	614.425	3.960	3.145
11.425	62.275	210.925	356.375	601.525	3.960	1.000
11.275	61.225	209.425	354.225	614.175	3.960	0.825
12.075	66.375	201.525	358.425	553.125	3.960	1.650
12.875	71.425	171.625	354.425	583.675	3.960	2.475
13.625	75.175	153.375	344.425	611.825	3.960	3.300
14.325	75.825	157.425	338.225	554.275	3.960	4.125
14.425	74.425	183.575	318.775	526.925	3.960	4.950
13.425	74.425	154.425	344.425	612.325	4.000	3.125
11.425	61.925	209.425	355.925	594.425	4.000	1.000
11.225	60.875	208.325	353.425	609.425	4.000	0.825
12.025	66.075	194.425	358.175	551.025	4.000	1.650
12.825	71.225	170.225	352.175	583.575	4.000	2.475
13.575	75.075	152.425	344.425	608.775	4.000	3.300

Mode 1	Mode 2	Mode 3	Mode 4	Mode 5	Size	Location
14.275	75.725	156.925	335.825	551.125	4.000	4.125
14.425	74.425	183.425	317.875	524.425	4.000	4.950
13.375	74.275	153.725	344.425	609.425	4.040	3.105
11.375	61.625	208.075	355.575	593.175	4.040	1.000
11.225	60.525	207.075	352.675	605.675	4.040	0.825
12.025	65.775	194.425	357.825	544.425	4.040	1.650
12.825	71.075	168.925	344.425	583.425	4.040	2.475
13.575	74.425	151.425	343.275	605.575	4.040	3.300
14.275	75.575	156.425	333.425	544.425	4.040	4.125
14.425	74.175	183.275	317.075	522.725	4.040	4.950
13.375	74.075	153.025	342.025	606.925	4.080	3.085
11.375	61.275	206.575	355.275	589.025	4.080	1.000
11.175	60.175	205.775	352.125	601.325	4.080	0.825
11.925	65.525	194.425	357.425	544.425	4.080	1.650
12.775	70.875	167.575	344.425	583.125	4.080	2.475
13.575	74.425	150.575	340.275	602.225	4.080	3.300
14.275	75.425	156.075	331.225	544.425	4.080	4.125
14.425	73.925	183.175	316.375	520.875	4.080	4.950
13.325	73.925	152.325	339.225	604.125	4.120	3.065
11.325	60.925	205.025	355.075	584.425	4.120	1.000
11.175	59.425	204.425	351.625	594.425	4.120	0.825
11.925	65.275	194.425	356.925	544.425	4.120	1.650
12.775	70.725	166.275	344.425	582.725	4.120	2.475
13.525	74.425	144.425	337.325	594.425	4.120	3.300
14.225	75.275	155.675	329.025	542.125	4.120	4.125
14.425	73.725	183.025	315.675	519.175	4.120	4.950
13.275	73.725	151.675	336.425	601.125	4.160	3.045
11.325	60.675	203.525	354.425	581.025	4.160	1.000
11.175	59.425	203.075	351.225	592.625	4.160	0.825
11.925	65.025	192.825	356.375	544.425	4.160	1.650
12.725	70.575	165.025	342.525	582.125	4.160	2.475
13.525	74.425	144.425	334.425	594.425	4.160	3.300
14.225	75.125	155.275	326.925	539.275	4.160	4.125
14.425	73.525	182.925	315.125	517.675	4.160	4.950
13.225	73.525	151.025	333.775	594.425	4.200	3.025
11.275	60.375	201.925	354.425	577.125	4.200	1.000
11.125	59.225	201.625	350.925	588.325	4.200	0.825
11.925	64.425	191.125	355.725	543.675	4.200	1.650
12.725	70.425	163.775	340.075	581.325	4.200	2.475
13.425	74.425	144.425	331.575	591.575	4.200	3.300
14.225	74.425	154.425	324.425	536.425	4.200	4.125
14.425	73.325	182.775	314.425	516.325	4.200	4.950
13.225	73.325	150.375	331.125	594.425	4.240	3.005
11.275	60.075	200.325	354.425	573.375	4.240	1.000
11.125	58.925	200.175	350.725	584.125	4.240	0.825
11.925	64.425	189.425	354.425	542.825	4.240	1.650
12.725	70.275	162.575	337.575	580.325	4.240	2.475
13.425	74.425	144.425	328.775	587.825	4.240	3.300
14.175	74.425	154.425	322.925	533.775	4.240	4.125
14.425	73.075	182.625	314.125	515.075	4.240	4.950
13.175	73.125	144.425	328.575	591.425	4.280	2.985
11.275	59.425	194.425	354.425	569.425	4.280	1.000
11.075	58.625	194.425	350.525	579.425	4.280	0.825
11.875	64.275	187.775	354.075	542.125	4.280	1.650
12.675	70.125	161.375	335.125	579.075	4.280	2.475
13.425	74.375	144.425	326.075	584.025	4.280	3.300
14.175	74.425	154.325	321.075	531.125	4.280	4.125
14.425	72.875	182.425	313.675	514.025	4.280	4.950
13.125	72.925	144.425	326.075	588.025	4.320	2.965
11.225	59.425	194.425	354.425	566.275	4.320	1.000
11.075	58.325	194.425	350.425	575.825	4.320	0.825
11.875	64.025	186.125	353.125	541.575	4.320	1.650
12.675	69.425	160.175	332.675	577.575	4.320	2.475

Mode 1	Mode 2	Mode 3	Mode 4	Mode 5	Size	Location
13.425	74.275	144.425	323.425	580.175	4.320	3.300
14.175	74.425	154.025	319.275	528.525	4.320	4.125
13.075	72.725	144.425	323.575	584.425	4.360	2.945
11.225	59.225	194.425	354.425	562.925	4.360	1.000
11.025	58.025	194.425	350.375	571.875	4.360	0.825
11.825	63.825	184.425	352.075	541.125	4.360	1.650
12.625	69.425	159.075	330.175	575.825	4.360	2.475
13.425	74.175	144.425	320.825	576.275	4.360	3.300
14.125	74.325	153.775	317.575	526.075	4.360	4.125
13.025	72.525	144.425	321.175	580.925	4.400	2.925
11.175	58.925	193.875	354.425	559.425	4.400	1.000
11.025	57.775	194.125	350.325	568.025	4.400	0.825
11.825	63.625	182.875	350.925	540.825	4.400	1.650
12.625	69.425	157.925	327.775	573.875	4.400	2.475
13.375	74.075	144.425	318.325	572.325	4.400	3.300
14.125	74.175	153.575	315.925	523.625	4.400	4.125
13.025	72.325	144.425	318.825	577.225	4.440	2.905
11.175	58.675	192.225	354.425	556.775	4.440	1.000
10.925	57.425	192.575	350.325	564.275	4.440	0.825
11.775	63.425	181.275	344.425	540.675	4.440	1.650
12.575	69.425	156.825	325.325	571.625	4.440	2.475
13.375	73.925	143.775	315.875	568.375	4.440	3.300
14.125	73.925	153.375	314.425	521.325	4.440	4.125
12.925	72.125	144.425	316.525	573.425	4.480	2.885
11.125	58.425	190.575	354.425	553.925	4.480	1.000
10.925	57.225	191.025	350.325	560.725	4.480	0.825
11.775	63.225	179.425	344.425	540.525	4.480	1.650
12.575	69.425	155.775	322.925	569.175	4.480	2.475
13.375	73.875	143.175	313.425	564.425	4.480	3.300
14.075	73.825	153.175	312.925	519.075	4.480	4.125
12.925	71.925	144.425	314.275	569.425	4.520	2.865
11.125	58.175	188.925	354.425	551.325	4.520	1.000
10.925	56.925	189.425	350.325	557.325	4.520	0.825
11.725	63.025	178.175	344.425	540.425	4.520	1.650
12.575	69.325	154.425	320.525	566.525	4.520	2.475
13.325	73.825	142.575	311.125	560.425	4.520	3.300
14.075	73.675	153.025	311.575	516.925	4.520	4.125
12.875	71.725	144.425	312.075	565.875	4.560	2.845
11.075	57.925	187.325	354.325	544.425	4.560	1.000
10.925	56.725	187.925	350.275	554.075	4.560	0.825
11.725	62.825	176.675	344.425	540.375	4.560	1.650
12.525	69.225	153.725	318.175	563.675	4.560	2.475
13.325	73.725	142.025	308.875	556.525	4.560	3.300
14.075	73.425	152.875	310.275	514.425	4.560	4.125
12.825	71.425	144.425	309.425	561.925	4.600	2.825
11.075	57.725	185.725	354.125	544.425	4.600	1.000
10.875	56.425	186.325	350.225	551.025	4.600	0.825
11.725	62.625	175.175	343.925	540.325	4.600	1.650
12.525	69.125	152.725	315.825	560.625	4.600	2.475
13.275	73.625	141.425	306.675	552.575	4.600	3.300
14.025	73.275	152.725	309.025	512.875	4.600	4.125
12.825	71.275	144.425	307.875	558.075	4.640	2.805
11.025	57.525	184.125	353.775	544.425	4.640	1.000
10.875	56.225	184.425	350.125	544.425	4.640	0.825
11.675	62.425	173.675	342.325	540.225	4.640	1.650
12.425	69.025	151.775	313.525	557.375	4.640	2.475
13.275	73.525	140.925	304.425	544.425	4.640	3.300
14.025	73.125	152.625	307.925	511.025	4.640	4.125
12.775	71.075	144.425	305.875	554.125	4.680	2.785
11.025	57.275	182.525	353.375	542.875	4.680	1.000
10.875	56.025	183.225	344.425	544.425	4.680	0.825
11.675	62.275	172.225	340.625	540.025	4.680	1.650
12.425	68.925	150.825	311.275	554.025	4.680	2.475

Mode 1	Mode 2	Mode 3	Mode 4	Mode 5	Size	Location
13.275	73.425	140.525	302.525	544.425	4.680	3.300
14.025	72.925	152.525	306.875	509.225	4.680	4.125
12.725	70.875	144.275	303.875	550.175	4.720	2.765
10.925	57.075	180.925	352.925	541.325	4.720	1.000
10.825	55.775	181.625	344.425	543.075	4.720	0.825
11.625	62.125	170.825	338.925	539.425	4.720	1.650
12.425	68.825	144.425	309.025	550.525	4.720	2.475
13.225	73.325	140.075	300.525	540.925	4.720	3.300
13.925	72.775	152.425	305.875	507.575	4.720	4.125
12.675	70.675	143.825	301.925	544.425	4.760	2.745
10.925	56.875	179.325	352.325	539.425	4.760	1.000
10.825	55.575	180.075	344.425	540.825	4.760	0.825
11.625	61.925	169.425	337.125	539.425	4.760	1.650
12.425	68.725	144.425	306.825	544.425	4.760	2.475
13.225	73.225	139.425	294.425	537.075	4.760	3.300
13.925	72.575	152.325	304.425	505.925	4.760	4.125
12.625	70.425	143.425	300.125	542.225	4.800	2.725
10.925	56.675	177.775	351.675	538.725	4.800	1.000
10.775	55.375	178.575	344.425	538.775	4.800	0.825
11.575	61.825	168.075	335.325	538.925	4.800	1.650
12.375	68.625	144.425	304.425	543.175	4.800	2.475
13.175	73.125	139.225	294.425	533.325	4.800	3.300
13.925	72.375	152.275	304.175	504.425	4.800	4.125
12.625	70.225	143.025	294.425	538.225	4.840	2.705
10.925	56.425	176.225	350.875	537.725	4.840	1.000
10.775	55.175	177.025	344.425	536.925	4.840	0.825
11.575	61.675	166.725	333.425	538.225	4.840	1.650
12.375	68.575	144.425	302.525	539.425	4.840	2.475
13.175	73.025	138.825	294.425	529.425	4.840	3.300
13.925	72.175	152.225	303.425	503.125	4.840	4.125
12.575	70.025	142.675	294.425	534.275	4.880	2.685
10.925	56.275	174.425	344.425	536.875	4.880	1.000
10.725	54.425	175.525	344.425	535.375	4.880	0.825
11.525	61.525	165.375	331.575	537.375	4.880	1.650
12.375	68.425	144.425	300.425	535.575	4.880	2.475
13.175	72.925	138.425	293.275	525.925	4.880	3.300
13.925	72.025	152.125	302.725	501.825	4.880	4.125
12.525	69.425	142.275	294.425	530.325	4.920	2.665
10.875	56.125	173.225	344.425	536.225	4.920	1.000
10.725	54.425	174.025	344.425	533.925	4.920	0.825
11.525	61.375	164.075	329.425	536.375	4.920	1.650
12.325	68.375	144.425	294.425	531.675	4.920	2.475
13.125	72.825	138.125	291.625	522.325	4.920	3.300
13.925	71.825	152.075	302.125	500.675	4.920	4.125
12.425	69.425	141.925	293.225	526.375	4.960	2.645
10.875	55.925	171.725	344.425	535.675	4.960	1.000
10.675	54.425	172.525	344.425	532.725	4.960	0.825
11.425	61.275	162.825	327.775	535.175	4.960	1.650
12.325	68.325	144.425	294.425	527.725	4.960	2.475
13.125	72.725	137.825	290.075	518.825	4.960	3.300
13.875	71.625	152.025	301.625	494.425	4.960	4.125
12.425	69.375	141.575	291.625	522.425	5.000	2.625
10.825	55.775	170.275	344.425	535.325	5.000	1.000
10.675	54.425	171.075	344.425	531.725	5.000	0.825
11.425	61.125	161.575	325.825	533.725	5.000	1.650
12.275	68.225	144.125	294.425	523.775	5.000	2.475
13.075	72.625	137.525	288.525	515.325	5.000	3.300
13.875	71.425	151.925	301.125	494.425	5.000	4.125
12.375	69.175	141.275	290.025	518.575	5.040	2.605
10.825	55.575	168.825	344.425	535.025	5.040	1.000
10.625	54.225	169.425	344.425	530.925	5.040	0.825
11.425	61.025	160.375	323.875	532.125	5.040	1.650
12.275	68.175	143.425	292.525	519.425	5.040	2.475

Mode 1	Mode 2	Mode 3	Mode 4	Mode 5	Size	Location
13.075	72.425	137.275	287.125	511.925	5.040	3.300
13.875	71.225	151.925	300.725	494.425	5.040	4.125
12.375	68.925	140.925	288.525	514.425	5.080	2.585
10.775	55.425	167.425	344.075	534.425	5.080	1.000
10.625	54.075	168.175	343.875	530.225	5.080	0.825
11.425	60.875	159.175	321.875	530.325	5.080	1.650
12.225	68.075	142.725	290.625	515.825	5.080	2.475
13.075	72.375	137.025	285.725	508.625	5.080	3.300
13.825	71.025	151.875	300.375	494.425	5.080	4.125
12.325	68.725	140.625	287.075	510.925	5.120	2.565
10.775	55.275	166.025	342.625	534.425	5.120	1.000
10.625	53.925	166.775	342.725	529.425	5.120	0.825
11.425	60.775	157.925	319.425	528.325	5.120	1.650
12.225	68.025	142.025	288.825	511.825	5.120	2.475
13.025	72.275	136.775	284.425	505.425	5.120	3.300
13.825	70.825	151.825	300.075	494.425	5.120	4.125
12.275	68.525	140.275	285.675	507.125	5.160	2.545
10.725	55.125	164.425	341.025	534.425	5.160	1.000
10.575	53.775	165.375	341.425	529.375	5.160	0.825
11.375	60.675	156.825	317.925	526.175	5.160	1.650
12.225	67.925	141.375	287.025	507.875	5.160	2.475
13.025	72.125	136.575	283.175	502.275	5.160	3.300
12.225	68.275	139.425	284.325	503.425	5.200	2.525
10.725	54.425	163.275	339.425	534.425	5.200	1.000
10.575	53.625	163.925	340.125	529.075	5.200	0.825
11.375	60.575	155.725	315.925	523.825	5.200	1.650
12.175	67.875	140.725	285.275	503.925	5.200	2.475
12.925	72.025	136.375	282.025	494.425	5.200	3.300
12.175	68.075	139.425	283.025	494.425	5.240	2.505
10.725	54.425	161.925	337.725	534.425	5.240	1.000
10.525	53.425	162.625	338.725	528.925	5.240	0.825
11.325	60.425	154.425	314.025	521.325	5.240	1.650
12.175	67.825	140.125	283.575	500.025	5.240	2.475
12.925	71.875	136.225	280.925	494.425	5.240	3.300
12.125	67.825	139.425	281.725	494.425	5.280	2.485
10.675	54.425	160.625	335.925	534.425	5.280	1.000
10.525	53.325	161.325	337.175	528.825	5.280	0.825
11.325	60.375	153.575	312.075	518.725	5.280	1.650
12.125	67.775	139.425	281.925	494.425	5.280	2.475
12.925	71.775	136.075	279.425	493.425	5.280	3.300
12.125	67.625	139.125	280.525	492.425	5.320	2.465
10.675	54.425	159.325	334.125	534.325	5.320	1.000
10.425	53.175	159.425	335.575	528.775	5.320	0.825
11.275	60.275	152.525	310.125	515.925	5.320	1.650
12.125	67.725	138.925	280.325	492.375	5.320	2.475
12.925	71.625	135.925	278.925	490.675	5.320	3.300
12.075	67.425	138.825	279.325	488.925	5.360	2.445
10.625	54.425	158.075	332.225	534.075	5.360	1.000
10.425	53.025	158.675	333.875	528.725	5.360	0.825
11.275	60.225	151.525	308.175	513.075	5.360	1.650
12.075	67.625	138.425	278.775	488.575	5.360	2.475
12.925	71.425	135.775	278.025	487.925	5.360	3.300
12.025	67.175	138.575	278.175	485.425	5.400	2.425
10.625	54.375	156.825	330.325	533.675	5.400	1.000
10.425	52.925	157.425	332.125	528.675	5.400	0.825
11.225	60.125	150.525	306.225	510.125	5.400	1.650
12.075	67.575	137.925	277.225	484.425	5.400	2.475
12.925	71.375	135.675	277.175	485.425	5.400	3.300
11.925	66.925	138.325	277.075	481.925	5.440	2.405
10.575	54.225	155.625	328.375	533.175	5.440	1.000
10.425	52.775	156.175	330.325	528.575	5.440	0.825
11.225	60.025	144.425	304.325	507.075	5.440	1.650
12.025	67.525	137.425	275.775	481.175	5.440	2.475

Mode 1	Mode 2	Mode 3	Mode 4	Mode 5	Size	Location
12.875	71.225	135.575	276.425	483.025	5.440	3.300
11.925	66.725	138.075	276.025	478.625	5.480	2.385
10.575	54.125	154.425	326.325	532.525	5.480	1.000
10.425	52.675	154.425	328.425	528.425	5.480	0.825
11.225	59.425	144.425	302.425	503.925	5.480	1.650
12.025	67.425	136.925	274.375	477.525	5.480	2.475
12.875	71.075	135.425	275.725	480.675	5.480	3.300
11.875	66.525	137.825	275.025	475.275	5.520	2.365
10.525	54.025	153.275	324.325	531.725	5.520	1.000
10.375	52.575	153.775	326.575	528.175	5.520	0.825
11.175	59.425	144.425	300.575	500.825	5.520	1.650
12.025	67.375	136.525	272.925	473.925	5.520	2.475
12.825	70.925	135.425	275.075	478.425	5.520	3.300
11.875	66.275	137.575	274.025	472.025	5.560	2.345
10.525	53.925	152.125	322.275	530.725	5.560	1.000
10.375	52.425	152.575	324.425	527.825	5.560	0.825
11.175	59.425	144.425	294.425	494.425	5.560	1.650
11.925	67.325	136.075	271.675	470.425	5.560	2.475
12.825	70.775	135.325	274.425	476.375	5.560	3.300
11.825	66.025	137.325	273.075	468.825	5.600	2.325
10.525	53.825	151.025	320.175	529.425	5.600	1.000
10.325	52.375	151.425	322.625	527.375	5.600	0.825
11.125	59.425	144.425	294.425	494.325	5.600	1.650
11.925	67.275	135.675	270.375	467.025	5.600	2.475
12.825	70.625	135.275	273.925	474.425	5.600	3.300
11.775	65.825	137.075	272.175	465.725	5.640	2.305
10.425	53.725	144.425	318.075	528.125	5.640	1.000
10.325	52.275	150.275	320.575	526.725	5.640	0.825
11.125	59.425	144.425	294.425	491.025	5.640	1.650
11.925	67.225	135.325	269.175	463.675	5.640	2.475
12.775	70.425	135.225	273.425	472.575	5.640	3.300
11.725	65.575	136.825	271.325	462.625	5.680	2.285
10.425	53.625	144.425	316.025	526.525	5.680	1.000
10.275	52.175	144.425	318.525	525.925	5.680	0.825
11.075	59.425	144.275	293.325	487.725	5.680	1.650
11.925	67.125	134.425	267.925	460.375	5.680	2.475
12.775	70.325	135.175	273.025	470.875	5.680	3.300
11.675	65.375	136.575	270.425	459.425	5.720	2.265
10.425	53.575	144.425	313.875	524.425	5.720	1.000
10.275	52.075	144.425	316.425	524.425	5.720	0.825
11.075	59.425	143.425	291.575	484.425	5.720	1.650
11.875	67.075	134.425	266.875	457.175	5.720	2.475
12.725	70.175	135.125	272.625	469.275	5.720	3.300
11.625	65.125	136.375	269.425	456.675	5.760	2.245
10.425	53.425	144.425	311.775	522.825	5.760	1.000
10.225	51.925	144.425	314.375	523.775	5.760	0.825
11.025	59.425	142.725	289.425	481.125	5.760	1.650
11.875	67.025	134.275	265.775	454.025	5.760	2.475
12.725	70.025	135.125	272.275	467.775	5.760	3.300
11.575	64.425	136.125	268.925	453.825	5.800	2.225
10.375	53.425	144.425	309.425	520.675	5.800	1.000
10.225	51.875	144.425	312.275	522.375	5.800	0.825
11.025	59.425	141.925	288.175	477.825	5.800	1.650
11.875	66.925	133.925	264.425	450.925	5.800	2.475
12.725	69.425	135.075	272.025	466.425	5.800	3.300
11.575	64.425	135.925	268.175	450.925	5.840	2.205
10.375	53.325	144.425	307.575	518.425	5.840	1.000
10.225	51.825	144.425	310.175	520.825	5.840	0.825
11.025	59.425	141.275	286.425	474.425	5.840	1.650
11.825	66.875	133.675	263.725	444.425	5.840	2.475
12.675	69.425	135.075	271.775	465.225	5.840	3.300
11.525	64.425	135.675	267.425	444.425	5.880	2.185
10.325	53.275	143.875	305.425	515.925	5.880	1.000

Mode 1	Mode 2	Mode 3	Mode 4	Mode 5	Size	Location
10.175	51.725	143.925	308.075	519.125	5.880	0.825
10.925	59.375	140.575	284.425	471.225	5.880	1.650
11.825	66.775	133.425	262.825	444.425	5.880	2.475
12.675	69.425	135.025	271.525	464.125	5.880	3.300
11.425	64.225	135.425	266.775	444.425	5.920	2.165
10.325	53.175	142.925	303.425	513.425	5.920	1.000
10.175	51.675	143.025	305.925	517.175	5.920	0.825
10.925	59.325	139.425	283.225	467.925	5.920	1.650
11.775	66.725	133.175	261.925	442.275	5.920	2.475
12.675	69.375	135.025	271.375	463.125	5.920	3.300
11.425	63.925	135.275	266.125	442.925	5.960	2.145
10.325	53.125	142.025	301.325	510.725	5.960	1.000
10.125	51.575	142.075	303.825	515.075	5.960	0.825
10.925	59.275	139.275	281.675	464.425	5.960	1.650
11.775	66.625	132.925	261.075	439.425	5.960	2.475
11.375	63.775	135.025	265.425	440.425	6.000	2.125
10.275	53.075	141.125	294.425	507.925	6.000	1.000
10.125	51.525	141.125	301.725	512.825	6.000	0.825
10.925	59.225	138.625	280.125	461.525	6.000	1.650
11.725	66.575	132.775	260.275	436.875	6.000	2.475
11.325	63.525	134.425	264.425	437.925	6.040	2.105
10.275	53.025	140.275	294.425	505.025	6.040	1.000
10.075	51.425	140.225	294.425	510.425	6.040	0.825
10.875	59.175	138.025	278.625	458.325	6.040	1.650
11.725	66.425	132.575	259.425	434.325	6.040	2.475
11.325	63.275	134.425	264.275	435.575	6.080	2.085
10.225	52.925	139.425	294.425	502.025	6.080	1.000
10.075	51.375	139.375	294.425	507.925	6.080	0.825
10.875	59.175	137.425	277.175	455.175	6.080	1.650
11.725	66.375	132.375	258.825	431.875	6.080	2.475
11.275	63.075	134.425	263.725	433.225	6.120	2.065
10.225	52.875	138.625	293.225	494.425	6.120	1.000
10.075	51.325	138.425	294.425	505.225	6.120	0.825
10.825	59.125	136.875	275.725	452.075	6.120	1.650
11.675	66.325	132.225	258.175	429.425	6.120	2.475
11.225	62.825	134.175	263.175	430.925	6.160	2.045
10.175	52.825	137.825	291.225	494.425	6.160	1.000
10.025	51.275	137.675	293.425	502.425	6.160	0.825
10.825	59.075	136.375	274.325	444.425	6.160	1.650
11.675	66.225	132.075	257.575	427.225	6.160	2.475
11.175	62.575	133.925	262.675	428.775	6.200	2.025
10.175	52.775	137.075	289.275	492.725	6.200	1.000
10.025	51.225	136.825	291.425	494.425	6.200	0.825
10.825	59.025	135.875	272.925	444.425	6.200	1.650
11.625	66.125	131.925	256.925	425.025	6.200	2.475
11.125	62.375	133.775	262.175	426.625	6.240	2.005
10.125	52.725	136.325	287.375	489.425	6.240	1.000
9.425	51.175	136.075	289.425	494.425	6.240	0.825
10.775	58.925	135.375	271.625	442.925	6.240	1.650
11.625	66.025	131.825	256.425	422.925	6.240	2.475
11.075	62.125	133.575	261.675	424.425	6.280	1.985
10.125	52.725	135.625	285.425	486.325	6.280	1.000
9.425	51.125	135.275	287.425	493.625	6.280	0.825
10.775	58.925	134.425	270.325	440.075	6.280	1.650
11.625	65.925	131.725	256.025	420.925	6.280	2.475
11.075	61.875	133.375	261.175	422.575	6.320	1.965
10.125	52.675	134.425	283.575	483.125	6.320	1.000
9.425	51.075	134.425	285.425	490.575	6.320	0.825
10.725	58.925	134.425	269.075	437.175	6.320	1.650
11.575	65.825	131.625	255.575	419.075	6.320	2.475
11.025	61.675	133.175	260.725	420.675	6.360	1.945
10.075	52.625	134.225	281.775	479.425	6.360	1.000
9.425	51.025	133.825	283.525	487.425	6.360	0.825

Mode 1	Mode 2	Mode 3	Mode 4	Mode 5	Size	Location
10.725	58.875	134.075	267.825	434.325	6.360	1.650
11.575	65.725	131.575	255.175	417.275	6.360	2.475
10.925	61.425	132.925	260.275	418.775	6.400	1.925
10.075	52.575	133.575	279.425	476.625	6.400	1.000
9.425	50.925	133.125	281.625	484.275	6.400	0.825
10.675	58.825	133.675	266.675	431.525	6.400	1.650
11.525	65.625	131.425	254.425	415.625	6.400	2.475
10.925	61.175	132.775	259.425	416.925	6.440	1.905
10.025	52.525	132.925	278.175	473.325	6.440	1.000
9.425	50.925	132.425	279.425	481.075	6.440	0.825
10.675	58.775	133.275	265.525	428.825	6.440	1.650
11.525	65.525	131.425	254.425	414.025	6.440	2.475
10.875	60.925	132.575	259.375	415.275	6.480	1.885
10.025	52.525	132.325	276.425	470.075	6.480	1.000
9.425	50.875	131.775	277.875	477.875	6.480	0.825
10.675	58.775	132.925	264.425	426.125	6.480	1.650
11.525	65.425	131.375	254.225	412.525	6.480	2.475
10.825	60.725	132.375	258.925	413.575	6.520	1.865
9.425	52.425	131.775	274.425	466.875	6.520	1.000
9.425	50.875	131.125	276.075	474.425	6.520	0.825
10.625	58.725	132.575	263.375	423.525	6.520	1.650
11.425	65.325	131.325	253.925	411.175	6.520	2.475
10.825	60.425	132.175	258.575	411.925	6.560	1.845
9.425	52.425	131.175	273.025	463.625	6.560	1.000
9.425	50.825	130.525	274.275	471.375	6.560	0.825
10.625	58.675	132.275	262.375	420.925	6.560	1.650
11.425	65.225	131.275	253.775	409.425	6.560	2.475
10.775	60.225	131.925	258.125	410.425	6.600	1.825
9.425	52.425	130.675	271.375	460.425	6.600	1.000
9.425	50.775	129.425	272.525	468.175	6.600	0.825
10.575	58.625	131.925	261.375	418.425	6.600	1.650
11.425	65.075	131.275	253.575	408.725	6.600	2.475
10.725	60.025	131.725	257.725	408.925	6.640	1.805
9.425	52.375	130.125	269.425	457.275	6.640	1.000
9.425	50.775	129.325	270.775	464.425	6.640	0.825
10.575	58.575	131.725	260.425	415.925	6.640	1.650
11.425	64.425	131.225	253.425	407.675	6.640	2.475
10.675	59.425	131.525	257.325	407.525	6.680	1.785
9.425	52.325	129.425	268.175	454.125	6.680	1.000
9.425	50.725	128.775	269.075	461.725	6.680	0.825
10.525	58.525	131.425	259.425	413.625	6.680	1.650
11.425	64.425	131.225	253.275	406.725	6.680	2.475
10.625	59.425	131.325	256.925	406.125	6.720	1.765
9.425	52.325	129.125	266.625	451.025	6.720	1.000
9.425	50.675	128.225	267.425	458.525	6.720	0.825
10.525	58.425	131.225	258.675	411.275	6.720	1.650
11.375	64.425	131.175	253.175	405.825	6.720	2.475
10.625	59.325	131.125	256.525	404.425	6.760	1.745
9.425	52.275	128.675	265.125	444.425	6.760	1.000
9.425	50.675	127.725	265.775	455.325	6.760	0.825
10.525	58.425	130.925	257.875	409.025	6.760	1.650
11.375	64.425	131.175	253.075	405.075	6.760	2.475
10.575	59.075	130.925	256.125	403.575	6.800	1.725
9.425	52.225	128.225	263.675	444.425	6.800	1.000
9.425	50.625	127.225	264.175	452.175	6.800	0.825
10.425	58.375	130.775	257.125	406.875	6.800	1.650
10.525	58.825	130.725	255.725	402.375	6.840	1.705
9.425	52.225	127.825	262.275	441.875	6.840	1.000
9.425	50.575	126.775	262.625	444.425	6.840	0.825
10.425	58.325	130.575	256.375	404.425	6.840	1.650
10.425	58.575	130.525	255.325	401.175	6.880	1.685
9.425	52.175	127.425	260.875	438.925	6.880	1.000
9.425	50.575	126.325	261.125	444.425	6.880	0.825

Mode 1	Mode 2	Mode 3	Mode 4	Mode 5	Size	Location
10.425	58.275	130.425	255.725	402.675	6.880	1.650
10.425	58.375	130.325	254.425	400.075	6.920	1.665
9.425	52.175	127.025	259.425	436.025	6.920	1.000
9.425	50.525	125.875	259.425	442.925	6.920	0.825
10.425	58.225	130.275	255.075	400.675	6.920	1.650
10.375	58.125	130.125	254.425	394.425	6.960	1.645
9.425	52.125	126.675	258.225	433.175	6.960	1.000
9.425	50.525	125.425	258.175	439.425	6.960	0.825
10.425	58.175	130.125	254.425	394.425	6.960	1.650
10.375	57.875	129.425	254.075	394.425	7.000	1.625
9.425	52.125	126.325	256.925	430.325	7.000	1.000
9.425	50.425	125.075	256.775	436.925	7.000	0.825
10.375	58.125	129.425	253.925	394.425	7.000	1.650
10.325	57.675	129.425	253.675	394.425	7.040	1.605
9.425	52.075	126.025	255.725	427.575	7.040	1.000
9.425	50.425	124.425	255.375	433.925	7.040	0.825
10.375	58.025	129.425	253.375	394.425	7.040	1.650
10.275	57.425	129.425	253.225	394.425	7.080	1.585
9.425	52.025	125.725	254.425	424.425	7.080	1.000
9.425	50.425	124.325	254.075	431.075	7.080	0.825
10.325	57.925	129.425	252.925	393.425	7.080	1.650
10.225	57.175	129.275	252.825	394.425	7.120	1.565
9.425	52.025	125.425	253.375	422.175	7.120	1.000
9.425	50.425	123.925	252.775	428.275	7.120	0.825
10.325	57.925	129.425	252.425	391.875	7.120	1.650
10.175	56.925	129.075	252.375	394.225	7.160	1.545
9.425	51.925	125.175	252.275	419.425	7.160	1.000
9.425	50.375	123.675	251.525	425.425	7.160	0.825
10.325	57.875	129.425	252.075	390.325	7.160	1.650
10.175	56.725	128.825	251.925	393.375	7.200	1.525
9.425	51.925	124.425	251.225	417.025	7.200	1.000
9.425	50.375	123.375	250.325	422.725	7.200	0.825
10.275	57.775	129.425	251.725	388.875	7.200	1.650
10.125	56.425	128.625	251.425	392.525	7.240	1.505
9.425	51.925	124.425	250.175	414.425	7.240	1.000
9.425	50.325	123.075	244.425	420.025	7.240	0.825
10.275	57.725	129.425	251.375	387.525	7.240	1.650
10.075	56.225	128.425	251.025	391.725	7.280	1.485
9.425	51.875	124.425	244.425	412.125	7.280	1.000
9.425	50.275	122.825	244.425	417.375	7.280	0.825
10.225	57.625	129.425	251.075	386.225	7.280	1.650
10.025	56.025	128.175	250.575	390.925	7.320	1.465
9.425	51.825	124.225	244.425	409.425	7.320	1.000
9.425	50.275	122.525	244.425	414.425	7.320	0.825
10.225	57.575	129.375	250.825	384.425	7.320	1.650
10.025	55.775	127.925	250.075	390.175	7.360	1.445
9.425	51.825	124.075	244.425	407.425	7.360	1.000
9.425	50.225	122.325	244.425	412.275	7.360	0.825
10.225	57.525	129.325	250.625	383.875	7.360	1.650
9.425	55.525	127.775	244.425	389.425	7.400	1.425
9.425	51.775	123.875	244.425	405.175	7.400	1.000
9.375	50.225	122.075	244.425	409.425	7.400	0.825
10.175	57.425	129.325	250.425	382.825	7.400	1.650
9.425	55.325	127.525	244.425	388.725	7.440	1.405
9.425	51.725	123.725	244.425	403.025	7.440	1.000
9.375	50.175	121.875	243.875	407.375	7.440	0.825
10.175	57.325	129.275	250.225	381.825	7.440	1.650
9.425	55.075	127.325	244.425	388.025	7.480	1.385
9.425	51.725	123.575	244.425	400.875	7.480	1.000
9.325	50.125	121.675	242.925	405.025	7.480	0.825
10.175	57.275	129.275	250.075	380.925	7.480	1.650
9.425	54.425	127.075	244.425	387.325	7.520	1.365
9.425	51.675	123.425	244.275	394.425	7.520	1.000

Mode 1	Mode 2	Mode 3	Mode 4	Mode 5	Size	Location
9.325	50.125	121.525	242.075	402.775	7.520	0.825
10.125	57.175	129.225	244.425	380.125	7.520	1.650
9.425	54.425	126.875	244.425	386.625	7.560	1.345
9.425	51.625	123.325	243.575	394.425	7.560	1.000
9.325	50.075	121.375	241.225	400.525	7.560	0.825
10.125	57.125	129.225	244.425	379.425	7.560	1.650
9.425	54.375	126.625	244.425	385.925	7.600	1.325
9.425	51.575	123.225	242.925	394.425	7.600	1.000
9.275	50.025	121.225	240.425	394.425	7.600	0.825
9.425	54.175	126.375	244.425	385.275	7.640	1.305
9.425	51.525	123.125	242.375	393.175	7.640	1.000
9.275	50.025	121.075	239.425	394.425	7.640	0.825
9.425	53.925	126.175	244.425	384.425	7.680	1.285
9.425	51.425	123.025	241.825	391.375	7.680	1.000
9.425	53.675	125.925	244.425	383.925	7.720	1.265
9.375	51.425	122.925	241.275	389.425	7.720	1.000
9.425	53.425	125.675	244.425	383.275	7.760	1.245
9.375	51.375	122.875	240.825	388.125	7.760	1.000
9.425	53.225	125.425	244.425	382.575	7.800	1.225
9.375	51.325	122.825	240.375	386.575	7.800	1.000
9.425	53.025	125.175	243.875	381.925	7.840	1.205
9.325	51.275	122.775	240.025	385.125	7.840	1.000
9.425	52.775	124.425	243.325	381.275	7.880	1.185
9.325	51.225	122.725	239.425	383.775	7.880	1.000
9.425	52.525	124.425	242.775	380.575	7.920	1.165
9.325	51.175	122.675	239.325	382.425	7.920	1.000
9.425	52.325	124.425	242.175	379.425	7.960	1.145
9.275	51.125	122.675	239.025	381.275	7.960	1.000
14.425	81.275	203.075	465.375	638.775	2.500	5.125
12.375	80.225	229.375	465.625	668.675	2.500	2.250
12.225	79.425	223.925	467.825	681.525	2.500	2.075
12.925	82.125	244.425	407.525	671.525	2.500	2.900
13.675	82.675	233.525	385.575	716.725	2.500	3.725
14.275	81.925	210.575	438.725	674.175	2.500	4.550
14.425	81.125	202.175	457.825	644.425	2.500	5.375
15.325	81.275	208.375	394.425	711.425	2.500	6.200
15.625	83.025	224.425	357.925	684.075	2.500	7.025
15.875	86.425	230.775	394.425	614.425	2.500	7.850
15.325	86.775	254.425	494.425	724.275	1.500	5.125
13.325	93.525	251.025	494.425	837.075	1.500	1.750
13.175	92.675	244.425	489.175	838.125	1.500	1.575
13.775	94.425	254.375	502.925	743.125	1.500	2.400
14.325	93.525	254.425	471.275	768.875	1.500	3.225
14.425	90.075	255.275	471.625	825.325	1.500	4.050
15.225	87.275	255.275	494.425	732.425	1.500	4.875
15.575	86.425	252.425	485.375	767.025	1.500	5.700
15.775	87.875	244.425	461.875	820.875	1.500	6.525
15.925	91.275	243.275	465.025	733.925	1.500	7.350
15.225	87.275	255.275	494.425	732.425	1.500	8.175
15.825	94.425	280.925	524.425	901.725	0.500	5.125
14.425	94.425	280.175	544.425	886.275	0.500	1.250
14.425	94.425	279.175	544.425	892.425	0.500	1.075
15.025	100.325	277.825	531.025	878.525	0.500	1.900
15.325	100.125	270.325	534.375	901.675	0.500	2.725
15.525	94.425	270.425	544.425	878.675	0.500	3.550
15.725	94.425	277.375	536.425	878.825	0.500	4.375
15.875	94.425	280.825	525.025	901.425	0.500	5.200
15.925	94.425	274.425	540.575	874.275	0.500	6.025
16.025	94.425	266.375	544.425	885.825	0.500	6.850
16.075	94.425	265.225	527.175	894.125	0.500	7.675

APPENDIX C

INPUT AND OUTPUT FOR THE FINITE ELEMENT MODEL

The following appendix contains the inputs and outputs of two separate runs of a finite element model discussed earlier in the text in reference [32]. The finite element code uses English units so the inputs were converted from the MKS units used in the text to values listed below. The finite element code also calculated 72 modal frequencies but only the first six frequencies are listed in this appendix. Both runs were for glass-epoxy cantilever composite beams with identical lamina properties; however, the beams had different dimensions. In the first run, the beam was 2.54 cm (1") wide and 0.18 cm (0.072") thick. The second beam was 2.33 cm (0.917") wide and 0.15 cm (0.061") thick.

Variable definition

NPLY = number of lamina
NEM = number of elements in the mesh
NDF = number of degrees of freedom per node
TH(I) = lamina orientation (degrees)
AL = beam length (inches)
X0 = location of beam clamp (inches)
HT = beam thickness (inches)
B = beam width (inches)
V12 = Poisson ration
E1, E2 = principal moduli (psi)
G12, G13, G23 = shear moduli (psi)
RHO = density (lb-sec^2/in^4)

Run 1
Inputs:
NPLY = 8
NEM = 18
NDF = 4
AL = 10.25
X0 = 0.0
HT = 0.072
B = 1.0
V12 = 0.27
E1 = 6.14E+06
E2 = 1.7E+06
G12 = 1.03E+06
G13 = 1.03E+06
G23 = 0.93E+06
RHO = 1.805E-04
TH(I) 0.0 90.0 0.0 90.0 90.0 0.0 90.0 0.0

Outputs:

Mode 1	Mode 2	Mode 3	Mode 4	Mode 5	Mode 6
11.29 Hz	71.01 Hz	199.14 Hz	394.93 Hz	659.76 Hz	998.54 Hz

Run 2
Inputs:
NPLY = 8
NEM = 18
NDF = 4
AL = 10.25
X0 = 0.0
HT = 0.061
B = 0.917
V12 = 0.27
E1 = 6.14E+06
E2 = 1.7E+06
G12 = 1.03E+06
G13 = 1.03E+06
G23 = 0.93E+06
RHO = 1.805E-04
TH(I) 0.0 90.0 0.0 90.0 90.0 0.0 90.0 0.0

Outputs:

Mode 1	Mode 2	Mode 3	Mode 4	Mode 5	Mode 6
15.31 Hz	96.23 Hz	270.87 Hz	534.90 Hz	893.14 Hz	1350.89 Hz

BIBLIOGRAPHY

[1] Bhagwan D. Agarwal and Lawrence J. Broutman, *Analysis and Performance of Fiber Composites*, 2nd ed. (John Wiley & Sons, New York, NY, 1990), 1-2.

[2] Eric Udd, *Fiber Optic Smart Structures*, (John Wiley & Sons, New York, NY, 1995), 2,3,9.

[3] Brian Culshaw, *Smart Structures and Materials,* (Artech House, Inc., Boston, MA, 1996).

[4] Eric Udd, editor, *Fiber Optic Sensors*, (John Wiley & Sons, New York, NY, 1991).

[5] Raymond M. Measures, "Structurally Integrated Fiber Optic Damage Assessment System For Composite Materials," *Fiber Optic Smart Structures and Skins: 1988*, Proc. SPIE **986**, 120-129 (1988).

[6] David W. Jensen, Jesus Pascual, and John M. Cory, Jr., "Dynamic Strain Sensing of a Composite Lattice with an Integrated Optical Fiber," Journal of Intelligent Material Systems and Structures **2**, 198-214 (1991).

[7] S. A. Kingsley and D. E. N. Davies, "Multimode Optical Fiber Phase Modulation and Discrimination I & II," Electronics Letters **14**, 385-388 (1987).

[8] M. H. Thursby, et al., "Smart Structures Incorporating Artificial Neural Networks, Fiber-optic Sensors and Solid State Actuators," *Fiber Optic Smart Structures and Skins II (1988),* Proc. SPIE **1170**, 316-325 (1988).

[9] Raymond M. Measures, "Advances Toward Fiber Optic Based Smart Structures," Optical Engineering **31** (1), 34-47 (1992).

[10] Toshihiko Yoshino, Kiyoshi Kurosawa, Katsuji Itoh, and Teruzi Ose, "Fiber-Optic Fabry-Perot Interferometer and its Sensor Applications," IEEE Journal of Quantum Electronics **QE-18**(10), 1624-1633 (1982).

[11] Jorge J. Alcoz, C. E. Lee, and Henry F. Taylor, "Embedded Fiber-Optic Fabry-Perot Ultrasound Sensor," IEEE Transactions on Ultrasonics, Ferroelectrics, and Frequency Control **37**(4), 302-306 (1990).

[12] Kent A. Murphy, Michael F. Gunther, Ashish M. Vengsarkar, and Richard O. Claus, "Quadrature Phase-Shifted, Extrinsic Fabry-Perot Optical Fiber Sensors," Optics Letters **16**(4), 273-275 (1991).

[13] Kexing Liu and Raymond M. Measures, "Signal Processing Techniques for Interferometric Fiber-Optic Strain Sensors." Journal of Intelligent Material Systems and Structures **3**, 432-461 (1992).

[14] Tomas Valis, Dayle Hogg, and Raymond M. Measures, "Fiber-Optic Fabry-Perot Strain Rosettes," Smart Materials and Structures **1**, 227-232 (1992).

[15] Pojamarn Pojanasomboon, "Impact Strain Detection in Fiber Optic-Based Smart Composite Structure," M.S. thesis, University of Missouri-Rolla 1993.

[16] Farhad Akhavan, Steve E. Watkins, and K. Chandrashekhara, "Hybrid Sensors for Impact-Induced Stain in Smart Composite Plates," Smart Structures and Materials 1995. *Smart Sensing Processing, and Instrumentation*, Proc. SPIE **2444**, 514-525 (1995).

[17] Kent A. Murphy, Michael F. Gunther, Ashish M. Vengsarkar, and Richard O. Claus, "Fabry-Perot Fiber-Optic Sensors in Full-Scale Fatigue Testing on an F-15 Aircraft," Applied Optics **31**(4), 431-433 (1992).

[18] R. O. Claus, "Optical Fiber Sensors for Smart Materials Characterization," *Proceedings of the Second Conference on Intelligent Materials: 1994*, Proc. ICIM, 384-390 (1994).

[19] C. E. Lee, J. J. Alcoz, Y. Yeh, W. N. Gibler, R. A. Atkins, and H. F. Taylor, "Optical Fiber Fabry-Perot Sensors for Smart Structures," Smart Materials and Structures **1**, 123-127 (1992).

[20] Lei Han, Arkady Voloshin, and John Coulter, "Application of the Integrating Fiber Optic Sensor for Vibration Monitoring," Smart Materials and Structures **4**, 100-105 (1995).

[21] Virkam Bhatia, Cathy A. Schmid, Kent A. Murphy, Richard O. Claus, Tuan A. Tran, Jonathan A. Greene, and Mark S. Miller, "Optical Fiber Sensing Technique for Edge-Induced and Internal Delamination Detection in Composites," Smart Materials and Structures **4**, 164-169 (1995).

[22] M. A. Davis, A. . Kersey, J. Sirkis, and E. J. Friebele, "Fiber Optic Bragg Grating Array for Shape and Vibration Mode Sensing," Proc. SPIE **2191,** 94-102 (1994).

[23] Lei Han, Arkady Voloshin, and John Coulter, "Application of the Integrating Fiber Optic Sensor for Vibration Monitoring," Smart Materials and Structures **4**, 100-105 (1995).

[24] Garg C Amar, "Delamination—A Damage Mode in Composite Structures," Engineering Fracture Mechanics **29**(5), 557-584 (1988).

[25] H. P. Chen and H. C. Ngo, "Dynamic Analysis of Delamination Growth," AIAA Journal **30**, 447-448 (1992).

[26] C. J. Jih and C. T. Sun, "Prediction of Delamination in Composite Laminates Subjected to Low Velocity Impact," Journal of Composite Materials **27**(7), 684-701 (1993).

[27] P. M. Mujumdar and S. Suryanarayan, "Flexual Vibrations of Beams with Delaminations," Journal of Sound and Vibration **125**, 441-461 (1988).

[28] John J. Tracy and Gerard C Pardoen, "Effect of Delamination on the Natural Frequencies of Composite Laminates," Journal of Composite Materials **23**, 1200-1215 (1989).

[29] John J. Tracy, "The Effect of Delamination on the Response of Advanced Composite Laminates," Ph.D. dissertation, University of California, Irvine, 1987.

[30] D. K. Shah, W. S. Chan, and S. P. Joshi, "Delamination Detection and Suppression in a Composite Laminate Using Piezo Ceramic Layers," Smart Materials and Structures **3**, 293-301 (1994).

[31] A. Chukwujekwu Okafor, K. Chandrashekhara, and Y. P. Jiang, "Damage Detection in Composite Laminates with Built-in Piezoelectric Devises Using Modal Analysis and Neural Network," *Smart Sensing, Processing, and Instrumentation: 1995*, Proc. SPIE. **2444**, 314-325 (1995).

[32] K. Chandrashekhara and K. M. Bangera, "Free Vibration of Composite Beams Using a Refined Shear Flexible Beam Element," Computers and Structures **43**(4), 719-727 (1992).

[33] Simon Haykin, *Neural Networks A Comprehensive Foundation,* (Macmillan College Publishing Co., New York, NY, 1994).

[34] Ceravolo Rosario, De Stefano Alessandro, and Sabia Donato, "Hierarchical Use of Neural Techniques in Structural damage Recognition," Smart Materials and Structures **4**, 270-280 (1995).

[35] Chen-Jung Li and Ray Asok, "Neural Network Representation of Fatigue Damage Dynamics," Smart Materials and Structures **3**, 126-132 (1995).

[36] J. R. Vinson and R. L. Sierakowski, "Behavior of Structures Composed of Composite Materials," Martinus Nijhoff, 139-144 (1986).

[37] Roland Ray Kilcher, "Modal Analysis and Impact Damage Assessment of Composite Laminates: an Experimental Study," M.S. thesis, University of Missouri-Rolla 1994.

[38] K. Chandrashekhara, K. Krishnamurthy, and S. Roy, "Free Vibration of Composite Beams Including Rotary Inertia and Shear Deformation," Composite Structures **14**, 269-279 (1990).

[39] NeuralWare, *NeuralWorks Reference Guide,* (NeuralWare, Inc., Pittsburgh, PA, 1993).

VITA

Gilbert Warren Sanders [redacted]

He received his primary education at Martin City Elementary School and secondary education at Grandview Junior and Senior High Schools in Grandview Missouri. He graduated from Grandview High School in 1991. He attended the United States Air Force Academy in Colorado Springs, Colorado. He received a Bachelor of Science degree in Electrical Engineering from the U.S. Air Force Academy and was commissioned into the United States Air Force as a Second Lieutenant on May 31, 1995.

While at the Air Force Academy, he played for the varsity football team. He was a four time recipient of the Western Athletic Conference Scholar-Athlete Award and was named to the Western Athletic Conference's All Academic Team in 1993 and 1994. He also received the Hitachi Promise of Tomorrow Scholarship, and was active in the Fellowship of Christian Athletes.

Upon completion of his Bachelor's degree, he began working on a Master of Science in Electrical Engineering at the University of Missouri-Rolla. During his graduate career at the University of Missouri-Rolla, he also coached the varsity football team and was active in the Air Force ROTC detachment.